Strange Particle Production Via The Weak Interaction

By
Gashaw Bekele Adera

Thesis presented in partial fulfilment
of the requirements for the degree of
Master of Science
at Stellenbosch University

Supervisor: Dr B. I. S. Van Der Ventel
Co-Supervisor: Prof G. C. Hillhouse
March 2009

Declaration

I, the undersigned, hereby declare that the work contained in this thesis is my own original work and has not previously, in its entirety or in part, been submitted at any university for a degree.

---------- ----------

Gashaw Bekele Adera Date

Abstract

In this thesis a general relativistic formalism for neutrino-induced weak production of strange particles is presented. In our formalism it is shown that the differential cross section is constructed as a contraction between a leptonic tensor and a hadronic tensor. The electroweak theory of Glashow, Salam and Weinberg is used to calculate the leptonic tensor exactly. The hadronic current is determined from the newly derived general form of the weak hadronic current which is expressed in terms of eighteen invariant amplitudes that parametrize the hadron vertex. The Born diagram is used to approximate the unknown hadronic vertex and the numerical calculation is made by evaluating the tree diagrams in terms of standard weak form factors and the strong coupling constants in the framework of the Cabibbo theory and SU(3) symmetry. The investigation is made for charged current reactions in terms of the angular distribution of the differential cross section with respect to the outgoing kaon angle and the results are discussed.

Dedication

I would like to dedicated this work to my mother, Gete Yadeta.

Acknowledgements

Above all, blessed be the name of the Lord Jesus whose majesty is full of grace and honour. He established the universe with his wisdom. He perfected the heavens by his Sprite. He destroyed ignorance and the shadow of death with his power. He always restores my soul, leads me beside the still water, and keeps peace in my heart. All things are for of him, through him, and to him: to whom be glory forever!

I would like to express my sincere gratitude to my supervisor Dr B. I. S. Van Der Ventel for his great support in my work and also other aspect of my life, sharing his knowledge and guidance from the start right up until the finalization of this work. I am always fascinated by his enthusiasm that carried me along my work and has helped me to pave a way for my future academic and professional endeavours.

I am also thankful to Prof. G. C. Hillhouse who created the welcoming atmosphere in the physics department throughout my stay. Prof. Terry Mart definitely deserves my special thanks for the discussions we made and the resources he provided me with in his area of expertise specially regarding the strong coupling constants.

My sister, Mebrat Adera is the blessing who has ever been happened to my life. She always stands by my side in her prayers, which was one of the most important things I needed in my study life. My acknowledgement also goes to the physics department librarian, Ms Avdil Davids, who was very helpful to me. I am lucky enough to meet my best friends during my studies: Rachel Frans from USA and Fernanda Almeida from Brazil, who were always there for me at the times I needed them. I always love you both. You are my eternal friends.

This work is financially supported in part by African Institute for Mathematical Sciences (AIMS), by Physics Department University of Stellenbosch, and by South African National Research Foundation (NRF), to whom I am very grateful.

Contents

Abstract i

List of Figures iv

List of Tables vii

1 Introduction 1

2 Theoretical Overview 4

2.1 Dirac Spinor Fields 4

2.1.1 Energy-spin projection operators 5

2.1.2 Helicity state 7

2.2 The SU(3) flavour quark model 8

2.2.1 SU(3) Current Octet 11

2.3 Weak Interaction 12

2.4 Electromagnetic Current in SU(2) Framework 14

2.5 Electroweak Gauge Theory 17

2.6 Strange particle production 20

3 General Formalism 22

3.1 Kinematic Description 23

3.2 Cross Section 27

3.3 Invariant Amplitude Evaluation 31

4 Hadronic Weak Current **35**

4.1 Weak Form factors in Two-body transitions 35

4.2 Model-independent Form factors of Three-body Weak Transition 38

5 SU(3) Current Algebra **42**

5.1 Cabibbo Theory and Conserved Vector Current 42

5.2 Weak Transition of Mesons 49

5.3 Strong Coupling constants 49

6 Neutrino-induced Strange Particle Production **51**

6.1 Born Term Model 51

6.2 Associated production of strange particles 53

6.2.1 s-channel: Fig. 6.2 53

6.2.2 t-channel: Fig. 6.3 54

6.2.3 u-channel: Fig. 6.4 55

6.2.4 Extraction of the Eighteen Structure Functions 56

7 Numerical Results and Discussion **59**

8 Summary and Conclusions **76**

Appendices **78**

A Dirac Algebra of Gamma Matrix **78**

A.1 Dirac Algebra 79

A.2 Trace Theorems 80

B Leptonic Tensor **82**

B.1 Weak Neutral Current 82

B.1.1 Feynman's Trace Technique 84

B.2 Weak Charged Current 86

C Gordon-like Identities **88**

D Born Approximation of the Weak Hadronic Current Amplitudes **91**

Bibliography **96**

List of Figures

2.1 The fundamental SU(3) triplets of quark and antiquark with the action of the step operators. 9

2.2 The octet of pseudoscalar-mesons which is constructed from 3(quark) and $\bar{3}$(antiquark) of SU(3) representations by using the weight diagrams. 11

2.3 The SU(3) octet representation of the ground state baryons. 12

2.4 The weak quark currents: (a) refers to the strangeness conserving transition, $d \to u$; whereas (b) represents the strangeness changing transition, $s \to u$. . . 15

3.1 The lowest order Feynman diagram of neutrino-induced weak production of strange particles at the hadronic level. 23

3.2 kinematics of the neutrino-induced weak production of strange particles in the rest frame of the target nucleon. 24

3.3 The Geometry of three-momenta of the reaction $\nu N \to lKY$. Here the momenta of the leptons and hadrons specified on the same coordinate system. 25

3.4 The general quark level Feynman diagram of strange particle production via neutrino-nucleon weak interaction and the associated factors according to the Feynman rules. 31

4.1 Tree diagram of the two-body weak process of fermions. 36

4.2 The Feynman diagram with a vertex of three external lines of hadrons and exchange particle carrying four-momentum transfer $q = p_1' + p_2' - p_1$. 39

6.1 The Born diagram of neutrino-induced weak production of strange particles. . 52

6.2 The Feynman diagram of the s-channel. 53

6.3 The Feynman diagram of the t-channel. 54

6.4 The Feynman diagram of the u-channel. 55

7.1 The differential cross section against the kaon angle for CC1 at $Q^2 = 0.035\,\mathrm{GeV}^2$ and $\theta' = 0.5$ deg. 65

7.2 The differential cross-section against the kaon angle for CC2 at $Q^2 = 0.035\,\mathrm{GeV}^2$ and $\theta' = 0.5$ deg. 66

7.3 The differential cross-section against the kaon angle for CC3 at $Q^2 = 0.035\,\mathrm{GeV}^2$ and $\theta' = 0.5$ deg. 67

7.4 The differential cross-section against the kaon angle for CC4 at $Q^2 = 0.035\,\mathrm{GeV}^2$ and $\theta' = 0.5$ deg. 68

7.5 The differential cross sections of CC1, CC2, CC3, and CC4 against the kaon angle for $\mathrm{h}' = -1$ and $\mathrm{h}' = +1$ helicity states as well as by summing over the two states at $Q^2 = 0.035\,\mathrm{GeV}^2$ and $\theta' = 0.5$ deg. 69

7.6 The differential cross section against the kaon angle for CC1 at $Q^2 = 0.25\,\mathrm{GeV}^2$ and $\theta' = 0.5$ deg. 70

7.7 The differential cross section against the kaon angle for CC2 at $Q^2 = 0.25\,\mathrm{GeV}^2$ and $\theta' = 0.5$ deg. 71

7.8 The differential cross section against the kaon angle for CC3 at $Q^2 = 0.25\,\mathrm{GeV}^2$ and $\theta' = 0.5$ deg. 72

7.9 The differential cross section against the kaon angle for CC4 at $Q^2 = 0.25\,\mathrm{GeV}^2$ and $\theta' = 0.5$ deg. 73

7.10 The differential cross sections of CC1, CC2, CC3, and CC4 against the kaon angle for $\mathrm{h}' = -1$ and $\mathrm{h}' = +1$ helicity states as well as the total by summing over the two states at $Q^2 = 0.25\,\mathrm{GeV}^2$ and $\theta' = 0.5$ deg. 74

7.11 The comparison of the angular distribution of the differential cross sections of CC1, CC2, CC3, and CC4 at $Q^2 = 0.035\,\mathrm{GeV}^2$ and $\theta' = 0.5$ deg (top) as well as $Q^2 = 0.25\,\mathrm{GeV}^2$ and $\theta' = 0.5$ deg (bottom). 75

B.1 The Feynman diagram for neutrino-nucleon interactions. 82

B.2 The Feynman diagram of the neutral current transition of the lepton. 83

B.3 The Feynman diagram of the charged current weak leptonic transition. 86

D.1 The Born diagram of $\nu n \to \mu^- K^+ \Sigma^0$ reaction channel. 95

List of Tables

2.1 The Clebsch-Gordan coefficients for structure functions f_{ijk} and d_{ijk}. 12

2.2 The mass of electron-, muon-, and tau-leptons in the units of MeV. 13

2.3 The standard model values of neutral vector and axial vector couplings coefficients. 20

2.4 The quark composition and mass of the eight 0^- mesons. 20

2.5 The quark composition and mass of the eight $\frac{1}{2}^-$ baryons. 21

2.6 Experimentally observed strange particle productions at ANL, BNL, and CERN. 21

3.1 The expression for η_l and η_h in terms of the weak coupling constant g. 32

5.1 The electromagnetic transitions among SU(3) baryon octet. 46

5.2 The matrix elements of the weak CC transition of SU(3) octet baryons. . . . 47

5.3 The determination of the standard weak form factors for CC transitions. . . . 48

6.1 The exchange particles and the corresponding propagators of the s-channel, t-channel, and u-channel. 52

6.2 Extraction of the unknown amplitudes for the $\nu n \to \mu^- K^+ \Lambda$ reaction process. 57

7.1 Physically allowed tree diagrams for the four reactions. 59

7.2 The kinematical inputs E_k and $E_{k'}$ at fixed values $Q^2 = 0.035\,\mathrm{GeV}^2$ and $\theta' = 0.5$ deg. 61

7.3 The kinematical inputs E_k and $E_{k'}$ at fixed values $Q^2 = 0.25\,\mathrm{GeV}^2$ and $\theta' = 0.5$ deg. 61

A.1 The summary of the Dirac gamma matrix properties. 79

C.1 Summary of Gordon-like identities for identical mass case 89

C.2 Summary of Gordon-like identities for different mass case 89

D.1 Extraction of the unknown amplitudes for the $\nu p \to \mu^- K^+ \Sigma^+$ reaction process. 93

D.2 Extraction of the unknown amplitudes for the $\nu n \to \mu^- K^0 \Sigma^+$ reaction process. 94

D.3 Extraction of the unknown amplitudes for the $\nu n \to \mu^- K^+ \Sigma^0$ reaction process. 95

Chapter 1

Introduction

The discovery of elementary particles and their interaction has brought about a better understanding of our universe from sub-nuclear scales to cosmological scales. In particular, the study of neutrino-nucleon weak interaction has become one of the frontiers of theoretical and experimental research in the field of astrophysics, cosmology, particle, and nuclear physics [1]. For instance, in neutrino physics the neutrino-nucleon weak interaction plays a significant role in the analysis of the neutrino oscillation experiments as well as neutrino mass [2]; in nuclear and particle physics it allows the detailed study of the strange-quark content of the nucleon [3] and the structure of the hadronic weak current [4]; in astrophysics it facilitates the investigation of supernova dynamics and energy production in the sun [5, 6].

The measurement of the strange-quark contribution to the nucleon spin and also the study of neutrino oscillation have been underway at the MiniBooNE experiment under the FINeSSE program [7, 8], which is one of the recent activities at Fermilab. In the near future experiments like Minerνa and SciBooNE will allow physicists to gain a considerable insight regarding the structure of the nucleon and the hadronic weak current via the neutrino-induced weak production of strange particles [9, 10]. However, the primary knowledge of neutrino-induced single and associated productions of strange particles comes from the experiments in the 1970's carried out at Argonne National Laboratory (ANL), Brookhaven National Laboratory (BNL), Fermi National Accelerator Laboratory (Fermilab), and CERN.

This study is done at the elementary level where spin-1/2 and spin-0 free particles can be described by the Dirac and Klein-Gordon wave equations, respectively. The main focus is the investigation of strange particle production via the weak interaction of the neutrino and nucleon near threshold energy. Since the neutrino is naturally left-handed, it is the best candidate for the study of the weak interaction. Moreover, it is a spin-1/2 and neutral

fermion which forms the SU(2) isospin doublet with the corresponding lepton. There are three generations of leptons but due to experimental reasons we only consider the weak leptonic transition of the muon isodoublet. Chapter 2 contains a brief review of the above argument.

In the mid 1970's and early 1980's, the first extensive theoretical studies of strange particle production via the weak interaction in comparison with experiment were made by Shrock [11], Mecklenburg [12], and Dewan [13]. Shrock and Mecklenburg independently studied the associated production of charged current (CC) reactions by employing the Cabibbo V-A theory with SU(3) symmetry and neutral current (NC) in the framework of the Weinberg-Salam model, whereas Dewan focused on the CC and strangeness changing ($\Delta S = 1$) strange particle production reactions. In their numerical calculation they used the method of determining the helicity amplitudes from the Born diagram and then they decomposed the norm squared invariant matrix element in terms of these amplitudes.

In the general formalism, the kinematical and dynamical descriptions of the strange particle production reactions is made in the relativistic framework. The differential cross section is constructed as the contraction between a leptonic tensor and a hadronic tensor. The kinematic part of the reactions is specified in two planes: the leptonic and the hadronic planes, for the sake of independent treatment of the leptonic and hadronic transitions. Moreover, the descriptions are made in the laboratory frame, that is the rest frame of the target nucleon. The construction of the leptonic tensor is performed via the Feynman trace technique in the framework of the electroweak theory. Similarly, the hadronic tensor is expressed as a trace of the product of matrices that involves the hadronic current operator, which is a complicated object to deal with. The detailed discussion on the kinematical and dynamical formalisms is given in chapter 3.

Unlike the leptonic transition current, there are no well developed and tested gauge theories that allow us to calculate the hadronic weak transition current. Therefore, we have developed the new model-independent approach to evaluate the invariant matrix element. Hence we derive, for the first time, the most general form of the three-body hadronic weak current operator for strange particle production based on the Dirac equation of on-shell particle and Dirac algebra. The hadronic weak transition current involves one initial state baryon and two final state hadrons: baryon and meson. The derivation is done by following the basic principles used for the derivation of the electromagnetic transition current of a fermion in terms of two form factors by Drell and Zachariasen [14]. The general expression of the current contains eighteen invariant amplitudes which fully parametrize the hadronic weak vertex. The detail of the above argument is given in chapter 4.

For the numerical calculation of the differential cross section for CC associated production, we follow similar scheme employed by Mecklenburg [12] to evaluating the tree diagrams that approximate the hadronic vertex represented by a "blob" in the generalized Feynman diagram of the reactions under consideration. As an important supplementary to chapter 6 and Appendix D in which the unknown invariant amplitudes of the weak hadronic current are extracted from the relevant Born diagrams, in chapter 5 we provide the detailed discussion of the Cabibbo V-A theory in relation to the conserved vector current hypothesis and the SU(3) predictions of the strong coupling constants. Appendix A and C contain the summary of Dirac algebra of gamma matrices and the Gordon-like identities, respectively.

A study of this kind may be used to test models and theories of the weak interaction. The representation of the weak hadronic current of the three-body processes in terms of eighteen scalar structure functions allows us to include all possible effects such as that of strong interaction. Hopefully the result of this study will motivate the undertaking of further experiments in the area of hadron physics for the detailed investigation of the quark structure of hadrons as well as in neutrino physics such as oscillation experiments for the investigation of the neutrino mass.

Chapter 2

Theoretical Overview

2.1 Dirac Spinor Fields

Consider a relativistic spin-1/2 particle with three-vector momentum $\mathbf{p}$, rest mass m, and energy E. The relativistic energy-momentum relation of the particle is given by

$$E^2 = \mathbf{p}^2 + m^2. \tag{2.1}$$

Based on the relativistic notation of four-vectors, energy and three-vector momentum gives rise to energy-momentum four-vector or four-vector momentum

$$p^\mu = (E,\, \mathbf{p}). \tag{2.2}$$

It is well established that relativistic spin-1/2 particles are described by the Dirac equation. In position space the Dirac equation for free particles is given by

$$i\frac{\partial}{\partial t}\psi(t,\mathbf{x}) = (-i\vec{\alpha}\cdot\vec{\nabla} + \beta m)\psi(t,\mathbf{x}), \tag{2.3}$$

where $\vec{\alpha}$ and β are 4×4 matrices and traditionally constructed from 2×2 Pauli matrices given in Eq. (A.1) in Appendix A and $\psi(t,\mathbf{x})$ is a wavefunction which is the four component column matrix. The solution of the Dirac equation for a free particle is

$$\psi(t,\mathbf{x}) = N_V u(\mathbf{p},s)\exp(-ix\cdot p), \tag{2.4}$$

where $u(\mathbf{p},s)$ represents the four component column matrix called the Dirac spinor and N_V is the volume normalization of the Dirac particle. Eq. (2.4) can also be rewritten in momentum space as

$$(\not{p} - m)u(\mathbf{p},s) = 0 \tag{2.5}$$

where $\not{p} = \gamma^\mu p_\mu$. We use Eq. (2.5) to derive the on-shell condition: $\not{p}^2 = p^2 = m^2$. On the other hand, off-shell particles are those which do not satisfy Eq. (2.5).

Note that Eq. (2.4) is the general solution of Eq. (2.3) and hence the spinor for positive energy solution becomes

$$u(\mathbf{p}, s) = C \begin{pmatrix} \phi^s \\ \dfrac{\vec{\sigma} \cdot \mathbf{p}}{E + m} \phi^s \end{pmatrix} \tag{2.6}$$

and the spinor for negative energy solution

$$\upsilon(\mathbf{p}, s) = C \begin{pmatrix} \dfrac{\vec{\sigma} \cdot \mathbf{p}}{E + m} \chi^s \\ \chi^s \end{pmatrix} \tag{2.7}$$

where ϕ^s and χ^s are the two component Pauli spinors representing spin states of the particle ($s = \pm\frac{1}{2}$). The normalization constant C can be determined by the condition:

$$C = \sqrt{\frac{E + m}{2m}}, \qquad \bar{u}(\mathbf{p}, s) u(\mathbf{p}, s') = \delta_{ss'}; \tag{2.8}$$

$$C = \sqrt{\frac{E + m}{2E}}, \qquad u^\dagger(\mathbf{p}, s) u(\mathbf{p}, s') = \delta_{ss'} \tag{2.9}$$

where Eq. (2.8) and (2.9) are covariant and non-covariant normalizations, respectively. The volume normalization N_V can now be determined by using the following relation

$$\psi^\dagger \psi = |N_V|^2 u^\dagger u = \rho, \tag{2.10}$$

where ρ refers to the number density of Dirac particles. If we assume that V is the normalization volume containing n number of the Dirac particles, then ρ can be written as

$$\rho = \frac{n}{V}. \tag{2.11}$$

Thus N_V would become

$$N_V = \sqrt{\frac{m}{EV} n}, \tag{2.12}$$

$$N_V = \sqrt{\frac{n}{V}} \tag{2.13}$$

for covariant and non-covariant normalizations, respectively.

2.1.1 Energy-spin projection operators

In many physics problems we might be interested in a particle with definite energy and spin states. Hence we can construct projection operators that act on the Dirac spinor fields that

allow us to specifically deal with one of the four components of the field at a time. The introduction of projection operators allows the application of the Feynman trace technique in the derivation of the invariant matrix element, which will be constructed as the contraction between the leptonic tensor and the hadronic tensor, which eliminates the cumbersome calculation procedure that requires the explicit use of gamma matrices and Dirac spinors. Thus for the Dirac particle one may write

$$u(\mathbf{p},s)\bar{u}(\mathbf{p},s) = \Lambda_+(\mathbf{p})\Sigma(s) \tag{2.14}$$

where

$$\Lambda_+ = \frac{\not{p}+m}{2E}; \qquad \Sigma(s) = \frac{I+\varepsilon_s\gamma_5\not{s}}{2} \tag{2.15}$$

which are the positive energy projection and spin projection operators, respectively, and $\varepsilon_{s=\pm\frac{1}{2}} = \pm 1$. If we sum over the spin of the particle we get

$$\sum_{s=\pm\frac{1}{2}} u(p,s)\bar{u}(p,s) = \Lambda_+(\mathbf{p}). \tag{2.16}$$

In other words, summing over all possible spin states eliminates the spin projection operator and it only takes into account the energy projection operator. Similarly for the negative energy case

$$v(\mathbf{p},s)\bar{v}(\mathbf{p},s) = -\Lambda_-(\mathbf{p})\Sigma(s), \tag{2.17}$$

where

$$\Lambda_-(\mathbf{p}) = \left(\frac{-\not{p}+m}{2E}\right). \tag{2.18}$$

Later we will use Eq. (2.16) in the derivation of the leptonic tensor and the hadronic tensor via Casimir's trick, because in this study we are considering unpolarized fermions except for the incident neutrino which naturally exists as a left-handed particle.

In the rest frame we define the polarization four-vector as $\hat{s}^\mu = (0,\, \hat{\mathbf{s}})$. In a given inertial frame where the three-momentum of the particle is $\mathbf{p}$, the Lorentz transformation of its polarization four-vector $\hat{s}^\mu$ then becomes

$$s^\mu = \left(\frac{\hat{\mathbf{s}}\cdot\mathbf{p}}{m},\ \hat{\mathbf{s}} + \frac{\hat{\mathbf{s}}\cdot\mathbf{p}}{m(E+m)}\mathbf{p}\right), \tag{2.19}$$

which satisfies the following two conditions in any frame

$$p^\mu s_\mu = 0; \tag{2.20}$$

$$s^\mu s_\mu = -1. \tag{2.21}$$

2.1.2 Helicity state

There are circumstances in which the orientation of the spin polarization is fixed specifically in the direction of the three-momentum of a particle. In such kind of situations the helicity representation of the Dirac spinor is more appropriate than the spin representation of the Dirac spinor to describe the state of the particle. In the limit of $m \ll E$ from the Dirac equation in momentum space we can derive the helicity operator and its action on the Pauli spinors with the corresponding helicity eigenstates

$$\frac{\sigma \cdot \mathbf{p}}{|\mathbf{p}|}\phi^s = +\phi^s \tag{2.22}$$

$$\frac{\sigma \cdot \mathbf{p}}{|\mathbf{p}|}\chi^s = -\chi^s \tag{2.23}$$

This can be generalized by defining helicity eigenvalues as $\lambda = \pm\frac{1}{2}$ in such a way that

$$\frac{1}{2}\frac{\vec{\sigma} \cdot \mathbf{p}}{|\mathbf{p}|}\phi^h(\hat{\mathbf{p}}) = \lambda\phi^h(\hat{\mathbf{p}}) \tag{2.24}$$

Thus the helicity state representation of Dirac spinor is given by

$$u(\mathbf{p}, h) = \sqrt{\frac{E+m}{2E}}\begin{pmatrix} \phi^h(\hat{\mathbf{p}}) \\ \dfrac{h|\mathbf{p}|}{E+m}\phi^h(\hat{\mathbf{p}}) \end{pmatrix} \tag{2.25}$$

where $h = 2\lambda$ and we have used the non-covariant normalization factor. In momentum space, the helicity operator can be written as

$$\frac{\sigma \cdot \hat{\mathbf{p}}}{2} = \sum_{i=1}^{3}\frac{\sigma_i \hat{p}_i}{2}, \qquad \hat{\mathbf{p}} = \mathbf{p}/|\mathbf{p}|. \tag{2.26}$$

Then in the spherical coordinate system, in terms of the polar angle θ and azimuthal angle φ of $\hat{\mathbf{p}}$ we get the following matrix expression of Eq. (2.26)

$$\frac{\sigma \cdot \hat{\mathbf{p}}}{2} = \frac{1}{2}\begin{pmatrix} \cos\theta & e^{-i\varphi}\sin\theta \\ e^{i\varphi}\sin\theta & -\cos\theta \end{pmatrix}. \tag{2.27}$$

Thus the normalized eigenstates of Eq. (2.27) with the corresponding eigenvalue $h = +1$ and $h = -1$ are

$$\phi^{h=+1}(\varphi,\, \theta) = \begin{pmatrix} \cos\frac{\theta}{2} \\ e^{i\frac{\varphi}{2}}\sin\frac{\theta}{2} \end{pmatrix} \quad \text{and} \quad \phi^{h=-1}(\varphi,\, \theta) = \begin{pmatrix} -e^{-i\frac{\varphi}{2}}\sin\frac{\theta}{2} \\ \cos\frac{\theta}{2} \end{pmatrix}. \tag{2.28}$$

Notice that in the rest frame of the particle the polarization three-vector is $\hat{\mathbf{s}} = h\mathbf{p}/|\mathbf{p}|$. If we set the polar angle θ and azimuthal angle φ to zero, we recover

$$\phi^{h=+1}(0,\, 0) = \begin{pmatrix} 1 \\ 0 \end{pmatrix}; \qquad \phi^{h=-1}(0,\, 0) = \begin{pmatrix} 0 \\ 1 \end{pmatrix} \tag{2.29}$$

Based on Eq. (2.19) for the particle having spin orientation along its three-momentum $\mathbf{p}$, one can show that the polarization four-vector s^μ becomes

$$s^\mu = \frac{1}{m}\left(\hat{\mathbf{s}}\cdot\mathbf{p},\ E\frac{\mathbf{p}}{|\mathbf{p}|}\right). \tag{2.30}$$

Here it is worth noting that we have replaced ε_s with $h = \pm 1$. In case when $m \to E$, one can show that

$$s^\mu \to \frac{p^\mu}{m} \tag{2.31}$$

Now we redefine the projection operator in terms of the helicity representation

$$\frac{\not{p}+m}{2E}\ \frac{I+h\gamma_5\not{s}}{2} = \frac{1}{4E}(\not{p}I + h\not{p}\gamma_5\not{s} + mI + h\gamma_5 m\not{s}). \tag{2.32}$$

By using the anti-commutation relation of gamma matrices given in Appendix A we find that

$$\begin{aligned}\not{p}\gamma_5\not{s} &= \gamma_5\not{s}\not{p}\\ &= \gamma_5(2g^{\mu\nu} - \gamma^\nu\gamma^\mu)s_\mu p_\nu\\ &= 2\gamma_5 s^\nu p_\nu - \gamma_5\not{s}\not{p}\\ &= \gamma_5 s^\nu p_\nu.\end{aligned} \tag{2.33}$$

However, due to Eq. (2.20) we immediately notice that $\not{p}\gamma_5\not{s} = 0$. Moreover, in the limit $m \to 0$, Eq. (2.31) can be rewritten as $m\not{s} \simeq \not{p}$ and hence the projection operator in Eq. (2.32) becomes

$$\Lambda_+(\mathbf{p})\Sigma(h) \ = \frac{\not{p}}{2E}\ \frac{I-h\gamma_5}{2}. \tag{2.34}$$

For instance in the weak interaction only left-handed neutrinos participate. For a neutrino with four-momentum k^μ, the projection operator is given by

$$\nu(\mathbf{k},\,h)\bar{\nu}(\mathbf{k},\,h) = \Lambda_+(\mathbf{k})\Sigma(h=-1) = \frac{\not{k}}{2E}\ \frac{I+\gamma_5}{2}, \tag{2.35}$$

where ν is the Dirac spinor of the neutrino.

2.2 The SU(3) flavour quark model

In 1964, Gell-Mann and Zweig [15, 16], independently, introduced the classification of mesons and baryons using group theory. They used the SU(3) scheme based on three quark flavours up-, down-, and strange-quark. The group SU(3) is the three dimensional generalization of SU(2) of up-and down-quarks by including strange-quark; and hence the new quantum number called Strangeness is introduced to the symmetric group of strongly interacting particles. In addition, the s-quark is also characterized by isotopic spin. Note that SU(3) contains two

fundamental representations 3 and $\bar{3}$: the former contains the three quarks and the later contains the corresponding antiquarks. Fig. 2.1 shows the weight diagram of 3 and $\bar{3}$. Due to the mass difference amongst the quark flavours and also the existence of other flavours such as charm-, top-, and bottom-quarks, it has been found that the SU(3) flavour quark is not an exact symmetry of nature.

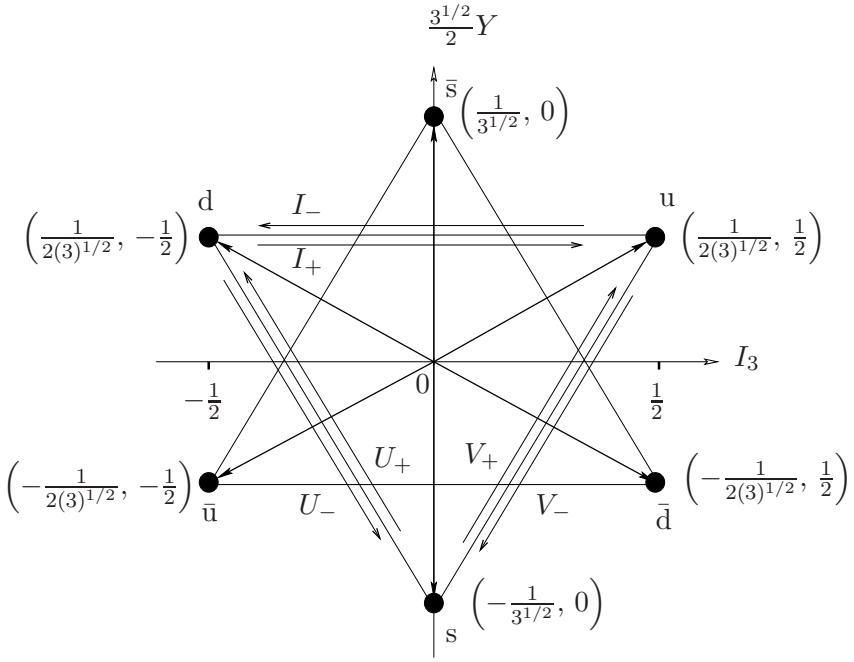

Fig. 2.1: The fundamental SU(3) triplets of quark and antiquark with the action of the step operators.

Let q be the three-component quark field

$$q = \begin{pmatrix} u \\ d \\ s \end{pmatrix} \tag{2.36}$$

where u, d, and s are the Dirac spinor fields of up-, down-, and strange-quarks. The Lagrangian of this field, by ignoring the mass difference, is defined as

$$\mathcal{L} = \bar{q}(x)(i\partial\!\!\!/ - m)q(x), \tag{2.37}$$

where m is the quark mass. All 3-dimensional unimodular and unitary matrices whose action on q leave $\mathcal{L}$ unchanged or invariant forms the group SU(3). Let $U \in \text{SU}(3)$, hence it can be written as:

$$U = \exp(i\Lambda) \tag{2.38}$$

where Λ is a linear combination of eight independent 3×3 traceless matrices. Hence

$$U(\vartheta) = \exp\left(i \sum_{i=1}^{8} \vartheta_i \frac{\lambda_i}{2}\right) \tag{2.39}$$

where $\{\vartheta_i\}_{i=1}^{8}$ are real parameters and $\{\lambda_i\}_{i=1}^{8}$ are called the generators of SU(3) group and a standard choice is [17]

$$\begin{aligned}
\lambda_1 &= \begin{pmatrix} 0 & 1 & 0 \\ 1 & 0 & 0 \\ 0 & 0 & 0 \end{pmatrix}, \quad \lambda_2 = \begin{pmatrix} 0 & -i & 0 \\ i & 0 & 0 \\ 0 & 0 & 0 \end{pmatrix}, \quad \lambda_3 = \begin{pmatrix} 1 & 0 & 0 \\ 0 & -1 & 0 \\ 0 & 0 & 0 \end{pmatrix}, \\
\lambda_4 &= \begin{pmatrix} 0 & 0 & 1 \\ 0 & 0 & 0 \\ 1 & 0 & 0 \end{pmatrix}, \quad \lambda_5 = \begin{pmatrix} 0 & 0 & -i \\ 0 & 0 & 0 \\ i & 0 & 0 \end{pmatrix}, \quad \lambda_6 = \begin{pmatrix} 0 & 0 & 0 \\ 0 & 0 & 1 \\ 0 & 1 & 0 \end{pmatrix}, \\
\lambda_7 &= \begin{pmatrix} 0 & 0 & 0 \\ 0 & 0 & -i \\ 0 & i & 0 \end{pmatrix}, \quad \lambda_8 = \frac{1}{3^{1/2}} \begin{pmatrix} 1 & 0 & 0 \\ 0 & 1 & 0 \\ 0 & 0 & -2 \end{pmatrix}.
\end{aligned} \tag{2.40}$$

The quark flavours combine in a specific pattern to form many-quark system such as three-quark or quark-antiquark systems that reproduce the same quantum numbers of the well know hadronic particles. In an other word, higher dimensional representations such as the baryons and mesons octets of SU(3) can be built out of the Kronecker product of the fundamental representations [18, p. 116]. For instance, the Kronecker product of 3 and $\bar{3}$, $3 \otimes \bar{3} = 8 \dot{+} 1$, allows the construction of higher dimensional multiplets of particles composed of quark-antiquark pairs. The 8 (octet) representation is the multiplet that contains eight mesons with $B = 0$ and $J^\pi = 0^-$ and is called the pseudoscalar meson octet. The construction of the octet representation by using the the weight diagrams is shown in Fig. 2.2.

In a similar fashion, the Kronecker product of three fundamental quark representations generates the baryon multiplets (i.e., $3 \otimes 3 \otimes 3 = 10 \dot{+} 8 \dot{+} 8 \dot{+} 1$); because of its relevance to our problem we choose only the baryon octet containing eight bound state particles with $B = 1$ and $J^\pi = \frac{1}{2}^+$ (see Fig. 2.3). In this irreducible representation, (p, n) and (Ξ^0, Ξ^-) form isospin doublets; whereas (Σ^+, Σ^0, Σ^-) form an isospin triplet. Moreover, Λ is an isospin singlet.

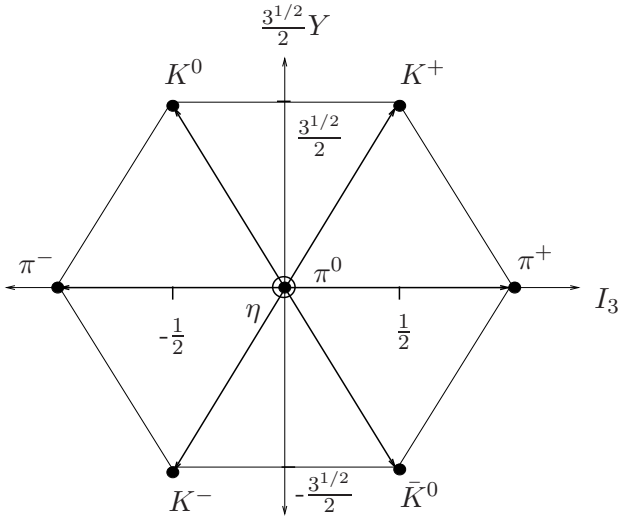

Fig. 2.2: The octet of pseudoscalar-mesons which is constructed from 3(quark) and $\bar{3}$(antiquark) of SU(3) representations by using the weight diagrams.

2.2.1 SU(3) Current Octet

Now one can construct the step operators as follows

$$\begin{aligned} I_{\pm} &= \frac{\lambda_1 \pm i\lambda_2}{2}, \\ U_{\pm} &= \frac{\lambda_6 \pm i\lambda_7}{2}, \\ V_{\pm} &= \frac{\lambda_4 \pm i\lambda_5}{2}. \end{aligned} \tag{2.41}$$

Since λ_i are members of the SU(3) group, their algebra closes under the commutation relation

$$\left[\frac{\lambda_i}{2},\ \frac{\lambda_j}{2}\right] = if_{ijk}\frac{\lambda_k}{2} \tag{2.42}$$

where f_{ijk} are the anti-symmetric structure constants of SU(3). They also satisfy the following anti-commutation relation

$$\{\lambda_i,\ \lambda_j\} = \frac{4}{3}\delta_{ij}I + 2d_{ijk}\lambda_k \tag{2.43}$$

where d_{ijk} are the symmetric structure constants of SU(3). Note that f_{ijk} and d_{ijk} are the SU(3) Clebsch-Gordan coefficients summarized in Table 2.1 [19, p. 214]. In general, the transition current of the baryons that belong to the SU(3) octet also form an SU(3) symmetry group.

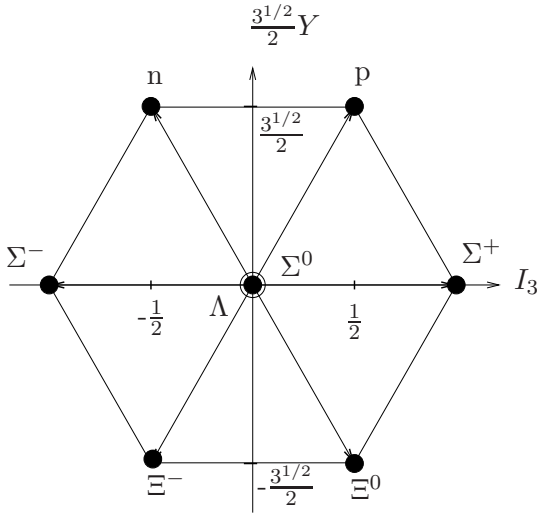

Fig. 2.3: The SU(3) octet representation of the ground state baryons.

Table. 2.1: The Clebsch-Gordan coefficients for structure functions f_{ijk} and d_{ijk}.

ijk	f_{ijk}	ijk	d_{ijk}	ijk	d_{ijk}
123	1	118	$1/\sqrt{3}$	366	$-1/2$
147	$1/2$	146	$1/2$	377	$-1/2$
156	$-1/2$	157	$1/2$	448	$-1/2\sqrt{3}$
246	$1/2$	228	$1/\sqrt{3}$	558	$-1/2\sqrt{3}$
257	$1/2$	247	$-1/2$	668	$-1/2\sqrt{3}$
345	$1/2$	256	$1/2$	778	$-1/2\sqrt{3}$
367	$-1/2$	338	$1/\sqrt{3}$	888	$-1/2\sqrt{3}$
458	$\sqrt{3}/2$	344	$1/2$		
678	$\sqrt{3}/2$	355	$1/2$		

2.3 Weak Interaction

Fermi for the first time established the phenomenological study of weak interaction by using β decay. However, his theory of vector current interaction which he developed in analogy to the theory of quantum electrodynamics (QED) of the electromagnetic interaction, was found to be inconsistent with experiment. In his analogous approach he treated the β decay of the nucleon as a point interaction which disregarded the fact that the electromagnetic interaction takes place via the exchange of the vector gauge boson called the photon. Later the modification of Fermi's theory was made by the introduction of the massive gauge bosons, which is the reason for the weak interaction to be of short-range type.

The weak interaction is well distinguishable among the four fundamental interactions in that it violates parity. Parity violation was, for the first time, predicted by T. D. Lee and C. N. Yang in 1956 and then in 1957 C. S. Wu found the first experimental evidence of violation of parity by using nuclear beta-decay [20, 21]. In addition, in the weak interaction the quark flavour and isospin quantum numbers are not conserved as well. It has been well established that the violation of parity by the weak interaction is described by the vector - axial (V-A) form of the weak current operator. For a particle that has the spin orientation along the direction of the motion, the general Dirac equation of the particle contains both helicity states that can be separated using the projection operators.

$$\mathcal{P}_L = \frac{1}{2}(I - \gamma^5); \qquad \mathcal{P}_R = \frac{1}{2}(I + \gamma^5) \tag{2.44}$$

For instance, in the neutrino-induced weak interaction the violation of parity conservation arises from the strict selection of left-handed neutrino. Based on experimental observation leptons are classified by using SU(2) weak isospin symmetry in to three generations as

$$\begin{pmatrix} e \\ \nu_e \end{pmatrix}; \quad \begin{pmatrix} \mu \\ \nu_\mu \end{pmatrix}; \quad \begin{pmatrix} \tau \\ \nu_\tau \end{pmatrix}. \tag{2.45}$$

Weak transition is allowed only within an isodoublet. That means there does not exist weak transition across generations. The neutrinos belonging to the three isodoublets are considered to be massless; the mass of electron-, muon-, and tau-leptons are given in Table. 2.2.

Table. 2.2: The mass of electron-, muon-, and tau-leptons in the units of MeV.

Lepton	e	μ	τ
Mass	0.511	105.66	1784.1

In general, there are three kinds of weak transitions: pure leptonic, semi-leptonic, and non-leptonic. The weak transitions which involve hadrons are parametrized by form factors in order to incorporate the effects that arise from their spatial structure and strong interactions. But the weak interaction can be studied at the quark level in order to obtain a better picture of what is going on at the hadronic level. On the fundamental level it is the quark weak current that couples to the gauge boson. Like leptons, quarks are also of three generations

$$\begin{pmatrix} u \\ d \end{pmatrix}, \quad \begin{pmatrix} c \\ s \end{pmatrix}, \quad \begin{pmatrix} t \\ b \end{pmatrix}. \tag{2.46}$$

However, from experimental observations the universality of the weak interaction is violated in the semi-leptonic transitions. That is, strangeness changing ($\Delta S = 1$) CC processes are suppressed by a factors of $\tan^2\theta_c$ with respect to the strangeness conserving ($\Delta S = 0$) CC ones[1]. In 1963, Cabibbo restored the universality of weak coupling by proposing that the weak interaction eigenstates of up-, down-, and strange-quarks are not the same as that of the strong interaction eigenstates [22]. Thus he hypothesised that the eigenstates of weak interaction are obtained by taking the superposition of the strong interaction ones. That is, there exists cross-generation in the coupling involving the three quark flavours. Note that θ_c is the Cabibbo mixing angle; the experimental estimation of this parameter is 13.1 deg [23, p. 318]. By including this factor one can restore the universality of weak coupling at the hadronic vertex [24].

Therefore, we can build the weak isospin doublets for the SU(3) quark flavours by using the following isospin rotation:

$$\begin{pmatrix} d_c \\ s_c \end{pmatrix} = \begin{pmatrix} \cos\theta_c & \sin\theta_c \\ -\sin\theta_c & \cos\theta_c \end{pmatrix} \begin{pmatrix} d \\ s \end{pmatrix}, \tag{2.47}$$

where d_c and s_c are the Cabibbo "rotated" quarks; and hence the weak eigenstates become

$$\begin{pmatrix} u \\ d_c \end{pmatrix} = \begin{pmatrix} u \\ d\cos\theta_c + s\sin\theta_c \end{pmatrix}, \quad \begin{pmatrix} c \\ s_c \end{pmatrix} = \begin{pmatrix} c \\ -d\sin\theta_c + s\cos\theta_c \end{pmatrix}. \tag{2.48}$$

In a similar fashion to the leptons, the charged current weak transitions of the quarks are shown in Fig. 2.4. Thus the current operator for Fig. 2.4 (a) is

$$J^{\mu}_{d\to u}(\Delta S = 0) = \frac{-ig}{2\sqrt{2}}\bar{u}_u\gamma^{\mu}(1-\gamma^5)u_d\cos\theta_c \qquad \text{(Cabibbo favoured)} \tag{2.49}$$

and the current operator for Fig. 2.4 (b) is

$$J^{\mu}_{s\to u}(\Delta S = 1) = \frac{-ig}{2\sqrt{2}}\bar{u}_u\gamma_{\mu}(1-\gamma^5)u_s\sin\theta_c \qquad \text{(Cabibbo suppressed).} \tag{2.50}$$

2.4 Electromagnetic Current in SU(2) Framework

In the absence of electromagnetic field, the proton and neutron display more or less similar behaviour. Hence they can be treated as two different states of a single particle known as a nucleon. This treatment is developed in analogy with the spin state of a fermion. Let us

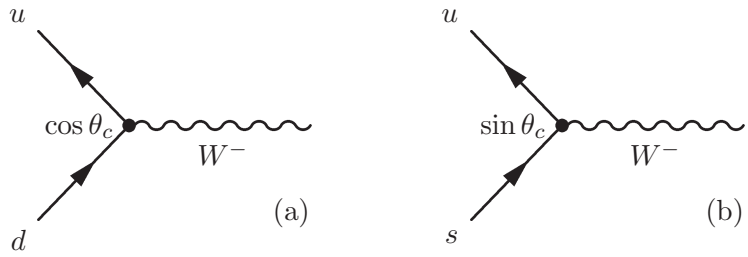

Fig. 2.4: The weak quark currents: (a) refers to the strangeness conserving transition, $d \to u$; whereas (b) represents the strangeness changing transition, $s \to u$.

construct the eight dimensional spinor field u_N (which is called the two-component isospinor) of the nucleon from the four dimensional proton and neutron spinor fields. That is

$$u_N = \begin{pmatrix} \tilde{u}_p \\ \tilde{u}_n \end{pmatrix} \tag{2.51}$$

where $\tilde{u}_p$ and $\tilde{u}_n$ are the Dirac spinors of the proton and neutrino, respectively. In general, Eq. (2.51) is called an SU(2) isospin doublet state (i.e., it behaves like a two dimensional spinor field in isospin space). Hence, one can apply the SU(2) algebra to describe the dynamics of the nucleon. Let $\tilde{\tau}_1$, $\tilde{\tau}_2$, and $\tilde{\tau}_3$ be the 2×2 Pauli matrix representations (given in Appendix A Eq. (A.1)) which generate all the algebraic structure of SU(2) symmetry group; and also $\tilde{\gamma}^\mu$ and $\tilde{\gamma}_5$ are the standard 4×4 Dirac gamma matrices which are defined in Appendix A Eq. (A.3). Note that they may have the 8×8 matrix representations which can be constructed by taking their Kronecker product. That is

$$\gamma^\mu = I_2 \otimes \tilde{\gamma}^\mu. \tag{2.52}$$

In the presence of the electromagnetic field, the neutron does not have a current that couples to the photon (the gauge field of QED) due to its zero charge quantum number unlike the proton. Moreover, electromagnetic transition always preserves charge quantum number unlike the weak interaction. Now we can define the eight dimensional spinor field $\tilde{u}_p$ of the proton by using the isospin projection operator as

$$u_p = \hat{P}_+ \begin{pmatrix} \tilde{u}_p \\ \tilde{u}_n \end{pmatrix} = \frac{I_8 + \tau_3}{2} \begin{pmatrix} \tilde{u}_p \\ \tilde{u}_n \end{pmatrix} = \begin{pmatrix} \tilde{u}_p \\ 0 \end{pmatrix} \tag{2.53}$$

where I_i are $i \times i$ identity matrices and τ_i are the eight dimensional extensions of the Pauli matrices which would be built as

$$\tau_i = \tilde{\tau}_i \otimes I_4; \quad i = 1, 2, 3, \tag{2.54}$$

and hence

$$\tau_1 = \begin{pmatrix} 0 & I_4 \\ I_4 & 0 \end{pmatrix}; \quad \tau_2 = \begin{pmatrix} 0 & -iI_4 \\ iI_4 & 0 \end{pmatrix}; \quad \tau_3 = \begin{pmatrix} I_4 & 0 \\ 0 & -I_4 \end{pmatrix}, \tag{2.55}$$

from which one may also construct the isospin operators of SU(2) algebra

$$\tau_\pm = \frac{\tau_1 \pm i\tau_2}{2}. \tag{2.56}$$

The electromagnetic transition current of the point proton can therefore be written as

$$\begin{aligned} J^\mu_{em} = \quad \overline{u}_p \gamma^\mu u_p \quad &= (\hat{P}_+ u_N)^\dagger \gamma_0 \gamma^\mu \hat{P}_+ u_N \\ &= \overline{u}_N \gamma^\mu \hat{P}_+ u_N \end{aligned} \tag{2.57}$$

where the following identities are used

$$\gamma_0 \hat{P}^\dagger_+ \gamma_0 = \hat{P}_+; \;\; \hat{P}_+ \gamma^\mu = \gamma^\mu \hat{P}_+; \text{ and } \hat{P}^2_+ = \hat{P}_+. \tag{2.58}$$

One can explicitly write Eq. (2.57) in terms of two components: isoscalar current and isovector current, as follows

$$J^\mu_{em} = \overbrace{\overline{u}_N \gamma^\mu \frac{I}{2} u_N}^{\text{Isoscalar}} + \overbrace{\overline{u}_N \gamma^\mu \frac{\tau_3}{2} u_N}^{\text{Isovector}}, \tag{2.59}$$

Therefore, one may deduce that the electromagnetic transition current of hadrons can always be written as the sum of the isoscalar current (which is invariant under SU(2) transformation) and isovector current (which transforms as the third component of isotriplet vector of current operator) components in the following form

$$J^\mu_{em} = J^\mu_{IS} + J^\mu_{IV} \tag{2.60}$$

where J^μ_{IS} and J^μ_{IV} are the generalized forms of isoscalar and isovector components of the electromagnetic current. The expression in Eq. (2.60) is applicable to the electromagnetic transition of composite hadrons which are characterized by parametrization form factors. The importance of Eq. (2.60) is that it holds true not only for the proton but also the neutron in that the values of their form factors can easily be extracted from experiment [19, p. 74].

In terms of the Dirac and Pauli form factors of the nucleon, the proton electromagnetic transition can be written as

$$J^\mu_{em} = \bar{u}_p \left\{ \frac{1}{2}(F_1^{IS} + F_1^{IV})\gamma^\mu + \frac{1}{2}\frac{i(F_2^{IS} + F_2^{IV})}{2M}\sigma^{\mu\nu} q_\nu \right\} u_p \tag{2.61}$$

which gives the electromagnetic form factor of the proton as

$$f_{1,2}^{p} = \frac{F_{1,2}^{IS} + F_{1,2}^{IV}}{2}. \tag{2.62}$$

Note that the SU(2) ladder operator τ_- defined in Eq. (2.56) flips the nucleon from the proton state, $\left|\{I = \frac{1}{2}; I_3 = \frac{1}{2}\}\right\rangle$, to the neutron state, $\left|\{I = \frac{1}{2}; I_3 = -\frac{1}{2}\}\right\rangle$, by leaving the sign of the isoscalar part unchanged. However, the sign of the isovector part changes by the transformation. Thus the electromagnetic transition form factors of the neutron become

$$f_{1,2}^{n} = \frac{F_{1,2}^{IS} - F_{1,2}^{IV}}{2}. \tag{2.63}$$

Eq. (2.62) and (2.63) allow us to write F^{IS} and F^{IV} in terms f^p and f^n

$$\begin{aligned} F_{1,2}^{IS} &= f_{1,2}^{p} + f_{1,2}^{n} \\ F_{1,2}^{IV} &= f_{1,2}^{p} - f_{1,2}^{n} \end{aligned} \tag{2.64}$$

Hence Eq. (2.59) may be modified as

$$\begin{aligned} J_{em}^{\mu} &= \bar{u}_N \left\{ F_1^{IS}\gamma^{\mu} + \frac{iF_2^{IS}}{2M}\sigma^{\mu\nu}q_{\nu} \right\} \frac{I}{2} u_N \\ &+ \bar{u}_N \left\{ F_1^{IV}\gamma^{\mu} + \frac{iF_2^{IV}}{2M}\sigma^{\mu\nu}q_{\nu} \right\} \frac{\tau_3}{2} u_N \end{aligned} \tag{2.65}$$

Note also that $\{\tau_+, \tau_-, \tau_3\}$ forms the fundamental SU(2) basis for any vector current operator in isospin space. We later notice that via the conserved vector current hypothesis, the fundamental weak vector form factor of the SU(3) octet baryon transition is determined from the isovector form factor of the electromagnetic transition.

2.5 Electroweak Gauge Theory

The electroweak (GSW) theory of Glashow, Salam, and Weinberg describes the weak and electromagnetic interactions in a single and unified gauge theory in the framework of the gauge principle. In 1961 Glashow introduced a model which has the SU(2) × U(1) gauge symmetry. Then Weinberg and Salam proposed the Higgs mechanism which is associated with the mass generation of the vector gauge boson. This theory implies that there exists the neutral gauge boson Z^0 which in turn indicates the presence of neutral weak current.

In the gauge model of the electroweak interactions SU(2) refers to the weak isospin, and U(1) refers to weak hypercharge; $\tau = (\tau^1, \tau^2, \tau^3)$ is an isospin operator and $\tau^i (i = 1, 2, 3)$ are the generators of SU(2) group. For individual generators τ^i we associate vector gauge fields W_{μ}^{i}

which are the three components of $\mathbf{W}_\mu$ (i.e., $\mathbf{W}_\mu = (W^1_\mu, W^2_\mu, W^3_\mu)$) in isospin space. Note that $\mathbf{W}_\mu$ may represent three massless gauge bosons W^+, W^-, W^0, where

$$W^\pm_\mu = \frac{1}{\sqrt{2}}(W^1_\mu \pm iW^2_\mu) \tag{2.66}$$

$$W^0_\mu = W^3_\mu. \tag{2.67}$$

The SU(2) × U(1) Lagrangian is

$$\mathcal{L} = \bar{\psi} i\gamma^\mu D_\mu \psi - \frac{1}{4}\mathbf{W}_{\mu\nu} \cdot \mathbf{W}^{\mu\nu} - \frac{1}{4}B_{\mu\nu}B^{\mu\nu} \tag{2.68}$$

where

$$D_\mu = \partial_\mu - ig\vec{\tau} \cdot \mathbf{W}_\mu - i\frac{g'}{2}YB_\mu \tag{2.69}$$

$$\mathbf{W}_{\mu\nu} = \partial_\mu \mathbf{W}_\nu - \partial_\nu \mathbf{W}_\mu - g\mathbf{W}_\mu \times \mathbf{W}_\nu \tag{2.70}$$

$$B_{\mu\nu} = \partial_\mu B_\nu - \partial_\nu B_\mu. \tag{2.71}$$

In the unified gauge theory, left-handed structure of charged current couplings needs to be implemented. The basic electroweak interaction term of the Lagrangian in Eq. (2.68) is therefore

$$\begin{aligned} \mathcal{L}_{int} &= g(\bar{\psi}\gamma^\mu \vec{\tau}\psi)\mathbf{W}_\mu + \frac{g'}{2}(\bar{\psi}\gamma^\mu Y\psi)B_\mu) \\ &= g\mathbf{J}^\mu \cdot \mathbf{W}_\mu + \frac{g'}{2}J^\mu_Y B_\mu, \end{aligned} \tag{2.72}$$

where $\mathbf{J}^\mu = (J^\mu_1, J^\mu_2, J^\mu_3)$ and J^μ_Y are weak isospin and hypercharge currents and g and g' are the corresponding couplings to the weak isotriplet of the intermediate vector bosons, $\mathbf{W}$, and an isosinglet intermediate vector boson, B, respectively. Since the weak hypercharge is defined as $Q = I_3 + (1/2)Y$, the weak hypercharge current, J^μ_Y, becomes

$$J^\mu_{em} = J^\mu_3 + \frac{1}{2}J^\mu_Y, \tag{2.73}$$

where J^μ_{em} and J^μ_3 are the electromagnetic current and the third component of the weak isospin current, respectively. In fact, the masses of the bosons are generated by means of symmetry breaking; the two neutral fields W^3_μ and B^μ mix in such a way that two physical states (i.e., the mass eigenstates) would evolve

$$A_\mu = B_\mu \cos\theta_W + W^3_\mu \sin\theta_W \tag{2.74}$$

$$Z_\mu = -B_\mu \sin\theta_W + W^3_\mu \cos\theta_W \tag{2.75}$$

where A^μ and Z^μ are electromagnetic (massless) and neutral weak (massive) gauge fields, respectively; and θ_W is the Weinberg or the weak mixing angle, which is not predicted by this

model but instead needs to be measured from experiment. Using the definition $g' = g\tan\theta_W$,

$$B_\mu = \frac{-g'Z_\mu + gA_\mu}{(g^2+g'^2)^{1/2}} \tag{2.76}$$

$$W^3_\mu = \frac{gZ_\mu + g'A_\mu}{(g^2+g'^2)^{1/2}}. \tag{2.77}$$

Therefore, we can rewrite the electroweak interaction Lagrangian in terms of $J^\mu_\pm = J^\mu_1 \pm iJ^\mu_2$, J^μ_3, and J^μ_Y [23, 25]

$$\begin{aligned}\mathcal{L}_{int} &= g\left[\frac{1}{\sqrt{2}}J^\mu_+W^+_\mu + \frac{1}{\sqrt{2}}J^\mu_-W^-_\mu\right] \\ &+ \left[g\cos\theta_W J^\mu_3 - \frac{g'}{2}\sin\theta_W J^\mu_Y\right]Z_\mu \\ &+ \left[g\sin\theta_W J^\mu_3 + \frac{g'}{2}\cos\theta_W J^\mu_Y\right]A_\mu\end{aligned} \tag{2.78}$$

where the first, second, and third terms represent weak charged, weak neutral, and electromagnetic currents, respectively. From QED the electromagnetic coupling is $eJ^\mu_{em}A_\mu$, where e is the elementary charge. Thus the following relation between the weak and electromagnetic coupling constants may be found

$$g\sin\theta_W = g'\cos_W = e. \tag{2.79}$$

For the weak neutral current we define

$$g_z = \frac{g}{\cos\theta_W} = \frac{e}{\cos\theta_W\sin\theta_W}. \tag{2.80}$$

Thus

$$\mathcal{L}_{int} = \frac{g}{\sqrt{2}}\left[J^\mu_+W^+_\mu + J^\mu_-W^-_\mu\right] + g_z\left[J^\mu_3 - \sin^2\theta_W J^\mu_{em}\right]Z_\mu + eJ^\mu_{em}A_\mu. \tag{2.81}$$

Hence a coupling of a given elementary fermion with the gauge boson can be determined form Eq. (2.81). The vertex factor for charged currents of the underlying lepton and quark processes always maintain pure universal V-A form

$$\frac{-ig}{2\sqrt{2}}\gamma^\mu(I-\gamma_5), \tag{2.82}$$

whereas neutral currents are no longer of pure V-A form but instead can be generalized as

$$\frac{-ig_z}{2}\gamma^\mu(c^f_V - c^f_A\gamma_5), \tag{2.83}$$

where the coefficients c^f_V and c^f_A depend of the particular quark or lepton involved. The standard GSW theory determines the values of these coefficients in terms of the Weinberg angle, θ_W, and summarized in Table. 2.3

Table. 2.3: The standard model values of neutral vector and axial vector couplings coefficients.

Fermion	c_V^f	c_A^f
ν_e, ν_μ, ν_τ	1/2	1/2
e, μ, τ	-1/2 + 2 sin θ_W	-1/2
u, c, t	1/2 − (4/3) sin^2 θ_W	1/2
d, s, b	-1/2 + (2/3) sin^2 θ_W	-1/2

2.6 Strange particle production

The production of strange particles via neutrino-nucleon weak interaction involves leptons and hadrons and hence it is a semi-leptonic process. In the standard model, hadrons are described as the bound states of quarks. As mentioned before, this study is based on SU(3) symmetry that takes into account three quark flavours: up-, down-, and strange-quarks. The Standard model classifies hadrons into two families: mesons and baryons. If the final state of the reaction contains a pair of strange particles: one from $\{K^0, K^+\}$ with $S = 1$ and another from $\{\Lambda, \Sigma^0, \Sigma^\pm\}$ with $S = -1$, then it is called associated production. This kind of reaction channel can be induced by both CC and NC. On the other hand, we may also have the final state with only a single strange particle (commonly pseudoscalar meson), whereas the other hadron in the final channel may possibly be a nucleon having $S = 0$. The quark structure and masses of the pseudoscalar mesons ($J^\pi = 0^-$) and baryons ($J^\pi = \frac{1}{2}^+$) are summarized in Table. 2.4 and 2.5 [26].

Table. 2.4: The quark composition and mass of the eight 0^- mesons.

Meson	Composition	Mass (GeV)
π^+	$u\bar{d}$	0.140
π^0	$(u\bar{u} + d\bar{d})/\sqrt{2}$	0.135
π^-	$\bar{u}d$	0.140
K^+	$u\bar{s}$	0.494
K^0	$d\bar{s}$	0.498
$\bar{K}^0$	$\bar{d}s$	0.498
K^-	$\bar{u}s$	0.494
η	$(u\bar{u} + d\bar{d} - 2s\bar{s})/\sqrt{6}$	0.549

In 1970's and 80's the cross sections of strange-particle production reactions were measured

Table. 2.5: The quark composition and mass of the eight $\frac{1}{2}^-$ baryons.

Baryon	Composition	Mass (GeV)
p	uud	0.938
n	udd	0.940
Σ^+	uus	1.189
Σ^0	uds	1.192
Σ^-	dds	1.197
Ξ^0	uss	1.321
Ξ^-	dss	1.315
Λ	uds	1.116

at ANL, BNL, and CERN by using bubble chamber experiments [27]. Listed in Table. 2.6 are some of the neutrino-induced strange particle production reactions [9, 28].

Table. 2.6: Experimentally observed strange particle productions at ANL, BNL, and CERN.

Reaction channel CC, $\Delta S = 0$	Reaction channel CC, $\Delta S = 1$	Reaction channel NC
$\nu_\mu + \mathrm{p} \rightarrow \mu^- + K^+ + \Sigma^+$	$\nu_\mu + \mathrm{p} \rightarrow \mu^- + K^+ + \mathrm{p}$	$\nu_\mu + \mathrm{p} \rightarrow \nu + K^0 + \Sigma^+$
$\nu_\mu + \mathrm{n} \rightarrow \mu^- + K^0 + \Sigma^+$	$\nu_\mu + \mathrm{n} \rightarrow \mu^- + K^0 + \mathrm{p}$	$\nu_\mu + \mathrm{p} \rightarrow \nu + K^+ + \Sigma^0$
$\nu_\mu + \mathrm{n} \rightarrow \mu^- + K^+ + \Sigma^0$		$\nu_\mu + \mathrm{p} \rightarrow \nu + K^+ + \Lambda$
$\nu_\mu + \mathrm{n} \rightarrow \mu^- + K^+ + \Lambda$		$\nu_\mu + \mathrm{n} \rightarrow \nu + K^+ + \Sigma^-$
		$\nu_\mu + \mathrm{n} \rightarrow \nu + K^0 + \Sigma^0$
		$\nu_\mu + \mathrm{n} \rightarrow \nu + K^0 + \Lambda$

Chapter 3

General Formalism

To date the most formal way of theoretical and experimental investigations of the interaction of particles are the derivation and measurement of the cross sections, respectively. In relativistic quantum mechanics it is possible and convenient to treat the kinematical process and the dynamical process, separately. The kinematics is developed in the relativistic framework in the rest frame of the target (i.e., the laboratory frame of reference). It contains information of the phase space available for the reaction processes under question. On the other hand, the Feynman rules are used to derive the invariant amplitude (which carries all the dynamical information) from the appropriate Feynman diagrams that describe the process.

The general form of the reaction we consider is given by

$$\nu(k,h) + N(p_1,s_1) \rightarrow \begin{pmatrix} \nu_\mu \\ \mu \end{pmatrix} (k',h') + K(p_1') + Y(p_2',s_2'), \tag{3.1}$$

where ν and N are the initial neutrino and nucleon, respectively and K and Y are the final state pseudoscalar K-meson and hyperon, respectively. The final state lepton is either muon-neutrino or muon and we label it from now on by l. Moreover, k, p_1, k', p_1', p_2' are the corresponding four-momenta; s_1, s_2' are spin polarization four vectors; and h and h' specify helicity states of the participating leptons. As mentioned in chapter 2, the neutrino is assumed to be massless. Let m_l, M, M_K, and M_Y be the masses of final lepton, nucleon, K-meson, and hyperon, respectively. As a consequence of gauge theory, such a reaction is mediated by the gauge boson denoted by $W \in \{W^{\pm}, Z^0\}$. The lowest order Feynman diagram for this reaction is given in Fig. 3.1

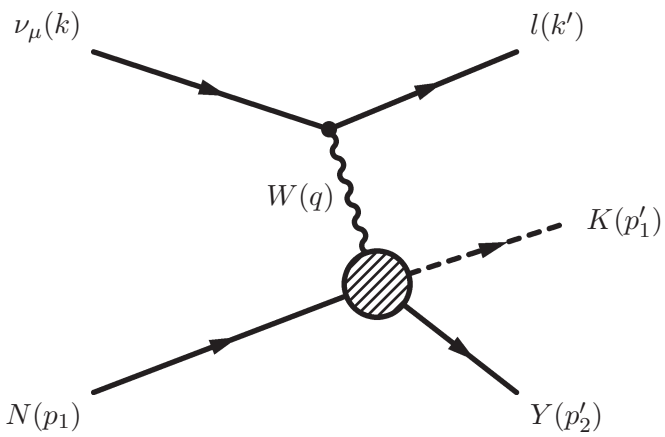

Fig. 3.1: The lowest order Feynman diagram of neutrino-induced weak production of strange particles at the hadronic level.

3.1 Kinematic Description

It is more convenient to describe the kinematics in two planes: a leptonic (scattering) plane and a hadronic (production) plane (Fig. 3.2). The leptonic xz-plane contains the incoming neutrino and the outgoing lepton. The gauge boson, that mediates the interaction, has the three-vector momentum transfer directed along the z-axis. The hadronic plane is defined in such a way that it is the SO(3) transformation of the leptonic plane about the z-axis by an angle ϕ and it contains the hadronic final state particles produced by the neutrino incident on the target nucleon. It is worth noting the kinematics of the differential cross section depends on the masses, energies, and momenta of the particles involved in the interaction. This dependence would be shown in the general expression of the phase space factor.

The four-vector momenta can conventionally can be written in the following relativistic notation.

$$k^\mu = (E_k, \mathbf{k}), \quad k'^\mu = (E_{k'}, \mathbf{k}') \tag{3.2}$$

for incoming and outgoing leptons, respectively,

$$p_1^\mu = (E_{p_1}, \mathbf{p}_1) \tag{3.3}$$

for the target nucleon in its rest frame, and

$$p_1'^\mu = (E_{p_1'}, \mathbf{p}_1'), \quad p_2'^\mu = (E_{p_2'}, \mathbf{p}_2') \tag{3.4}$$

for the final state meson and baryon, respectively. The four-momentum of W is given by

$$q^\mu = k^\mu - k'^\mu = (q^0, \mathbf{q}). \tag{3.5}$$

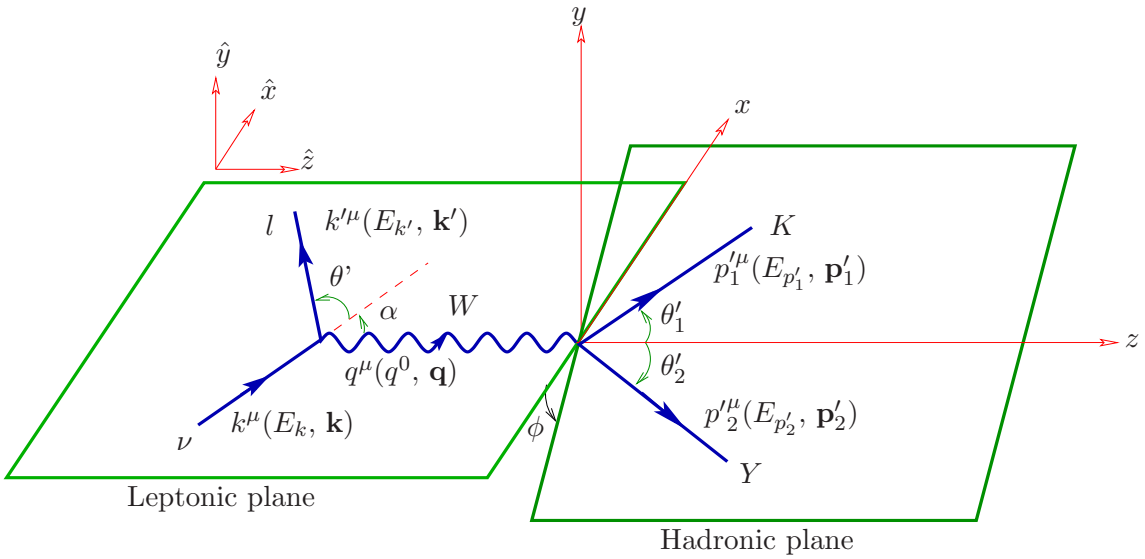

Fig. 3.2: kinematics of the neutrino-induced weak production of strange particles in the rest frame of the target nucleon.

Careful analysis of Fig. 3.2 leads to treating the leptonic scattering and the strange particle production, separately, as shown in Fig. 3.3 which gives a clear illustration as to how we should impose the geometrical conditions on the kinematic variables.

In terms of the cartesian components the three-momenta of leptons and the gauge boson can be written as

$$\begin{aligned} \mathbf{k} &= (k_x,\, k_y,\, k_z) & \mathbf{p}_1 &= (p_{1x},\, p_{1y},\, p_{1z}) \\ \mathbf{k}' &= (k_x',\, k_y',\, k_z') & \mathbf{p}_1' &= (p_{1x}',\, p_{1y}',\, p_{1z}') \\ \mathbf{q} &= (q_x,\, q_y,\, q_z) & \mathbf{p}_2' &= (p_{2x}',\, p_{2y}',\, p_{2z}'). \end{aligned} \tag{3.6}$$

In the leptonic plane, $\mathbf{k}$ and $\mathbf{k}'$ become

$$\begin{aligned} \mathbf{k} &= |\mathbf{k}| \sin\alpha\hat{x} + 0\hat{y} + |\mathbf{k}| \cos\alpha\hat{z} \\ \mathbf{k}' &= |\mathbf{k}'| \sin(\alpha+\theta')\hat{x} + 0\hat{y} + |\mathbf{k}'| \cos(\alpha+\theta')\hat{z}. \end{aligned} \tag{3.7}$$

In Fig. 3.2, since the three-vector momentum transfer $\mathbf{q} = \mathbf{k} - \mathbf{k}'$, which is carried by the gauge boson, is defined in such a away that $\mathbf{q} = (0,\, 0,\, q_z)$, this in turn allows the determination of the incident angle $\alpha \equiv \alpha(E_k,\, E_{k'},\, \theta')$ from input variables E_k, $E_{k'}$, θ'. The following relation may be found

$$\sin\alpha = \pm\sqrt{\frac{A^2}{A^2+B^2}}, \qquad \cos\alpha = \pm\sqrt{\frac{B^2}{A^2+B^2}} \tag{3.8}$$

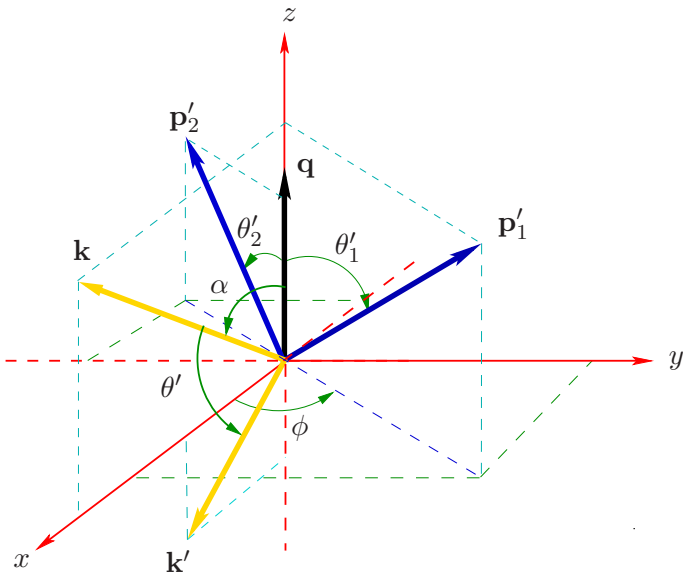

Fig. 3.3: The Geometry of three-momenta of the reaction $\nu N \to lKY$. Here the momenta of the leptons and hadrons specified on the same coordinate system.

where

$$\begin{aligned} A &= |\mathbf{k}| - |\mathbf{k}'|\cos\theta' \\ B &= |\mathbf{k}'|\sin\theta', \end{aligned} \tag{3.9}$$

and the signs for both $\sin\alpha$ and $\cos\alpha$ can be taken as inputs.

In the hadronic plane, there are two outgoing particles with three-momenta $\mathbf{p}'_1$ and $\mathbf{p}'_2$ at angles θ'_1 and θ'_2 from z-axis. Since this plane may be connected to the leptonic plane via the SO(3) group transformation, it's coordinates become

$$\begin{aligned} \hat{x}' &= \cos\phi\hat{x} + \sin\phi\hat{y} + 0\hat{z} \\ \hat{y}' &= -\sin\phi\hat{x} + \cos\phi\hat{y} + 0\hat{z} \\ \hat{z}' &= 0\hat{x} + 0\hat{y} + \hat{z}. \end{aligned} \tag{3.10}$$

Thus Eq. (3.10) leads to the following expression of $\mathbf{p}'_1$ and $\mathbf{p}'_2$

$$\begin{aligned} \mathbf{p}'_1 &= |\mathbf{p}'_1|\sin\theta'_1\cos\phi\hat{x} + |\mathbf{p}'_1|\sin\theta'_1\sin\phi\hat{y} + |\mathbf{p}'_1|\cos\theta'_1\hat{z} \\ \mathbf{p}'_2 &= |\mathbf{p}'_2|\sin(-\theta'_2)\cos\phi\hat{x} + |\mathbf{p}'_2|\sin(-\theta'_2)\sin\phi\hat{y} + |\mathbf{p}'_2|\cos(-\theta'_2)\hat{z}. \end{aligned} \tag{3.11}$$

In momentum space, the following spherical coordinate treatments can be applied for the

final state particles $l(k)$, $K(p'_1)$ and $Y(p'_2)$

$$\begin{aligned} d^3\mathbf{k}' &= |\mathbf{k}'|^2 d|\mathbf{k}'| d\Omega(\phi', \theta') \\ d^3\mathbf{p}'_1 &= |\mathbf{p}'_1|^2 d|\mathbf{p}'_1| d\Omega(\phi'_1, \theta'_1) \\ d^3\mathbf{p}'_2 &= |\mathbf{p}'_2|^2 d|\mathbf{p}'_2| d\Omega(\phi'_2, \theta'_2), \end{aligned} \tag{3.12}$$

where $\Omega(\phi, \theta) = d(\cos\theta)d\phi$ is called as a solid angle. Since there exists an azimuthal symmetry for the outgoing lepton, $d^3\mathbf{k}'$ is integrated over ϕ' and hence can be written as $d^3\mathbf{k}' = 2\pi|\mathbf{k}'|^2 d|\mathbf{k}'| d(\cos\theta')$. However, both ϕ'_1 and ϕ'_2 may be chosen to be the same as ϕ.

Here we introduce the most important problem that will be encountered later. It is the one with the four-dimensional Dirac delta function

$$\begin{aligned} (2\pi)^4\delta(k - k' + p_1 - p'_1 - p'_2) = \; & (2\pi)\delta(E_k - E_{k'} + E_p - E_{p'_1} - E_{p'_2}) \\ & \times (2\pi)^3\delta(\mathbf{k} - \mathbf{k}' + \mathbf{p} - \mathbf{p}'_1 - \mathbf{p}'_2). \end{aligned} \tag{3.13}$$

Based on the properties associated with the delta function, the space component enforces the conservation of three-momentum at the hadronic vertex of the Feynman diagram shown in Fig. 3.1. As a result, after integrating over $d^3\mathbf{p}'_2$, the following relation can be obtained

$$\mathbf{p}'_2 = \mathbf{k} - \mathbf{k}' + \mathbf{p} - \mathbf{p}'_1. \tag{3.14}$$

Then Eq. (3.13) remains with the time component which contains two unknown variables: $E_{p'_1}$ and $E_{p'_2}$. Let $f(E_{p'_1}, E_{p'_2}) = E_k - E_{k'} + E_p - E_{p'_1} - E_{p'_2}$. However, it is inappropriate to express a function in terms of variables which are not independent. On the other hand, based on Eq. (2.1) we can easily establish a relationship between $E_{p'_1}$ and $E_{p'_2}$. Thus $f(E_{p'_1}, E_{p'_2})$ can be redefined as $f(E_{p'_1})$ (i.e., it is only the function of the energy of the outgoing pseudoscalar-meson); and hence the energy dependent delta function in Eq. (3.13) can be written as $\delta[f(E_{p'_1})]$. Therefore, after a few algebraic steps $f(E_{p'_1})$ becomes

$$f(z) = a - z - \left(b + z^2 - c\left[z^2 - {M_K}^2\right]^{\frac{1}{2}}\right)^{\frac{1}{2}}, \tag{3.15}$$

where

$$\begin{aligned} a &= E_k - E'_k + M \\ b &= |\mathbf{q}|^2 - {M_K}^2 + {M_Y}^2 \\ c &= 2|\mathbf{q}|\cos\theta'_1 \end{aligned} \tag{3.16}$$

and for convenience $E_{p'_1}$ has been relabelled by z. Once again by invoking the property of the Dirac delta function, it is possible to demand the conservation of energy at the hadronic vertex, which in turn leads to the determination of the all possible roots of $f(z) = 0$ by

integrating over all kinematically available range of z. One may apply certain mathematical trick such as the following quadratic expression, in order to obtain the roots of $f(z) = 0$, analytically.

$$A_0 + A_1 z + A_2 z^2 = 0, \tag{3.17}$$

where

$$\begin{aligned} A_0 &= (b - a^2)^2 + M_K^2 c^2, \\ A_1 &= 4a(b - a^2), \\ A_2 &= 4a^2 - c^2. \end{aligned} \tag{3.18}$$

In this section it is appropriate to introduce the Mandelstam variables which are Lorentz invariant quantities.

$$s = (q + p_1)^2 = (p_1' + p_2')^2, \tag{3.19}$$

$$t = (q - p_1')^2 = (p_2' - p_1)^2, \tag{3.20}$$

$$u = (q - p_2')^2 = (p_1' - p_1)^2. \tag{3.21}$$

Since the study is focused in the threshold energy region, it is of paramount importance to determine this energy.

$$E_{th} = \frac{(m_l + M_Y + M_K)^2 - m^2 - M^2}{2M}. \tag{3.22}$$

3.2 Cross Section

The most general form of the differential cross section of the reaction type give in Eq. (3.1) is constructed based on Fermi's Golden rule that relates the rate of transition per unit volume with the lowest order matrix element (transition probability) between initial state $|i\rangle$ and final state $|j\rangle$ [24, 23].

$$W_{fi} = \frac{|S_{fi}|^2}{TV}, \tag{3.23}$$

where V and T are the normalization volume and the total time a particle spends in V, respectively, and according to [29, 30, 31] the transition probability S_{fi} is defined as

$$S_{fi} = -i \underbrace{(N_{V_1} N_{V_2} N_{V_3} N_{V_4} N_{V_5})}_{\text{volume normalization factor}} (2\pi)^4 \delta(k - k' + p_1 - p_1' - p_2')\mathcal{M}, \tag{3.24}$$

where $\mathcal{M}$ is the invariant amplitude that contains all the dynamics of the processes under question, the role of the Dirac delta function is to impose energy-momentum conservation at the interaction vertex.

The differential cross section for the neutrino-induced production of strange particles is defined as

$$\begin{aligned} d\sigma = \; & \frac{(2\pi)^4 \delta(k - k' + p_1 - p_1' - p_2') \left(N_{V_1} N_{V_2} N_{V_3} N_{V_4} N_{V_5}\right)^2}{TV \times (\text{Initial Flux})} |\mathcal{M}|^2 \\ & \underbrace{\times \left(\frac{V}{(2\pi)^3} \frac{d^3\mathbf{k}'}{n'}\right) \left(\frac{V}{(2\pi)^3} \frac{d^3\mathbf{p}_1'}{n_1'}\right) \left(\frac{V}{(2\pi)^3} \frac{d^3\mathbf{p}_2'}{n_2'}\right)}_{\text{phase space factor}}, \end{aligned} \tag{3.25}$$

where the n's are number of particles per unit volume and the initial flux may be written as

$$\text{Initial Flux} = \frac{n|\mathbf{v}_\nu - \mathbf{v_1}|}{V} \frac{n_1}{V} \tag{3.26}$$

where $|\mathbf{v} - \mathbf{v_1}|$ is the relative velocity of the incident neutrino with respect to the target nucleon and it can be written as

$$\frac{|\mathbf{v} - \mathbf{v_1}|}{4} = \frac{\left((k \cdot p_1)^2 - m^2 M^2\right)^{\frac{1}{2}}}{2E_k 2E_{p_1'}}. \tag{3.27}$$

The following normalizations are chosen:

- The number of particles is normalized such that there is one particle per unit volume, and this sets n to unity for all particles participated in the reaction process.
- For free spin-$\frac{1}{2}$ fermions, the non-covariant normalization to the free particle solution of the Dirac equation is used.
- For spin-0 bosons, the usual normalization to the solution of the Klein-Gordon equation is applied. That is

$$\int_V N_V^2 2E d^3\mathbf{x} = 1 \quad \Rightarrow \quad N_V = \frac{1}{\sqrt{2EV}}. \tag{3.28}$$

Thus one may able to rewrite Eq. (3.25) as

$$d\sigma = \frac{2E_k\,2E_{p_1}}{4\left((k\cdot p_1)^2 - m^2M^2\right)^{\frac{1}{2}}}(2\pi)^4\delta(k+p_1-k'-p_1'-p_2')|\mathcal{M}|^2 \times\frac{1}{(2\pi)^3}d^3\mathbf{k}'\frac{1}{(2\pi)^3}\frac{d^3\mathbf{p}_1'}{2E_{p_1'}}\frac{1}{(2\pi)^3}d^3\mathbf{p}_2' \quad . \tag{3.29}$$

Obviously the mass m of the neutrino is zero and the three-momentum of the initial nucleon $\mathbf{p}_1 = \mathbf{0}$. Hence these argument reduces the right-hand side of Eq. (3.27) to

$$\frac{2E_k\,2E_{p_1}}{4\left((k\cdot p_1)^2 - (mM)^2\right)^{\frac{1}{2}}} \longrightarrow 1. \tag{3.30}$$

For both charged current and neutral current processes, the final state K-meson is considered as an experimentally observed particle, and hence one may rather integrate over all available phase space of the final state baryon. As it has been pointed out earlier, the presence of the four-dimensional delta function in the general expression of the differential cross section simplifies the evaluation. Thus, by referring back to Eq. (3.12) and arguments given in section 3.1 regarding the Dirac delta function, the differential cross section becomes

$$d\sigma = \frac{1}{2(2\pi)^5}\delta\left(E_k + M - E_{k'} - E_{p_1'} - E_{p_2'}(E_{p_1'})\right)|\mathcal{M}|^2 \chi(E_{k'})\left(E_{p_1'}^2 - M_K^2\right)^{\frac{1}{2}} dE_{k'}d(\cos\theta')dE_{p_1'}d\Omega_1' \tag{3.31}$$

where

$$\chi(E_{k'}) = \begin{cases} 2\pi E_{k'}^2 & \text{for NC process} \\ 2\pi E_{k'}\left(E_{k'}^2 - m_l^2\right)^{\frac{1}{2}} & \text{for CC process} \end{cases} \quad . \tag{3.32}$$

In the charged current processes the final state lepton is a muon which is detectable for it is relatively massive and carries electric charge. The differential cross section may be measured along with the scattering angle θ' and the energy $E_{k'}$. Therefore, one can theoretically calculate the angular and energy distribution of the differential cross section and compare results with experimental data. On the contrary, for neutral current processes the final state lepton is the muon-neutrino and being a neutral particle with zero mass makes it very difficult to detect [32]. One therefore integerates over the polar angle and the energy of the final state neutrino.

The most appropriate differential cross section for charged current reaction may be rewritten as

$$\frac{d^3\sigma}{dE_{k'}d(\cos\theta')d\Omega_1'} = \frac{1}{2(2\pi)^5}\int \delta\left[f(E_{p_1'})\right]\chi(E_{k'})\left(E_{p_1'}^2 - M_K^2\right)^{\frac{1}{2}}|\mathcal{M}|^2 dE_{p_1'}, \tag{3.33}$$

where $f(E_{p_1'})$ is the same as the function defined in Eq. (3.15). The following identity of the Dirac delta function is applied

$$\int \delta[f(z)]dz = \sum_{z_i}\int \frac{1}{|f'(z)|}\delta(z-z_i)dz = \sum_{z_i}\frac{1}{|f'(z_i)|} \tag{3.34}$$

where z_i are the roots of $f(z)$. It is worth noting that only one of the two roots of Eq. (3.17) is physical as far $f(E_{p_1'})$ is concerned. Finally, we obtain

$$\frac{d^3\sigma}{dE_{k'}d(\cos\theta')d\Omega_1'} = \frac{1}{2(2\pi)^5}\left[\frac{1}{|f'(E_{p_1'})|}\right]\chi(E_{k'})\left(E_{p_1'}^2 - M_K^2\right)^{\frac{1}{2}}|\mathcal{M}|^2, \tag{3.35}$$

where $E_{p_1'}$ is fixed as a result of the above argument. All kinematical quantities can be determined by specifying the following set:

$$\{E_k,\, E_{k'},\, \theta',\, \theta_1',\, \phi\}.$$

In general, Eq. (3.35) may be used to investigate the angular distribution of differential cross section with respect to either of muon angle or K-meson angle as well as its energy distribution with respect to muon energy for the charged current weak production of strange particles.

However, for the neutral current case the proper form of the differential cross section would be

$$\frac{d\sigma}{d\Omega_1'} = \int dE_{k'}\int d(\cos\theta')\left[\frac{1}{2(2\pi)^5}\left[\frac{1}{|f'(E_{p_1'})|}\right]\chi(E_{k'})\left(E_{p_1'}^2 - M_K^2\right)^{\frac{1}{2}}|\mathcal{M}|^2\right]. \tag{3.36}$$

The integrations are supposed to be taken in kinematically allowed ranges of final state lepton energy and angle. Clearly, with Eq. (3.36) one can study the angular distribution of differential cross section with respect to the outgoing K-meson angle.

3.3 Invariant Amplitude Evaluation

It has been made apparent that the differential cross section is proportional to the norm squared invariant amplitude. But this quantity has not been determined yet. In what follows the derivation of this amplitude will be done. The Feynman rules may be applied as a math-

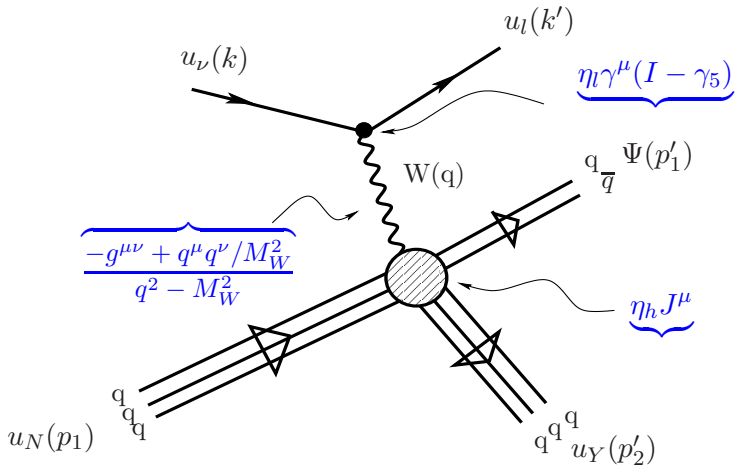

Fig. 3.4: The general quark level Feynman diagram of strange particle production via neutrino-nucleon weak interaction and the associated factors according to the Feynman rules.

ematical tool to construct the invariant amplitude directly from the lowest order Feynman diagram, Fig. 3.1, for the reaction processes in question. In general the diagram contains four major elements: the leptonic transition, the hadronic transition, the propagator, and the interaction vertices. Thus the Feynman rules allow us to extract the associated factor at indicated in Fig. 3.4 and it is possible to construct the general expression of $\mathcal{M}$ as

$$-i\mathcal{M} = \overbrace{\left[\bar{u}_l(k',h')\eta_l\gamma_\mu(I-\gamma_5)\nu(k,h)\right]}^{\text{leptonic weak current}} iD^{\mu\nu} \underbrace{\left\langle K(p_1')Y(p_2')\left|\eta_h\hat{J}_\nu(q)\right|N(p_1)\right\rangle}_{\text{hadronic weak current}}, \tag{3.37}$$

where for convenience the neutrino's Dirac spinor is represented by $\nu(k,h)$ instead of $u_\nu(k,h)$ and $D^{\mu\nu}$ is the gauge boson propagator

$$D^{\mu\nu} = \frac{-g^{\mu\nu}+q^\mu q^\nu/M_W^2}{q^2-M_W^2}, \tag{3.38}$$

and the hadronic transition current can be written as [33]

$$\left\langle K(p_1')Y(p_2')\left|\eta_h\hat{J}_\nu\right|N(p_1)\right\rangle = \bar{u}_Y(p_2',s_2')\eta_h J_\nu(q)u_N(p_1,s_1) \tag{3.39}$$

and the two factors η_l and η_h are given in Table. 3.1[1].

Table. 3.1: The expression for η_l and η_h in terms of the weak coupling constant g.

	CC	NC
η_l	$\frac{-ig}{2\sqrt{2}}$	$\frac{-ig}{4}\frac{M_Z}{M_{W^+}}$
η_h	$\frac{-ig}{2\sqrt{2}}\eta_c$	$\frac{-ig}{4}\frac{M_Z}{M_{W^+}}\eta_c$

where η_c is Cabibbo factor and it has either of the following forms

$$\eta_c = \begin{cases} \cos\theta_c, & \text{for CC}, \Delta S = 0 \\ \sin\theta_c, & \text{for CC}, \Delta S = 1 \\ 1 & \text{for NC}, \end{cases} \tag{3.40}$$

where θ_c is Cabibbo angle. In this study, the condition $Q^2 \ll M_W^2$ ($Q^2 = -q^2$) must me satisfied such that $D^{\mu\nu} \to g^{\mu\nu}/M_W^2$, which in turn relates the weak coupling constant with the Fermi constant $G_F = 1.166 \times 10^{-05}\text{GeV}^{-2}$

$$\frac{G_F}{\sqrt{2}} = \frac{g^2}{8M_W^2}. \tag{3.41}$$

Then $\mathcal{M}$ becomes [32]

$$\mathcal{M} = \frac{G_F}{\sqrt{2}}\eta\left[\bar{u}_l(k',h')\gamma_\mu(I-\gamma_5)\nu(k,h)\right]\left[\bar{u}_Y(p_2',s_2')J^\mu(q)u_N(p_1,s_1)\right] \tag{3.42}$$

where

$$\eta = \begin{cases} \eta_c & \text{for CC} \\ \frac{\eta_c}{2} & \text{for NC}. \end{cases} \tag{3.43}$$

Thus the norm squared invariant amplitude may be written as the contraction between the leptonic tensor and the hadronic tensor as

[1]The coupling of lepton current with $W^\pm$ and Z^0 taken from [23, p. 336-337]

$$|\mathcal{M}|^2 = \frac{G_F^2 \eta^2}{2} L_{\mu\nu} W^{\mu\nu}, \tag{3.44}$$

where

$$L_{\mu\nu} = \left[\bar{u}_l(k', h')\gamma_\mu(I - \gamma_5)\nu(k, h)\right]\left[\bar{u}_l(k', h')\gamma_\nu(I - \gamma_5)\nu(k, h)\right]^* \tag{3.45}$$

and

$$W^{\mu\nu} = \left[\bar{u}_Y(p_2', s_2')J^\mu(q)u_N(p_1, s_1)\right]\left[\bar{u}_Y(p_2', s_2')J^\nu(q)u_N(p_1, s_1)\right]^*. \tag{3.46}$$

The leptonic tensor is derived from the leptonic weak transition current by applying the Feynman trace technique. The detailed derivation is given in Appendix B. This approach avoids the explicit use of the Dirac spinors and the gamma matrices for the calculation of the differential cross section.

$$L_{\mu\nu} = \frac{1}{8E_k E_{k'}} \mathrm{Tr}\left[\gamma_\mu(I - \gamma_5)\not{k}(I + \gamma_5)\gamma_\nu(I - \gamma_5)(\not{k}' + m_l)(I + h'\gamma_5\not{s}')\right]. \tag{3.47}$$

By applying the Dirac algebra repeatedly the leptonic tensor becomes

$$L_{\mu\nu}^{CC} = \frac{2}{E_k E_k'}\left[k_\mu K_\nu + k_\nu K_\mu - k \cdot K g_{\mu\nu} + i\epsilon_{\mu\nu\alpha\beta}k^\alpha K^\beta\right] \tag{3.48}$$

where $\varepsilon_{\mu\nu\alpha\beta}$ is the anti-symmetric Levi-Cevita tensor with convention $\varepsilon^{0123} = +1$, and

$$K^\mu = \frac{1}{2}(k'^\mu - h' m_l s'^\mu); \quad \text{and} \quad s'^\mu = \frac{1}{m_l}(|\mathbf{k}'|,\ E_{k'}\hat{\mathbf{k}}'), \tag{3.49}$$

where s'^μ is the spin polarization four vector of the final lepton. This procedure of deriving the leptonic tensor is generally called Casimir's trick. In the small mass limit, $m_l \to 0$,

$$K^\mu \longrightarrow k'^\mu \tag{3.50}$$

By using the zero mass limit the leptonic tensor for the NC weak transition may be deduced from Eq. (3.48).

$$L_{\mu\nu}^{NC} = \frac{2}{E_k E_k'}\left[k_\mu k'_\nu + k_\nu k'_\mu - k \cdot k' g_{\mu\nu} + i\epsilon_{\mu\nu\alpha\beta}k^\alpha k'^\beta\right]. \tag{3.51}$$

By employing a similar procedure as that of the leptonic case, the hadronic tensor becomes

$$W^{\mu\nu} = \frac{1}{2}\left\{\frac{1}{(2E_{p_1})(2E_{p_2'})}\mathrm{Tr}\left[\hat{J}^{\mu}(q)(\not{p}_1 + M_N)\overline{\hat{J}^{\nu}}(q)(\not{p}_2' + M_Y)\right]\right\} \tag{3.52}$$

where

$$\overline{\hat{J}^{\mu}}(q) = \gamma^0 \hat{J}^{\mu\,\dagger}(q)\gamma^0. \tag{3.53}$$

Following the assumption that the target nucleon is unpolarized and the final hyperon is not detected, we average over the nucleon spin state and sum over the final hyperon spin state. Eventually, the differential cross section given in Eq. (3.35) may be rewritten as

$$\frac{d^3\sigma}{dE_{k'}d(\cos\theta')d\Omega_1'} = \frac{1}{2(2\pi)^5}\frac{G_F^2\eta^2}{2}\chi(E_{k'})\left[\frac{\left(E_{p_1'}^2 - M_K^2\right)^{\frac{1}{2}}}{|f'(E_{p_1'})|}L_{\mu\nu}W^{\mu\nu}\right]. \tag{3.54}$$

However, the weak hadronic transition current $\hat{J}^{\mu}(q)$ is not well known due to the complication that arises from the strong interaction effects at the hadronic vertex which have not been well understood yet. The next chapter will focus on the model-independent construction of the most general form of hadronic weak current in the context of the three-body process.

Chapter 4

Hadronic Weak Current

In the previous discussion the leptonic part of the Feynman diagram shown in Fig. 3.4 is the well known leptonic current coupling with the gauge boson; and it is developed in analogy with QED. In contrast, the hadronic vertex must be parametrized by form factors to take into account the strong interaction effects. The role of the form factors is to parametrize the strong interaction effects.

Bjorken and Drell established the basic idea of describing the electromagnetic transitions in terms of two absolutely independent form factors (i.e., electric and magnetic form factors) in their book [29, p. 241-246]. In addition, as stated by Perkins in [34], the introduction of these form factors lead to the understanding that hadrons are no longer point-like particles rather they are composite particles and the typical properties of these hadrons are as a result of the individual contributions of the constituents [24]. In what follows, the model-independent derivation of the hadronic weak currents for a single particle transition as well as a three-body process will be made.

4.1 Weak Form factors in Two-body transitions

To begin with, it is quite relevant to consider the most general form of the weak current for a two-body process which can be represented by the Feynman diagram as shown in Fig. 4.1. As mentioned in [31, 35], a single spin-$\frac{1}{2}$ particle weak transition operator $\mathcal{O}^{\mu}(q)$ can be expanded in terms of the bilinear covariant basis given in Eq. (4.1)[1]. This is the consequence of the

[1]Brief explanation of the transformation behaviour of bilinear covariants and why they can definitely be used to construct any Lorentz vector and 4×4 square matrix is given in Ref [23, p. 224-225]

fact that $\mathcal{O}^\mu(q)$ is a Lorentz vector and a 4×4 matrix.

$$\Gamma = \{I,\, \gamma_5,\, \gamma^\mu,\, \gamma_5\gamma^\mu,\, \sigma^{\mu\nu}\}. \tag{4.1}$$

Let p_1 and p_2 be the initial and the final four-momenta of a particle which is weakly coupled to the gauge boson. For convenience, we define $q = p_1 - p_2$ and $k = p_1 + p_2$.

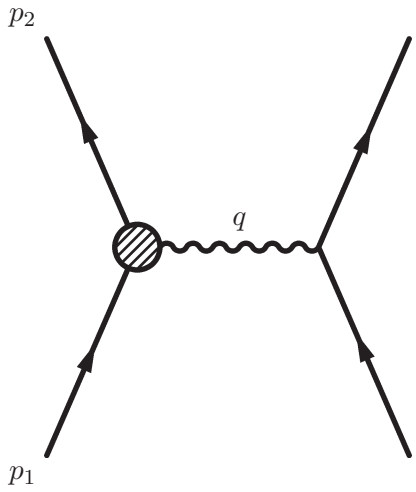

Fig. 4.1: Tree diagram of the two-body weak process of fermions.

The weak current may be decomposed via Γ into

$$\bar{u}(p_2')\mathcal{O}^\mu(q)u(p_1) = \bar{u}(p_2')\left\{A^\mu I + B^\mu\gamma_5 + C^{\mu\nu}\gamma_\nu + D^{\mu\nu}\gamma_5\gamma_\nu + E^{\mu\nu\alpha}\sigma_{\nu\alpha}\right\}u(p_1), \tag{4.2}$$

where A^μ, B^μ, $C^{\mu\nu}$, $D^{\mu\nu}$, $E^{\mu\nu\alpha}$ are unknown tensors. However, in such transitions these tensors depend on all available independent four-momenta. We, however, choose the two independent four-momenta q and k. In addition, the metric tensor $g^{\mu\nu}$, the Levi-Cevita tensor $\epsilon^{\mu\nu\alpha\beta}$ and their proper combination with q and k are also at our disposal to further expand the operator. For instance, A^μ and B^μ may be expanded in terms of the following basis

$$\tilde{\mathcal{A}} = \{q^\mu,\, k^\mu,\, \epsilon^{\mu\nu\alpha\beta}q_\nu q_\alpha q_\beta,\, \epsilon^{\mu\nu\alpha\beta}q_\nu q_\alpha k_\beta,\, \epsilon^{\mu\nu\alpha\beta}k_\nu k_\alpha q_\beta,\, \epsilon^{\mu\nu\alpha\beta}k_\nu k_\alpha k_\beta\}. \tag{4.3}$$

For $C^{\mu\nu}$ and $D^{\mu\nu}$ we have the following basis

$$\begin{aligned}\tilde{\mathcal{C}} = \;& \{g^{\mu\nu},\, q^\mu q^\nu,\, k^\mu k^\nu,\, q^\mu k^\nu + k^\mu q^\nu,\, q^\mu k^\nu - k^\mu q^\nu,\, \epsilon^{\mu\nu\alpha\beta}q_\alpha q_\beta,\, \epsilon^{\mu\nu\alpha\beta}q_\alpha k_\beta,\\ & \epsilon^{\mu\nu\alpha\beta}k_\alpha k_\beta\}.\end{aligned} \tag{4.4}$$

Note that the contraction

$$\epsilon^{\mu\nu\alpha\beta} a_i a_j = 0, \text{ for } i,j = \mu,\nu,\alpha,\beta \text{ and } i \neq j. \tag{4.5}$$

This tells us that all basis functions in $\tilde{\mathcal{A}}$ and $\tilde{\mathcal{C}}$ with the similar form as Eq. (4.5) vanish. The last tensor $E^{\mu\nu\alpha}$ can explicitly be written as the bases that can be carefully constructed from $\mathcal{C}$. However, it is worth noting that the basis with this amplitude is anti-symmetric in terms of Lorentz indices ν and α. Hence all the basis functions for $E^{\mu\nu\alpha}$ are also expected to be anti-symmetric. However, the contraction between symmetric and anti-symmetric tensors always vanishes. Hence,

$$\begin{aligned}\tilde{\mathcal{E}} = \; & \{q^\mu(q^\nu k^\alpha - k^\nu q^\alpha),\, k^\mu(q^\nu k^\alpha - k^\nu q^\alpha),\, q^\mu \epsilon^{\nu\alpha\beta\eta} q_\beta k_\eta,\, k^\mu \epsilon^{\nu\alpha\beta\eta} q_\beta k_\eta,\, \epsilon^{\mu\nu\alpha\beta} q_\beta, \\ & \epsilon^{\mu\nu\alpha\beta} k_\beta\}.\end{aligned} \tag{4.6}$$

Finally, the matrix element can be re-expressed as

$$\begin{aligned}\bar{u}(p_2')\mathcal{O}^\mu(q)u(p_1) = \; & \bar{u}(p_2')\,\{[A_1 q^\mu + A_2 k^\mu]I + [B_1 q^\mu + B_2 k^\mu]\gamma_5 + [C_1 g^{\mu\nu} + C_2 q^\mu q^\nu \\ & + C_3 k^\mu k^\nu + C_4(q^\mu k^\nu + k^\mu q^\nu) + C_5(q^\mu k^\nu - k^\mu q^\nu) \\ & + C_6 \epsilon^{\mu\nu\alpha\beta} q_\alpha k_\beta]\gamma_\nu + [D_1 g^{\mu\nu} + D_2 q^\mu q^\nu + D_3 k^\mu k^\nu + D_4(q^\mu k^\nu \\ & + k^\mu q^\nu) + D_5(q^\mu k^\nu - k^\mu q^\nu) + D_6 \epsilon^{\mu\nu\alpha\beta} q_\alpha k_\beta]\gamma_5\gamma_\nu \\ & + [E_1 q^\mu(q^\nu k^\alpha - k^\nu q^\alpha) + E_2 k^\mu(q^\nu k^\alpha - k^\nu q^\alpha) + E_3 q^\mu \epsilon^{\nu\alpha\beta\eta} q_\beta k_\eta \\ & + E_4 k^\mu \epsilon^{\nu\alpha\beta\eta} q_\beta k_\eta + E_5 \epsilon^{\mu\nu\alpha\beta} q_\beta + E_6 \epsilon^{\mu\nu\alpha\beta} k_\beta]\sigma_{\nu\alpha}\}\, u(p_1).\end{aligned} \tag{4.7}$$

At this stage one makes use of the algebra of gamma matrices (Table. A.1 in Appendix A) and the Dirac equation given in Eq. (2.5) in chapter 2, for the particle that satisfies the on-mass shell condition, over and over again in order to reach the following expression of $\mathcal{O}^\mu(q)$

$$\mathcal{O}^\mu = f_1 q^\mu + f_2 l^\mu + f_3 \gamma^\mu + f_4 q^\mu \gamma_5 + f_5 l^\mu \gamma_5 + f_6 \gamma^\mu \gamma_5. \tag{4.8}$$

Along the way it would become apparent that the last tensor $E^{\mu\nu\alpha}$ does not contain independent amplitudes. Besides, most of C_i's and D_i's are also absorbed by A_i's and B_i's.

Eventually, by exhaustively applying the Gordon-like identities ($\mathcal{GLI}$) (Table. C.1 in Appendix C) until l^μ is totally eliminated; we obtain

$$\mathcal{O}^\mu = f_1\gamma^\mu + \frac{f_2}{2m}\sigma^{\mu\nu}q_\nu + f_3 q^\mu + f_4\gamma^\mu\gamma_5 + f_5\epsilon^{\mu\nu\alpha\beta}\sigma_{\alpha\beta}q^\nu + f_6 q^\mu\gamma_5. \tag{4.9}$$

4.2 Model-independent Form factors of Three-body Weak Transition

What has been done in section 4.1 for the two-body case will be used as the basic foundation for the derivation of the most general hadronic weak current for the three-particle process such as strange particle production, which is the main subject of the study. In such expansion of the three-body weak current we use the following interpretation of the Feynman diagram in Fig. 4.2. The hadronic vertex represents the coupling of the generalized weak current, $J^\mu(B(p_1) \to B'(p_2')K(p_1'))$, with the exchange gauge boson with four-momentum q, where $B(p_1)$ is the initial state fermion, $B'(p_2')$ and $K(p_1')$ are the final state baryon and meson, respectively. We present, for the first time, the general form of the hadronic vertex for the three-body weak transitions.

This model-independent derivation is done by taking advantage of the fact that the weak interaction violates the most fundamental discrete symmetries such as parity ($\mathcal{P}$), time-reversal ($\mathcal{T}$), charge conjugation ($\mathcal{C}$), and the combination of parity and charge conjugation ($\mathcal{CP}$); and hence the general expression of the current will have relatively large number of independent parametrization form factors which possibly allow us to gain more insight about the weak interaction and structure of hadronic weak current. In addition, unlike the electromagnetic current, the non-conservation of the weak current, due to the massive gauge bosons exchange, does not allow the possibility of reducing the number of independent form factors.

To begin with, we choose p_1 and p_2' to be the four-momenta of spin-1/2 hadrons with mass M_1, and M_2, and p_1' to be the pseudoscalar-meson. The transition current at the hadronic vertex of Fig. 4.2 may be written as

$$\left\langle K(p_1')B(p_2')|\hat{J}^\mu(q)|B(p_1)\right\rangle = \bar{u}(p_2')J^\mu(q)u(p_1). \tag{4.10}$$

Once again, the derivation of the general expression of $\hat{J}^\mu(q)$ is based on the global structure that the current operator possesses. That is, the current operator is a 4×4 square matrix and

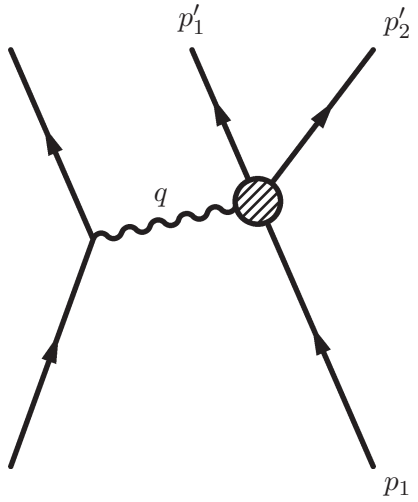

Fig. 4.2: The Feynman diagram with a vertex of three external lines of hadrons and exchange particle carrying four-momentum transfer $q = p_1' + p_2' - p_1$.

also first rank tensor or Lorentz vector; and hence a similar principle as in section 4.1 will be used to reach the most general hadronic weak current for three-body process. However, the only exception is that there is one additional independent variable. Eq. (4.11) summarizes the fundamental bases with which the first rank tensor $\hat{J}^\mu(q)$ will be constructed.

$$\begin{aligned} \tilde{\Gamma} = &\quad \{I,\, \gamma_5,\, \gamma^\mu,\, \gamma_5\gamma^\mu,\, \sigma^{\mu\nu}\}, \\ \tilde{\mathcal{P}} = &\quad \{q^\mu,\, p_1^\mu,\, p_2'^\mu\}, \\ \tilde{\mathcal{T}} = &\quad \{g^{\mu\nu},\, \varepsilon^{\mu\nu\alpha\beta}\}. \end{aligned} \tag{4.11}$$

As before the current operator $\hat{J}^\mu(q)$ which is sandwiched between Dirac spinors is can be expanded just like Eq. (4.2). For convenience sake the coefficients may be relabelled as $\tilde{A}^\mu$, $\tilde{B}^\mu$, $\tilde{C}^{\mu\nu}$, $\tilde{D}^{\mu\nu}$, $\tilde{E}^{\mu\nu\alpha}$. For instance, $\tilde{A}$ and $\tilde{B}$ can be further decomposed in terms of

$$\tilde{\mathcal{A}} = \{q^\mu,\, p_1^\mu,\, p_2'^\mu,\, \epsilon^{\mu\nu\alpha\beta} q_\nu p_{1\alpha} p'_{2\beta}\}. \tag{4.12}$$

$\tilde{C}$ and $\tilde{D}$ may also use the following set

$$\begin{aligned} \tilde{\mathcal{C}} = &\quad \{g^{\mu\nu},\, q^\mu q^\nu,\, p_1{}^\mu p_1{}^\nu,\, p_2'{}^\mu p_2'{}^\nu,\, q^\mu p_1{}^\nu \pm p_1{}^\mu q^\nu,\, q^\mu p_2'{}^\nu \pm p_2'{}^\mu q^\nu, \\ &\quad p_1{}^\mu p_2'{}^\nu \pm p_2'{}^\mu p_1{}^\nu,\, \epsilon^{\mu\nu\alpha\beta} q_\alpha p_{1\beta},\, \epsilon^{\mu\nu\alpha\beta} q_\alpha p_{1\beta} q_\alpha p'_{2\beta},\, \epsilon^{\mu\nu\alpha\beta} q_\alpha p_{1\beta} p_{1\alpha} p'_{2\beta}\}. \end{aligned} \tag{4.13}$$

By again noting that the symmetric behaviour arises from the exchange of the Lorentz indices, the last coefficient $\tilde{E}^{\mu\nu\alpha}$ may be restricted to take the following set

$$\begin{aligned}\tilde{\mathcal{E}} = \; & \{[q^\mu, p_1^\mu, p_2'^\mu](q^\mu {p_1}^\nu - {p_1}^\mu q^\nu), [q^\mu, p_1^\mu, p_2'^\mu](q^\mu {p_2'}^\nu - {p_2'}^\mu q^\nu), \\ & [q^\mu, p_1^\mu, p_2'^\mu]({p_1}^\mu {p_2'}^\nu - {p_2'}^\mu {p_1}^\nu), [q^\mu, p_1^\mu, p_2'^\mu]\epsilon^{\nu\alpha\beta\eta} q_\beta {p_1}_\eta, \\ & [q^\mu, p_1^\mu, p_2'^\mu]\epsilon^{\nu\alpha\beta\eta} q_\beta {p_2'}_\eta, [q^\mu, p_1^\mu, p_2'^\mu]\epsilon^{\nu\alpha\beta\eta} {p_1}_\beta {p_2'}_\eta, \epsilon^{\mu\nu\alpha\beta}[q_\beta, {p_1}_\beta, {p_2'}_\beta]\}.\end{aligned} \tag{4.14}$$

Terms like $a^\mu g^{\nu\alpha}$, $a^\mu a^\nu a^\alpha$, $a^\mu(b^\nu c^\alpha + c^\nu b^\alpha)$, and $a^\mu \epsilon^{\nu\alpha\beta\eta} a_\beta b_\eta$ would immediately vanish since they are symmetric in terms of ν and α. Thus by using Eq. (4.12)

$$\bar{u}(p_2')\tilde{A}^\mu I u(p_1) = \bar{u}(p_2')\{\tilde{A}_1 I q^\mu + \tilde{A}_2 I p_1^\mu + \tilde{A}_3 I p_2'^\mu, + \tilde{A}_4 I \epsilon^{\mu\nu\alpha\beta} q_\nu {p_1}_\alpha {p_2'}_\beta\} u(p_1), \tag{4.15}$$

$$\bar{u}(p_2')\tilde{B}^\mu \gamma_5 u(p_1) = \bar{u}(p_2')\{\tilde{B}_1 \gamma_5 q^\mu + \tilde{B}_2 \gamma_5 p_1^\mu + \tilde{B}_3 \gamma_5 p_2'^\mu, + \tilde{B}_4 \epsilon^{\mu\nu\alpha\beta} \gamma_5 q_\nu {p_1}_\alpha {p_2'}_\beta\} u(p_1). \tag{4.16}$$

It is also simple to write down the expression for $\bar{u}(p_2')\tilde{C}^{\mu\nu}\gamma_\nu u(p_1)$, $\bar{u}(p_2')\tilde{D}^{\mu\nu}\gamma_5\gamma_\nu u(p_1)$, and $\bar{u}(p_2')\tilde{E}^{\mu\nu\alpha}\sigma_{\nu\alpha} u(p_1)$ in terms of the linear combination of the bases in Eq. (4.13) and Eq. (4.14). For instance, one may consider $\bar{u}(p_2')\tilde{C}^{\mu\nu}\gamma_\nu u(p_1)$.

$$\begin{aligned}\bar{u}(p_2')\tilde{C}^{\mu\nu}\gamma_\nu u(p_1) = \; & \bar{u}(p_2')\{\tilde{C}_1\gamma^\mu + \tilde{C}_2 q^\mu \not{q} + \tilde{C}_3 {p_1}^\mu \not{p}_1 + \tilde{C}_4 {p_2'}^\mu \not{p}_2' + \tilde{C}_5(q^\mu \not{p}_1 + {p_1}^\mu \not{q}) \\ & + \tilde{C}_6(q^\mu \not{p}_1 - {p_1}^\mu \not{q}) + \tilde{C}_7(q^\mu \not{p}_2' + {p_2'}^\mu \not{q}) + \tilde{C}_8(q^\mu \not{p}_2' - {p_2'}^\mu \not{q}) \\ & + \tilde{C}_9({p_1}^\mu \not{p}_2' + {p_2'}^\mu \not{p}_1) + \tilde{C}_{10}({p_1}^\mu \not{p}_2' - {p_2'}^\mu \not{p}_1) + \tilde{C}_{11}\epsilon^{\mu\nu\alpha\beta}\gamma_\nu q_\alpha {p_1}_\beta \\ & + \tilde{C}_{12}\epsilon^{\mu\nu\alpha\beta}\gamma_\nu q_\alpha q_\alpha {p_2'}_\beta + \tilde{C}_{13}\epsilon^{\mu\nu\alpha\beta}\gamma_\nu {p_1}_\alpha {p_2'}_\beta\} u(p_1)\end{aligned} \tag{4.17}$$

where the Dirac slash notation $\not{a} = a^\nu \gamma_\nu$ is used. By exhaustively applying the Dirac equation for an on-shell particle (i.e., $\not{p} u(p) = M u(p)$ and $\bar{u}(p)\not{p} = M\bar{u}(p)$) as well as the identities given from Eq. (A.13) through (A.18) in Appendix A on Eq. (4.17) over and over again, all proportional terms can be eliminated and then the following expression may be obtained

$$\begin{aligned}\bar{u}(p_2')\tilde{C}^{\mu\nu}\gamma_\nu u(p_1) \; = \; & \bar{u}(p_2')\{\tilde{C}_1\gamma^\mu + \tilde{C}_1' q^\mu + \tilde{C}_2' p_1^\mu + \tilde{C}_3' p_2'^\mu + \tilde{C}_4'\gamma_5\gamma^\mu \\ & + \tilde{C}_5'\gamma_5 q^\mu + \tilde{C}_6'\gamma_5 {p_1}^\mu + \tilde{C}_7'\gamma_5 {p_2'}^\mu + \tilde{C}_2 q^\mu \not{q} \\ & + \tilde{C}_8' {p_1}^\mu \not{q} + \tilde{C}_9' {p_2'}^\mu \not{q} + \tilde{C}_{10}'\gamma_5 \not{q}\gamma^\mu\} u(p_1),\end{aligned} \tag{4.18}$$

where $\tilde{C}_1$ and $\{\tilde{C}_i'\}_{i=1}^{10}$ are coefficients obtained by factoring out all possible independent basis elements. It is worth noting that $\tilde{C}^{\mu\nu}\gamma_\nu$ introduces six new expansion basis elements such as γ^μ, $\gamma_5\gamma^\mu$, $q^\mu \not{q}$, ${p_1}^\mu \not{q}$, ${p_2'}^\mu \not{q}$, and $\gamma_5 \not{q}\gamma^\mu$, whereas the rest are proportional to the ones belonging

to $\bar{u}(p_2')\tilde{A}^\mu I u(p_1)$ and $\bar{u}(p_2')\tilde{B}^\mu\gamma_5 u(p_1)$ in Eq. (4.15) and Eq. (4.16), respectively. A similar procedure as for $\bar{u}(p_2')\tilde{C}^{\mu\nu}\gamma_\nu u(p_1)$ also yields the following expression for $\bar{u}(p_2')\tilde{D}^{\mu\nu}\gamma_5\gamma_\nu u(p_1)$

$$\begin{aligned}\bar{u}(p_2')\tilde{D}^{\mu\nu}\gamma_5\gamma_\nu u(p_1) &= \bar{u}(p_2')\{\tilde{D}_1\gamma_5\gamma^\mu + \tilde{D}_1' q^\mu + \tilde{D}_2' p_1^\mu + \tilde{D}_3' p_2'^\mu + \tilde{D}_4'\gamma^\mu \\ &\quad + \tilde{D}_5'\gamma_5 q^\mu + \tilde{D}_6'\gamma_5 {p_1}^\mu + \tilde{D}_7'\gamma_5 {p_2'}^\mu + \tilde{D}_2 q^\mu\gamma_5 q\!\!\!/ + \tilde{D}_8' {p_1}^\mu q\!\!\!/ \\ &\quad + \tilde{D}_9' {p_2'}^\mu q\!\!\!/ + \tilde{D}_{10}' {p_1}^\mu\gamma_5 q\!\!\!/ + \tilde{D}_{11}' {p_2'}^\mu\gamma_5 q\!\!\!/ + \tilde{D}_5 q\!\!\!/\gamma^\mu\} u(p_1).\end{aligned} \tag{4.19}$$

Hence $\bar{u}(p_2')\tilde{D}^{\mu\nu}\gamma_5\gamma_\nu u(p_1)$ contributes new parameters in terms of $q^\mu\gamma_5 q\!\!\!/$, ${p_1}^\mu\gamma_5 q\!\!\!/$, ${p_2'}^\mu\gamma_5 q\!\!\!/$, and $q\!\!\!/\gamma^\mu$. The remaining terms are proportional to the ones contained by either $\bar{u}(p_2')\tilde{A}^\mu I u(p_1)$, $\bar{u}(p_2')\tilde{B}^\mu\gamma_5 u(p_1)$, or $\bar{u}(p_2')\tilde{C}^{\mu\nu}\gamma_\nu u(p_1)$ and hence fuse into coefficients of the same basis. On the other hand, the last component $\bar{u}(p_2')\tilde{E}^{\mu\nu\alpha}\sigma_{\nu\alpha}u(p_1)$ does not carry new parameters instead all of them are absorbed by any of the previous ones.

Finally, the most general hadronic weak current for strange particle production may be expanded in terms of eighteen independent amplitudes; and in a more convenient rearrangement it may be written as

$$\begin{aligned}\bar{u}(p_2')J^\mu(q)u(p_1) = \; & \bar{u}(p_2')\{\tilde{A}^\mu I + \tilde{B}^\mu\gamma^5 + \tilde{C}_1\gamma^\mu + \tilde{C}^\mu q\!\!\!/ + \tilde{D}_1\gamma_5\gamma^\mu \\ & + \tilde{D}^\mu\gamma_5 q\!\!\!/ + \tilde{D}_5 q\!\!\!/\gamma^\mu + \tilde{D}_6\gamma_5 q\!\!\!/\gamma^\mu\} u(p_1),\end{aligned} \tag{4.20}$$

where

$$\begin{aligned}\tilde{A}^\mu &= \tilde{A}_1 q^\mu + \tilde{A}_2 p_1^\mu + \tilde{A}_3 {p_2'}^\mu + \tilde{A}_4\varepsilon^{\mu\nu\alpha\beta}q_\nu p_{1\alpha}p'_{2\beta}, \\ \tilde{B}^\mu &= \tilde{B}_1 q^\mu + \tilde{B}_2 p_1^\mu + \tilde{B}_3 {p_2'}^\mu + \tilde{B}_4\varepsilon^{\mu\nu\alpha\beta}q_\nu p_{1\alpha}p'_{2\beta}, \\ \tilde{C}^\mu &= \tilde{C}_2 q^\mu + \tilde{C}_3 p_1^\mu + \tilde{C}_4 {p_2'}^\mu, \\ \tilde{D}^\mu &= \tilde{D}_2 q^\mu + \tilde{D}_3 p_1^\mu + \tilde{D}_4 {p_2'}^\mu.\end{aligned} \tag{4.21}$$

These amplitudes are unknown. Recall that the electromagnetic current operator contains only two independent form factors (F_1 and F_2) for the two-body reaction. Hence we can apply a Rosenbluth separation formula to determine F_1 and F_2 experimentally as function of q^2. In contrast, we have eighteen independent structure functions, which necessitate the use of a model to determine them. However, this general form of the weak current operator avoids the recalculation of the differential cross section whenever we consider various reactions, introduce other models, or add more diagrams such as resonances to the Born diagram. Instead our formalism of the differential cross section can be used in all other considerations by only updating the eighteen invariant amplitudes of the most general hadronic weak current.

Chapter 5

SU(3) Current Algebra

5.1 Cabibbo Theory and Conserved Vector Current

A single particle weak transition vertex of a baryon is represented in terms of form factors of two-body process derived in section 4.1 particularly Eq. (4.9). Based on this equation, we specify the standard weak transition form factors at the hadronic vertex. We now consider a single baryonic weak transition, $B \to B'$, that can be written as

$$\begin{aligned}\langle B'|J^{\mu}(q)|B\rangle \quad &= \bar{u}_{B'}\left\{f_1(q^2)\gamma^{\mu} + \frac{if_2(q^2)}{2M}\sigma^{\mu\nu}q_{\nu} + f_3(q^2)q^{\mu}\right. \\ &\left. + g_1(q^2)\gamma^{\mu}\gamma_5 + \frac{ig_2(q^2)}{2M}\sigma^{\mu\nu}q_{\nu}\gamma_5 + \frac{g_3(q^2)}{2M}q^{\mu}\gamma_5\right\}u_B,\end{aligned} \tag{5.1}$$

where f_1, f_2, and f_3 are the vector, the weak magnetism and the induced scalar transition form factors, respectively; and on the other hand g_1, g_2, and g_3 are axial vector, the pseudotensor, and induced pseudoscalar transition form factors, respectively [26, p. 393].

Cabibbo in Ref. [22] hypothesised that in semi-leptonic weak interactions, weak transition currents of strongly interacting particles belong to the SU(3) current octet. Moreover, Feynman and Gell-mann in Ref. [36] proposed that the vector part of weak current is identified with the isovector part of the electromagnetic current belongs SU(3) octet; as a consequence they established the relationship between the vector weak current and the electromagnetic current by suggesting that since the electromagnetic current satisfies the conservation law $\partial_{\mu}J^{\mu} = 0$ and so does the vector weak current (i.e., $\partial_{\mu}J^{\mu}_{V} = 0$). This is what has become known as the conserved vector current (CVC) hypothesis.

Therefore, as an immediate consequence of the CVC hypothesis, the induced scalar form

factor, f_3, vanishes. In addition, it also allows the determination of the vector form factors, f_1 and f_2, from the electromagnetic transition form factors of the nucleon. Note that f_2, f_3, g_2, and g_3 arise from the effects of QCD [26]. This implies that the conservation laws associated with the strong interaction are supposed to be satisfied by these form factors. One of the symmetries of the strong interaction is the G-parity, $G = \mathcal{C}\mathcal{R}_2$, where $\mathcal{C}$ is charge conjugation and $\mathcal{R}_2$ is the rotation about 2-axis (I_2) of isospin space by an angle π. Under G-parity transformation the general weak current classified into two currents [37]. If the vector and the axial currents satisfy

$$GV^{\mu}G^{-1} = +V_V^{\mu}; \qquad GA^{\mu}G^{-1} = -A^{\mu} \tag{5.2}$$

they are called "first-class" currents; whereas, those ones with

$$GV^{\mu}G^{-1} = -V_V^{\mu}; \qquad GA^{\mu}G^{-1} = +A^{\mu} \tag{5.3}$$

are "second-class" currents. Thus, currents of $\gamma^{\mu}, \sigma^{\mu\nu}q_{\nu}, \gamma_5\gamma^{\mu}$, and $\gamma_5 q^{\mu}$ are first-class currents; however, currents formed from q^{μ} and $\sigma^{\mu\nu}\gamma_5 q_{\nu}$ are second-class currents. Therefore, the G-invariance demands the absence of second-class currents in the weak interaction which in turn results in the omission of f_3 and g_2; whereas currents with f_2 and g_3 survive. Then the weak hadronic current reduces to

$$\langle B'|J^{\mu}(q)|B\rangle = \bar{u}_{B'}\left\{f_1(q^2)\gamma^{\mu} + \frac{if_2(q^2)}{2M}\sigma^{\mu\nu}q_{\nu} + g_1(q^2)\gamma^{\mu}\gamma_5 + \frac{g_3(q^2)}{2M}q^{\mu}\gamma_5\right\}u_B. \tag{5.4}$$

Moreover, the induced pseudoscalar form factor g_3 can be connected to the axial vector form factor g_1 via the partially conserved axial current (PCAC) hypothesis and SU(3) symmetry [1]. But its contribution to the cross section of the neutrino-nucleon processes is proportional to m_{ν}/M_N; and hence this leads to neglect the current with g_3 [11]. Finally, it is worth noting that the weak current should always maintain the standard V-A form and hence Eq. (5.4) can be rewritten in a more appropriate form as

$$\langle B'|J^{\mu}(q)|B\rangle = \bar{u}_{B'}\left\{F_1(Q^2)\gamma^{\mu} + \frac{iF_2(Q^2)}{2M}\sigma^{\mu\nu}q_{\nu} - G_A(Q^2)\gamma^{\mu}\gamma_5\right\}u_B, \tag{5.5}$$

where $Q^2 = -q^2$. Therefore, Eq. (5.5) is the standard weak transition for a single fermion. Note also that F_1, F_2, and G_A are called the standard Dirac and Pauli, and axial form factors, respectively [32].

According to the standard model there are eight vector currents and axial vector currents that belong to the octet representation of SU(3) and defined as

$$V_i^{\mu} = \bar{q}\gamma^{\mu}\frac{\lambda_i}{2}q, \tag{5.6}$$

$$A_i^\mu = \bar{q}\gamma^\mu\gamma_5\frac{\lambda_i}{2}q. \tag{5.7}$$

Therefore, by choosing appropriate coefficients one can construct the electromagnetic current operator as well as the weak hadronic charged and neutral current operators from the linear combination of the vector currents and axial currents in Eq. (5.6) and (5.7). For instance, the electromagnetic current operator J_{em}^μ can be written as

$$J_{em}^\mu = V_3^\mu + \frac{1}{\sqrt{3}}V_8^\mu. \tag{5.8}$$

In what follows, the treatment of the weak transition current derivation in the SU(3) framework is done in analogy to the electromagnetic current dealt in Section 2.4. The three-component quark field q defined in Eq. (2.36) is used and the 4-dimensional Dirac gamma matrices $\tilde{\gamma}^\mu$ and $\tilde{\gamma}_5$ can be extended to 12×12 matrices γ^μ and γ_5 by using Kronecker product as follows

$$\gamma^\mu = I_3 \otimes \tilde{\gamma}^\mu; \quad \gamma_5 = I_3 \otimes \tilde{\gamma}_5 \tag{5.9}$$

Now let us define the 12-dimensional spinor field of u, d, and s quarks

$$\psi_u = \begin{pmatrix} u \\ 0 \\ 0 \end{pmatrix}, \ \psi_d = \begin{pmatrix} d \\ 0 \\ 0 \end{pmatrix}, \text{ and } \psi_s = \begin{pmatrix} s \\ 0 \\ 0 \end{pmatrix}. \tag{5.10}$$

One can construct projection operators $\hat{\Lambda}_1$, $\hat{\Lambda}_2$, and $\hat{\Lambda}_3$ which are 3×3 block matrices such that $\psi_u = \hat{\Lambda}_1 q, \psi_d = \hat{\Lambda}_2 q$, and $\psi_s = \hat{\Lambda}_3 q$; hence

$$\hat{\Lambda}_1 = \begin{pmatrix} I_4 & 0 & 0 \\ 0 & 0 & 0 \\ 0 & 0 & 0 \end{pmatrix}, \ \hat{\Lambda}_2 = \begin{pmatrix} 0 & I_4 & 0 \\ 0 & 0 & 0 \\ 0 & 0 & 0 \end{pmatrix}, \text{ and } \hat{\Lambda}_3 = \begin{pmatrix} 0 & 0 & I_4 \\ 0 & 0 & 0 \\ 0 & 0 & 0 \end{pmatrix}. \tag{5.11}$$

Thus the charged current transition at the fundamental level can be derived. For instance, we consider the weak processes where $\Delta S = 0$. The vector current for the transition d $\rightarrow$ u which is a charge raising process would have the following form

$$\bar{\psi}_u\gamma^\mu\psi_d = (\hat{\Lambda}_1 q)^\dagger\gamma^0\gamma^\mu\hat{\Lambda}_2 q \tag{5.12}$$

By applying the following properties

$$\gamma^0\hat{\Lambda}_i^\dagger\gamma^0 = \hat{\Lambda}_i^\dagger, \ \hat{\Lambda}_i^\dagger\gamma^\mu = \gamma^\mu\hat{\Lambda}_i^\dagger, \ i = 1,2,3; \text{ and } \hat{\Lambda}_1\hat{\Lambda}_j = \hat{\Lambda}_j, \ j = 2,3, \tag{5.13}$$

Eq. (5.12) becomes

$$\begin{aligned}\bar{\psi}_u\gamma^\mu\psi_d &= \bar{q}\{(I_3\otimes\tilde{\gamma}^\mu)\Lambda_2\}q \\ &= \bar{q}\left\{I_3\otimes\tilde{\gamma}^\mu\frac{\lambda_1+i\lambda_2}{2}\right\}q \\ &= V_1^\mu + iV_2^\mu.\end{aligned} \tag{5.14}$$

The form of the vector current for the inverse (i.e., the charge lowering) process u $\rightarrow$ d would also be straightforward

$$\begin{aligned}\bar{\psi}_d\gamma^\mu\psi_u &= \bar{q}\{(I_3\otimes\tilde{\gamma}^\mu)\Lambda_2^\dagger\}q \\ &= \bar{q}\left\{I_3\otimes\tilde{\gamma}^\mu\frac{\lambda_1-i\lambda_2}{2}\right\}q \\ &= V_1^\mu - iV_2^\mu.\end{aligned} \tag{5.15}$$

More importantly the strangeness changing weak processes u $\rightarrow$ s and s $\rightarrow$ u can be generalized from Eq. (5.14) and (5.15) as

$$\begin{aligned}J^\mu_{\substack{\mathrm{u}\rightarrow\mathrm{s}\\ \mathrm{s}\rightarrow\mathrm{u}}} &= \bar{q}\left\{I_3\otimes\tilde{\gamma}^\mu\frac{\lambda_4\pm i\lambda_5}{2}\right\}q \\ &= V_4^\mu \pm iV_5^\mu.\end{aligned} \tag{5.16}$$

The same argument applies for axial current transitions except that V_i^μ should be replaced with A_i^μ.

In the framework of the Cabibbo theory and SU(3) exact symmetry, the charge changing weak hadronic current operator $J^\mu_{CC,\,W_\pm}$ may be written as [26, p. 399]

$$J^\mu_{CC,\,W_\pm} = \{(V_1^\mu \pm iV_2^\mu) - (A_1^\mu \pm iA_2^\mu)\}\cos\theta_c + \{(V_4^\mu \pm iV_5^\mu) - (A_4^\mu \pm iA_5^\mu)\}\sin\theta_c; \tag{5.17}$$

whereas, based on the standard electroweak theory of Glashow, Salam and Weinberg, the weak hadronic neutral current operator $J^\mu_{NC,\,Z^0}$ may have the following form [11, 38]

$$J^\mu_{NC,\,Z^0} = V_3^\mu - A_3^\mu - \sin^2\theta_W J^\mu_{em} \tag{5.18}$$

where θ_c and θ_W the Cabibbo and Weinberg(mixing) angles, respectively.

Moreover, we introduce a more important SU(3) relation of a single-particle transition of baryons under the assumption of exact SU(3) symmetry. The matrix element of the transition between two baryon octet states B_i and B_k of currents, $\mathcal{J}_j$, which belong to SU(3) octet may be written in terms of two reduced matrix elements as follows

$$\langle B_i|\mathcal{J}_j|B_k\rangle = if_{ijk}F + d_{ijk}D \tag{5.19}$$

where F and D correspond to anti-symmetric and symmetric couplings of two SU(3) octet baryons, respectively [1]. Now we introduce the SU(3) octet states to form baryons

$$\begin{aligned} p &= \frac{1}{\sqrt{2}}(B_4 + iB_5), \quad n = \frac{1}{\sqrt{2}}(B_6 + iB_7), \quad \Sigma^{\pm} = \frac{1}{\sqrt{2}}(B_1 \pm iB_2), \\ \Xi^{-} &= \frac{1}{\sqrt{2}}(B_4 - iB_5), \quad \Xi^{0} = \frac{1}{\sqrt{2}}(B_4 + iB_5), \quad \Sigma^{0} = B_3, \ \Lambda = B_8. \end{aligned} \tag{5.20}$$

As a consequence of Eq. (5.19), the electromagnetic current J^{μ}_{em} would now be written as

$$\begin{aligned} \langle B_i \,| J^{\mu}_{em} |\, B_k \rangle &= \langle B_i |\, V^{\mu}_3 + \frac{1}{\sqrt{3}} V^{\mu}_8 \,| B_k \rangle \\ &= i \left\{ f_{i3k} + \frac{1}{\sqrt{3}} f_{i8k} \right\} F + \left\{ d_{i3k} + \frac{1}{\sqrt{3}} d_{i8k} \right\} D. \end{aligned} \tag{5.21}$$

Thus we can derive the general weak hadronic charged current transition between any two arbitrary baryon octet states B_i and B_k. For the case of CC and $\Delta S = 0$

$$\langle B_i |\, J^{\mu}_{CC,\,W^{\pm}} \,| B_k \rangle = \bar{u}_{B_i} \left\{ i(f_{i1k} \pm i f_{i2k}) F^{\mu} + (d_{i1k} \pm i d_{i2k}) D^{\mu} \right\} u_{B_k}, \tag{5.22}$$

with which the Cabibbo factor $\cos\theta_c$ must be associated, whereas, for CC and $\Delta S = \pm 1$ the hadronic process

$$\langle B_i |\, J^{\mu}_{CC,\,W^{\pm}} \,| B_k \rangle = \bar{u}_{B_i} \left\{ i(f_{i4k} \pm i f_{i5k}) F^{\mu} + (d_{i4k} \pm i d_{i5k}) D^{\mu} \right\} u_{B_k}, \tag{5.23}$$

with which the Cabibbo factor $\sin\theta_c$ must be associated. Note that F^{μ} and D^{μ} would have a form $F^{\mu}_V - F^{\mu}_A$ and $D^{\mu}_V - D^{\mu}_A$. Based on Eq. (5.21), Table. 5.1 summarizes the electromagnetic transition among baryons that belong to SU(3) octet in terms of the reduced

Table. 5.1: The electromagnetic transitions among SU(3) baryon octet.

Electromagnetic transition	$\mathcal{CG}$ coefficient of F	D
n $\to$ n	0	$-2/3$
p $\to$ p	1	$1/3$
$\Lambda \to \Lambda$	0	$-1/3$
$\Lambda \to \Sigma^0$	0	$1/\sqrt{3}$

matrix elements F and D with the corresponding Clebsch-Gordan ($\mathcal{CG}$) coefficients. Note that the electromagnetic current does not conserve isospin. Similarly, the weak hadronic charged current transition, say $J_{CC,\,W^{\pm}}$, between the $J^{\pi} = \frac{1}{2}^{+}$ baryons can also be summarized in Table. 5.2.

Table. 5.2: The matrix elements of the weak CC transition of SU(3) octet baryons.

CC Weak transition	$\lvert\Delta S\rvert$	$\mathcal{CG}$ coefficient of F	D
$p \to n$	0	1	1
$p \to \Lambda$	1	$-\sqrt{3}/\sqrt{2}$	$-1/\sqrt{6}$
$\Lambda \to \Sigma^{\pm}$	0	0	$\sqrt{2}/\sqrt{3}$
$\Sigma^0 \to \Sigma^{\pm}$	0	$\mp\sqrt{2}$	0

Table. 5.1 allows us to write down the electromagnetic transition of the nucleon (N → N) as

$$f^p(Q^2) = F(Q^2) + \frac{1}{3}D(Q^2), \tag{5.24}$$

$$f^n(Q^2) = -\frac{2}{3}D(Q^2). \tag{5.25}$$

Thus the vector parts of F and D are determined from these two from factors. That is

$$F_i^V(Q^2) = f_i^p(Q^2) + \frac{1}{2}f_i^n(Q^2), \quad i = 1, 2 \tag{5.26}$$

$$D_i^V(Q^2) = -\frac{3}{2}f_i^n(Q^2), \quad i = 1, 2 \tag{5.27}$$

where $f^p(Q^2)$ and $f^n(Q^2)$ are the nucleon form factors that are well known from experiment; and they are given by [39, 32]

$$f_1^p(Q^2) = \left(\frac{1 + \tau(1 + \lambda_p)}{1 + \tau}\right) G_D^V(Q^2), \tag{5.28}$$

$$f_2^p(Q^2) = \left(\frac{\lambda_p}{1 + \tau}\right) G_D^V(Q^2), \tag{5.29}$$

$$f_1^n(Q^2) = \left(\frac{\lambda_n \tau(1 - \eta)}{1 + \tau}\right) G_D^V(Q^2), \tag{5.30}$$

$$f_2^n(Q^2) = \left(\frac{\lambda_n(1 + \tau\eta)}{1 + \tau}\right) G_D^V(Q^2), \tag{5.31}$$

where $G_D^V(Q^2)$ is a dipole form factor

$$G_D^V(Q^2) = (1 + Q^2/M_V^2)^{-2} = (1 + 4.97\tau)^{-2}, \tag{5.32}$$

and

$$\eta = (1 + 5.6\tau)^{-1}, \quad \tau = Q^2/(4M^2); \qquad \lambda_p = 1.79, \quad \lambda_n = -1.91. \tag{5.33}$$

Therefore, the vector current form factors $F_1(Q^2)$ and $F_2(Q^2)$ of Eq. (5.5) of the CC weak transitions under consideration can easily be specified via the CVC hypothesis.

On the other hand, the standard axial current form factor $G_A(Q^2)$ is determined from the weak axial transition form factor of the nucleon as follows. From Table. 5.2 we realize that the nucleon transition has both F and D coupling. The axial parts $F^A(Q^2)$ and $D^A(Q^2)$ are given by

$$F^A(Q^2) = \frac{F}{F+D} g_A(Q^2), \tag{5.34}$$

$$D^A(Q^2) = \frac{D}{F+D} g_A(Q^2), \tag{5.35}$$

where we take $F = 0.45 \pm 0.02, D = 0.78 \pm 0.02$, and

$$g_A(Q^2) = (F+D) G_D^A(Q^2) \tag{5.36}$$

$$\tag{5.37}$$

where $F + D = 1.26$, and

$$G_D^A(Q^2) = (1 + Q^2/M_A)^{-2} = (1 + 3.31\tau(Q^2))^{-2}. \tag{5.38}$$

Thus the standard form factors of in Eq. (5.5) for some charged current weak transitions in terms of electromagnetic form factors $f^p(Q^2)$ and $f^n(Q^2)$ of the nucleon as well as $g_A(Q^2)$ are summarized in Table. 5.3; In the Born model these expressions will be used in order to determine the unknown structure functions, which are derived in Section 4.2 for three-body process, in terms of the algebraic relations arising from the assumption of exact SU(3) symmetry.

Table. 5.3: The determination of the standard weak form factors for CC transitions.

CC weak Transition	$F_1(Q^2)$	$F_2(Q^2)$	$G_A(Q^2)$
p $\to$ n	$f_1^p(Q^2) - f_1^n(Q^2)$	$f_2^p(Q^2) - f_2^n(Q^2)$	$g_A(Q^2)$
p $\to \Lambda$	$-\sqrt{\frac{3}{2}} f_1^p(Q^2)$	$-\sqrt{\frac{3}{2}} f_2^p(Q^2)$	$-\sqrt{\frac{1}{6}} \frac{3F+D}{F+D} g_A(Q^2)$
$\Sigma^\pm \to \Lambda$	$-\sqrt{\frac{3}{2}} f_1^n(Q^2)$	$-\sqrt{\frac{3}{2}} f_2^n(Q^2)$	$\sqrt{\frac{2}{3}} \frac{D}{F+D} g_A(Q^2)$
$\Sigma^\pm \to \Sigma^0$	$\mp\frac{1}{\sqrt{2}}(2f_1^p(Q^2)) + f_1^n(Q^2)$	$\mp\frac{1}{\sqrt{2}}(2f_2^p(Q^2) + f_2^n(Q^2))$	$\mp\sqrt{2}\frac{F}{F+D} g_A(Q^2)$

5.2 Weak Transition of Mesons

For the mesonic weak transition vertex we introduce four allowed matrix elements

$$\left\langle K^+(p_1')|J^\mu(q)|K^+\right\rangle = (2p_1' - q)^\mu F_{K^+}(q^2); \tag{5.39}$$

$$\left\langle K^0(p_1')|J^\mu(q)|K^0\right\rangle = (2p_1' - q)^\mu F_{K^0}(q^2); \tag{5.40}$$

$$\left\langle K^0(p_1')|J^\mu(q)|K^+\right\rangle = (2p_1' - q)^\mu F_{K^{0,+}}(q^2); \tag{5.41}$$

$$\left\langle K^+(p_1')|J^\mu(q)|K^0\right\rangle = (2p_1' - q)^\mu F^\mu_{K^{+,0}}(q^2). \tag{5.42}$$

Since Eq. (5.39) and (5.40) are carried out via neutral current, their transition form factors may also be related to that of the transition form factors of vector mesons as

$$F_{K^+} = F_{K,\rho} + F_{K,\omega} + F_{K,\phi} \tag{5.43}$$

$$F_{K^0} = -F_{K,\rho} + F_{K,\omega} + F_{K,\phi}; \tag{5.44}$$

whereas, Eq. (5.41) and (5.42) are charged current transitions and hence

$$F_{K^{+,0}} = F_{K^+} - F_{K^0} = +2F_{K,\rho} \tag{5.45}$$

$$F_{K^{0,+}} = F_{K^0} - F_{K^+} = -2F_{K,\rho}. \tag{5.46}$$

The vector meson form factors are given by

$$F_{K,\rho} = \frac{f_{\rho K\bar{K}}}{f_\rho}\frac{m_\rho^2}{m_\rho^2 - q^2}; \quad f_{\rho K\bar{K}}/f_\rho = 0.33 \pm 0.04 \tag{5.47}$$

$$F_{K,\omega} = \frac{f_{\omega K\bar{K}}}{f_\omega}\frac{m_\omega^2}{m_\omega^2 - q^2}; \quad f_{\omega K\bar{K}}/f_\omega = 0.17 \pm 0.04 \tag{5.48}$$

$$F_{K,\phi} = \frac{f_{\phi K\bar{K}}}{f_\phi}\frac{m_\phi^2}{m_\phi^2 - q^2}; \quad f_{\phi K\bar{K}}/f_\phi = 0.50, \tag{5.49}$$

where $m_\rho = 0.770$ GeV, $m_\omega = 0.783$ GeV, and $m_\phi = 1.020$ GeV.

5.3 Strong Coupling constants

One of the complications that arises when we deal with the Born term approximation for the numerical calculation of the cross section of the neutrino-induced strange particle production is the strong coupling constants, because their experimental values have not been precisely determined. However, the so far scarcely available experimental data allows SU(3) to estimate the bounds to the values of these coupling constants. Hence invoking the 20% broken SU(3)

symmetry leads to the prediction of $g_{K\Lambda N}$ and $g_{K\Sigma N}$ from the well-known coupling constant $g_{\pi NN}$ [40, 41].

$$g_{K^+\Lambda p} = -\frac{1}{\sqrt{3}}(3 - 2\alpha^D)g_{\pi NN}, \tag{5.50}$$

$$g_{K^+\Sigma^0 p} = +(2\alpha^D - 1)g_{\pi NN} \tag{5.51}$$

where α^D is a fraction of the D-type coupling, and the experimental value of $g_{\pi NN}$ is [42]

$$\frac{g^2_{\pi NN}}{4\pi} = 14.3 \pm 0.2; \quad \alpha^D = \frac{D}{F+D} = 0.644 \pm 0.006. \tag{5.52}$$

Thus the rough bounds on the values of $g_{K^+\Lambda p}$ and $g_{K^+\Sigma^0 p}$ would be

$$\frac{g_{K^+\Lambda p}}{\sqrt{4\pi}} = -4.4 \quad \text{to} \quad -3.0 \tag{5.53}$$

$$\frac{g_{K^+\Sigma^0 p}}{\sqrt{4\pi}} = +0.9 \quad \text{to} \quad +1.3. \tag{5.54}$$

However, for convenience sake we fix their values in this study to

$$\frac{g_{K^+\Lambda p}}{\sqrt{4\pi}} = -3.8; \quad \frac{g_{K^+\Sigma^0 p}}{\sqrt{4\pi}} = +1.2. \tag{5.55}$$

The values of the other strong coupling constants can be determined by making use of the isospin symmetry [43].

$$g_{K^+\Lambda p} = g_{K^0\Lambda n} \tag{5.56}$$

$$g_{K^+\Sigma^0 p} = -g_{K^0\Sigma^0 n} = g_{K^0\Sigma^+ p}/\sqrt{2} = g_{K^+\Sigma^- n}/\sqrt{2}. \tag{5.57}$$

Chapter 6

Neutrino-induced Strange Particle Production

The Feynman diagram for the reaction processes in question can be classified into two parts: the leptonic and the hadronic parts. The weak transitions of leptons are specified on the basis of the V-A theory due to their close analogy to the electromagnetic counterparts, which are completely described by QED [30, p. 111-123]. What makes the development of weak theory for lepton relatively simple is that leptons have been identified as structureless fermions. However, the structure of the weak hadronic interaction is not well understood as a result of hadron structure and the associated QCD effects at the vertex.

In order to perform numerical calculations of the differential cross section for the strange particle production processes, we introduce the Born term approximation. In this model the hadronic vertex is described by the lowest order Feynman diagrams (i.e., only those processes carried out via a single gauge boson exchange) with parametrization form factors which allows us to include the high order contributions and circumvent the QCD effect. The eighteen unknown parameters in the general hadronic current given in Eq. (4.20) will be extracted after carefully expanding the Born diagram in terms of the basis constructed in the expression of the weak hadronic current under consideration.

6.1 Born Term Model

This approximation was used in the study of associated production of strange particles by R. Shrock, H. Dewan, and W. Mechlenburg [11, 13, 12] and also in pion photoproduction by S. L. Adler *et al*, R. L. Workman *et al*, D. Drechsel *et al*, and Q. Zhao *et el* [44, 45, 46, 47].

The general form of the Born term model contains the three tree diagrams labelled as s-channel, t-channel, and u-channel. But at the practical level the all three channels may or may not contribute to the weak hadronic current of a particular reaction. Fig. 2.1 shows the expansion of the hadronic vertex in terms of tree diagrams. The mediators of these channels are the bound state hadrons. Table. 6.1 gives a summary of the exchange particles in the Born diagram [48, 49].

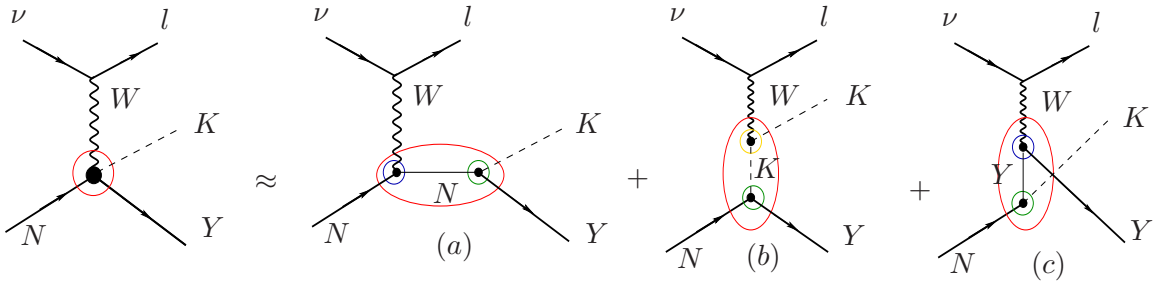

Fig. 6.1: The Born diagram of neutrino-induced weak production of strange particles.

Note that in Fig. 6.1, (a), (b), and (c), diagrams correspond to s-channel, t-channel, and u-channel, respectively. In what follows the detailed derivation of the weak hadronic current will be made. A quick look at Fig.6.1 would lead us to write the hadronic weak current operator as

$$\hat{J}^{\mu} = \hat{J}^{\mu}_{s} + \hat{J}^{\mu}_{t} + \hat{J}^{\mu}_{u}. \tag{6.1}$$

Table. 6.1: The exchange particles and the corresponding propagators of the s-channel, t-channel, and u-channel.

Channel	Exchange particle	Propagator
s-channel	N = $\{p(939), n(939)\}$	$\frac{\not{q} + \not{p}_1 + M_N}{s - M_N^2}$
t-channel	K = $\{K^0(498), K^+(494)\}$, K^* = $\{K^*(892), K_1^*(1270)\}$	$\frac{1}{t - M_K^2}$
u-channel	Y = $\{\Sigma^+(1189), \Sigma^0(1192), \Sigma^-(1197), \Lambda(1116)\}$	$\frac{\not{q} - \not{p}'_2 + M_Y}{u - M_Y^2}$

Note that s, t and u are the kinematical variables defined in Eq. (3.19), (3.20), and (3.21). Every tree diagram contains the weak and strong transition vertices. In the case of weak transition there might be either vertices for pure baryonic transition or pure mesonic

transition. On the other hand, the strong coupling vertices have three external lines associated with them: two baryon lines and one meson line.

6.2 Associated production of strange particles

Here we focus on the pair-production of pseudoscalar-meson with $S = 1$ (K^+ and K^0) and hyperon with $S = -1$ ($\Sigma^{\pm}$, Σ^0, and Λ) via the weak interaction of neutrino and nucleon.

To begin with, we first apply the Born term approximation to a typical reaction:

$$\nu + \mathrm{n} \to \mu^- + K^+ + \Lambda$$

which is the CC and $\Delta S = 0$ current-induced associated production. Then we extend the method we develop here to the other reaction channels under consideration for the calculation of the corresponding differential cross sections.

6.2.1 *s*-channel: Fig. 6.2

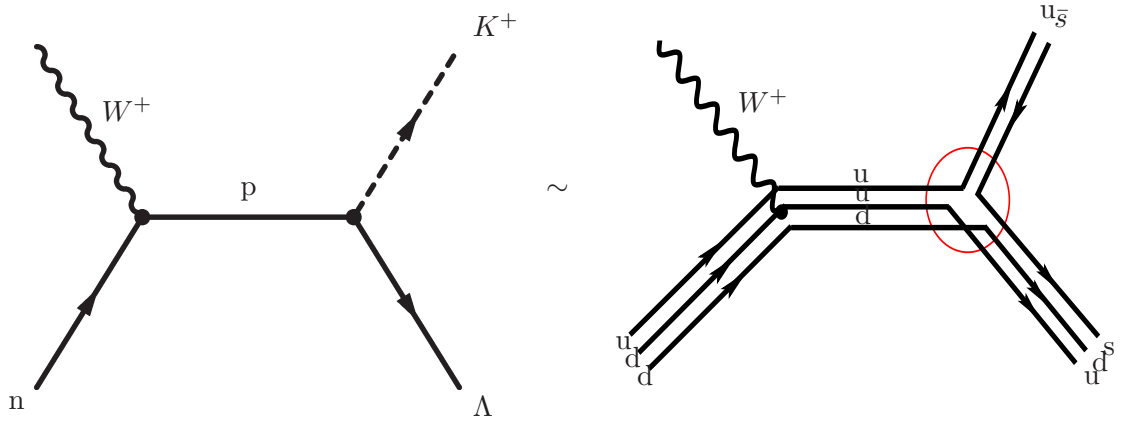

Fig. 6.2: The Feynman diagram of the *s*-channel.

This channel contains two vertices:

i. The weak charged current transition vertex of nucleon, n $\to$ p, which may be written in terms of the general weak transition form factors.

$$\langle p|\, \hat{J}^{\mu}_{CC,\,W^+}(q)\, |n\rangle = \bar{u}_p \left\{ F_1^N(q^2)\gamma^\mu + \frac{iF_2^N(q^2)}{2M}\sigma^{\mu\nu}q_\nu - G_A^N(q^2)\gamma^\mu\gamma_5 \right\} u_n. \tag{6.2}$$

In other words, the weak current coupling with the gauge boson can be parametrized by the standard vector and axial form factors.

ii. The pseudoscalar strong interaction vertex is denoted by

$$\langle K^+\Lambda|p\rangle = g_{K^+\Lambda p}\bar{u}_\Lambda\gamma_5 u_p. \tag{6.3}$$

We now apply the Feynman rules on the tree diagram, Fig. 6.2, of the s-channel. Note that the propagator of this channel is given in Table. 6.1. Thus the contribution of the s-channel to the total weak hadronic current would have the following form

$$\bar{u}_\Lambda J^\mu_{s,\,CC}u_n = \bar{u}_\Lambda\left[g_{K^+\Lambda p}\gamma_5\frac{\not{q}+\not{p}_1+M_N}{s-M_N^2}J^\mu_{CC,\,W^+}(n\to p)\right]u_n, \tag{6.4}$$

where we have used the notation $J^\mu_{CC,\,W^+}(B\to B') = \langle B'|\,\hat{J}^\mu_{CC,\,W^+}(q)\,|B\rangle$.

6.2.2 t-channel: Fig. 6.3

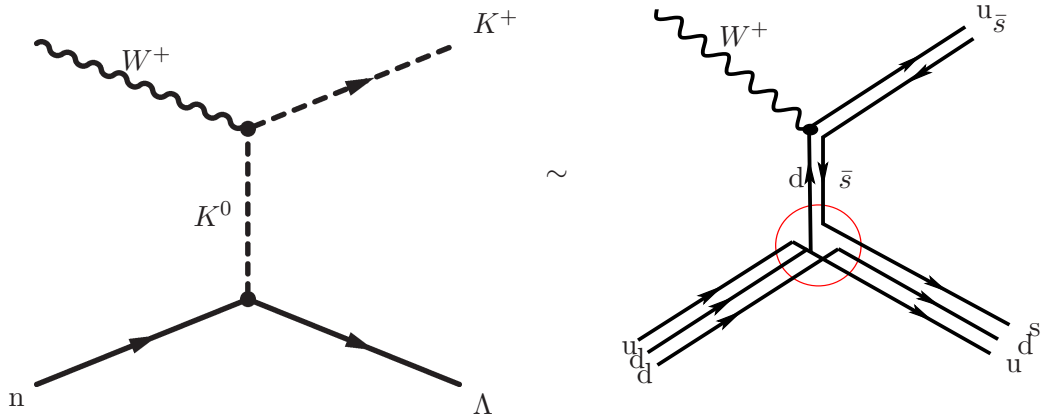

Fig. 6.3: The Feynman diagram of the t-channel.

The two vertices of the t-channel:

i. The weak charged current transition vertex of pseudoscalar meson $K^0\to K^+$ which takes the form of Eq. (5.42). That is

$$\langle K^+(p_1')|\,\hat{J}^\mu_{CC,\,W^+}(q)\,|K^0\rangle = (2p_1'-q)^\mu F_{K^+,0}(q^2)$$

ii. The strong interaction vertex has two baryon and two pseudoscalar meson external lines. Again the coupling takes the form

$$\langle K^0\Lambda|n\rangle = g_{K^0\Lambda n}\bar{u}_\Lambda\gamma_5 u_n \tag{6.5}$$

By referring to Table. 6.1 for the propagator of the t-channel, we may write down the contribution of this current as follows

$$\bar{u}_\Lambda J^\mu_{t,\,CC} u_n = \bar{u}_\Lambda \left[g_{K^0\Lambda n}\gamma_5 \frac{1}{t - M_K^2} J^\mu_{CC,\,W^+}(K^0 \to K^+) \right] u_n. \tag{6.6}$$

6.2.3 u-channel: Fig. 6.4

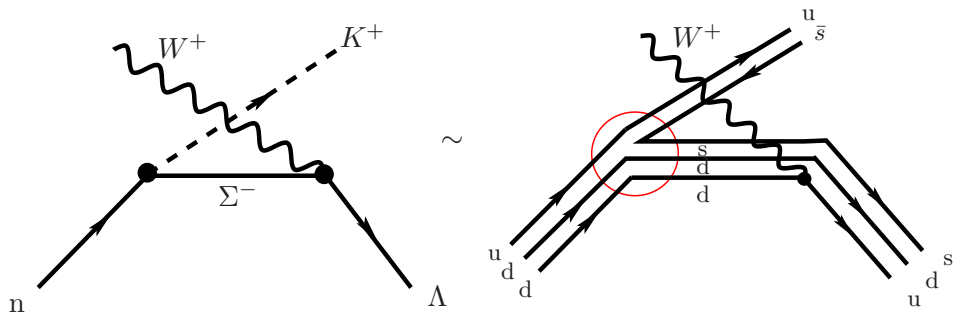

Fig. 6.4: The Feynman diagram of the u-channel.

Similarly, the two vertices of u-channel specified below

i. The weak charged current transition vertex is that of two hyperons: $\Sigma^- \to \Lambda$; hence the transition current has the same form as Eq. (6.2).

$$\langle \Lambda | \, \hat{J}^\mu_{CC,\,W^+}(q) \, | \Sigma^- \rangle = \bar{u}_\Lambda \left\{ F_1^Y(q^2)\gamma^\mu + \frac{iF_2^Y(q^2)}{2M}\sigma^{\mu\nu}q_\nu - G_A^Y(q^2)\gamma^\mu\gamma_5 \right\} u_{\Sigma^-} \tag{6.7}$$

ii. The strong interaction vertex connected to two baryons and one pseudoscalar-meson and the coupling is given by

$$\left\langle K^+\Sigma^- | n \right\rangle = g_{K^+\Sigma^- n}\bar{u}_{\Sigma^-}\gamma_5 u_n \tag{6.8}$$

Thus by recalling its propagator given in Table. 6.1 the current contribution of u-channel also becomes

$$\bar{u}_\Lambda J^\mu_{u,\,CC} u_n = \bar{u}_\Lambda \left[J^\mu_{CC,\,W^+}(\Sigma^- \to \Lambda) \frac{\not{q} - \not{p}'_2 + M_{\Sigma^-}}{u - M^2_{\Sigma^-}} g_{K^+\Sigma^- n}\gamma_5 \right] u_n. \tag{6.9}$$

6.2.4 Extraction of the Eighteen Structure Functions

The individual currents in Eq. (6.4), (6.6), and (6.9) will be expanded exhaustively in terms of the eighteen independent basis elements we developed for the most general weak hadronic transition of three-body processes in chapter 4 in Eq. (4.20). Then we proceed to identify the values of the unknown amplitudes corresponding to the same basis elements.

For the s-channel the expansion is done by making use of identities listed from Eq. (A.13) through (A.19) repeatedly and the Dirac equation Eq. (2.5) for the on-shell particles. After rigorous mathematical steps we finally obtain

$$\begin{aligned} J^{\mu}_{s,CC} &= G_s \left\{ -2G_A^N p_1^{\mu} + 2M_N G_A^N \gamma^{\mu} + \left(\frac{q^2}{2} + p_1 \cdot q \right) \frac{F_2^N}{M} \gamma_5 \gamma^{\mu} - \frac{M_N}{M} F_2^N q^{\mu} \gamma_5 \right. \\ &\left. + 2F_1^N p_1^{\mu} \gamma_5 + (F_1^N + \frac{M_N}{M} F_2^N) \gamma_5 \not{q} \gamma^{\mu} - G_A^N \not{q} \gamma^{\mu} - \frac{F_2^N}{2M} \gamma_5 q^{\mu} \not{q} - \frac{F_2^N}{M} \gamma_5 p_1^{\mu} \not{q} \right\}, \end{aligned} \tag{6.10}$$

where

$$G_s = g_{K^+ \Lambda p} \frac{1}{s - M_N^2} \tag{6.11}$$

The contribution of the t-channel would be

$$J^{\mu}_{t,CC} = G_t \left\{ (F_{K^+,0}) q^{\mu} \gamma_5 + (2F_{K^+,0}) p_1^{\mu} - (2F_{K^+,0}) p'^{\mu}_2 \gamma_5 \right\}, \tag{6.12}$$

where

$$G_t = g_{K^0 \Lambda n} \frac{1}{t - M_{K^0}^2}. \tag{6.13}$$

The t-channel clearly contributes only to the axial part of the total current.

Similar to the s-channel calculation, the u-channel contribution term Eq. (6.9) is expanded by applying the identities given from Eq. (A.13) through (A.19) and the on-shell condition and we would eventually obtain

$$\begin{aligned} J^{\mu}_{u,CC} &= G_u \left\{ 2G_A^Y q^{\mu} - 2G_A^Y p'^{\mu}_2 + (M_{\Lambda} - M_{\Sigma^-}) G_A^Y \gamma^{\mu} - \frac{F_2^Y}{2M} q^{\mu} \gamma_5 \not{q} - G_A^Y \not{q} \gamma^{\mu} \right. \\ &- 2F_1^Y p'^{\mu}_2 \gamma_5 + \frac{F_2^Y}{M} p'^{\mu}_2 \gamma_5 \not{q} - \left[(M_{\Lambda} + M_{\Sigma^-}) F_1^Y + \left(q \cdot p'_2 - \frac{q^2}{2} \right) \frac{F_2^Y}{M} \right] \gamma_5 \gamma^{\mu} \\ &\left. + \left[2F_1^Y + (M_{\Lambda} - M_{\Sigma^-}) \frac{F_2^Y}{2M} \right] q^{\mu} \gamma_5 - \left[F_1^Y + (M_{\Lambda} - M_{\Sigma^-}) \frac{F_2^Y}{2M} \right] \gamma_5 \not{q} \gamma^{\mu} \right\}, \end{aligned} \tag{6.14}$$

where

$$G_u = g_{K^+\Sigma^- n}\frac{1}{u - M_{\Sigma^-}}. \tag{6.15}$$

Note that Table. 5.3 gives the values of the standard weak form factors.

$$F_i^N(Q^2) = f_i^p(Q^2) - f_i^n(Q^2), \quad G_A^N(Q^2) = g_A(Q^2); \tag{6.16}$$

$$F_i^Y(Q^2) = -\sqrt{\frac{3}{2}}f_i^n(Q^2), \qquad G_A^Y(Q^2) = \sqrt{\frac{2}{3}}\frac{D}{F+D}g_A(Q^2). \tag{6.17}$$

Now by applying a method of identification of Eq. (6.10), (6.12), and (6.14) with Eq. (4.20), the unknown amplitudes can be determined for s-, t-, and u-channels, respectively. Then the total weak hadronic current of the $\nu n \to \mu^- K^+ \Lambda$ according to Born term model, therefore, is the sum of the individual contributions of these channels. Table. 6.2 lists the corresponding contribution to the unknown amplitudes of the most general weak hadronic transition current for the particular processes under question.

Table. 6.2: Extraction of the unknown amplitudes for the $\nu n \to \mu^- K^+ \Lambda$ reaction process.

Amplitudes	s-channel.	u-channel	t-channel
$\tilde{A}_1$	–	$2G_uG_A^Y$	–
$\tilde{A}_2$	$-2G_sG_A^N$	–	–
$\tilde{A}_3$	–	$-2G_uG_A^Y$	–
$\tilde{A}_4$	–	–	–
$\tilde{B}_1$	$-G_s\frac{M_N}{M}F_2^N$	$G_u\left[2F_1^Y + (M_\Lambda - M_{\Sigma^-})\frac{F_2^Y}{2M}\right]$	$G_tF_{K^+,0}$
$\tilde{B}_2$	$2G_sF_1^N$	–	$2G_tF_{K^+,0}$
$\tilde{B}_3$	–	$-2G_uF_1^Y$	$-2G_tF_{K^+,0}$
$\tilde{B}_4$	–	–	–
$\tilde{C}_1$	$2M_NG_sG_A^N$	$G_u(M_\Lambda - M_{\Sigma^-})G_A^Y$	–
$\tilde{C}_2$	–	–	–
$\tilde{C}_3$	–	–	–
$\tilde{C}_4$	–	–	–
$\tilde{D}_1$	$G_s\left(\frac{q^2}{2} + p_1\cdot q\right)\frac{F_2^N}{M}$	$-G_u\left[(M_\Lambda + M_{\Sigma^-})F_1^Y + \left(q\cdot p'_2 - \frac{q^2}{2}\right)\frac{F_2^Y}{M}\right]$	–
$\tilde{D}_2$	$-G_s\frac{F_2^N}{2M}$	$-G_u\frac{F_2^Y}{2M}$	–
$\tilde{D}_3$	$-G_s\frac{F_2^N}{M}$	–	–
$\tilde{D}_4$	–	$G_u\frac{F_2^Y}{M}$	–
$\tilde{D}_5$	$-G_sG_A^N$	$-G_uG_A^Y$	–
$\tilde{D}_6$	$G_s(F_1^N + \frac{M_N}{M}F_2^N)$	$-G_u\left[F_1^Y + (M_\Lambda - M_{\Sigma^-})\frac{F_2^Y}{2M}\right]$	–

Therefore, this result allows us to compare the differential cross section of individual chan-

nels to one another and to indicate a channel that contributes dominantly to the full term differential cross section of the Born approximation. Note that a similar calculation is made for the rest of CC and $\Delta S = 0$ reactions and the corresponding amplitudes of the general hadronic weak currents of these reaction channels are given in Appendix D.

Chapter 7

Numerical Results and Discussion

In what follows the result of numerical calculation via the Born term approximation is presented. Upon extracting the amplitudes of the weak hadronic current $J^{\mu}(q)$, we used the Fortran 90/95 and Python programming languages to code the numerical calculation of the differential cross sections for the CC and $\Delta S = 0$ associated production reactions given in Table. 2.6. The calculation is made in the threshold energy region. We now recall the expression given in Eq. (3.54) which allows us to investigate the angular distribution of the differential cross section with respect to the outgoing kaon angle for the reactions under consideration. Note also that we are working in the natural units ($\hbar = c = 1$).

Table. 7.1: Physically allowed tree diagrams for the four reactions.

Reaction	s-channel	u-channel	t-channel
ν_{μ} p $\rightarrow \mu^{-}K^{+}\Sigma^{+}$ (CC1)	–	2	1
ν_{μ} n $\rightarrow \mu^{-}K^{0}\Sigma^{+}$ (CC2)	1	2	–
ν_{μ} n $\rightarrow \mu^{-}K^{+}\Sigma^{0}$ (CC3)	1	1	1
ν_{μ} n $\rightarrow \mu^{-}K^{+}\Lambda$ (CC4)	1	1	1

In chapter 6 and Appendix D the unknown amplitudes are determined via the Born model. However, out of the eighteen amplitudes no contribution has come from $\tilde{A}_4, \tilde{B}_4, \tilde{C}_2, \tilde{C}_3$, and $\tilde{C}_4$ amplitudes for the four reaction channels. All the three channels contribute only to some reactions of the strange particle production. Table. 7.1 summarizes the channels allowed in

the corresponding Born diagrams of the four CC reactions. Moreover, the separate treatment of individual channels allows us to compare their contribution to the total differential cross section. The contributions of s-, u-, and t-channels comes through nine, ten, and three amplitudes of the general hadronic current, respectively.

The choice of the kinematical inputs: E_k, $E_{k'}$, and θ', is made in such a way that the square of the four-momentum transfer remains constant for all spectrum of calculations of individual reactions. We take two fixed values of $Q^2 = -q^2$. It is worth noting that we established the general formalism in chapter 3 in the limit of small q^2. Two fixed values are carefully selected in a region where the dominant contribution more or less comes from the tree diagrams relative to the nearby resonances. These two choices are $Q^2 = 0.035\,\mathrm{GeV}^2$ and $Q^2 = 0.25\,\mathrm{GeV}^2$. In this way seven sets of input values are constructed for individual choices of Q^2.

For the sake of relevance of this study we limit the range of the incident energy, E_k, of the neutrino in the threshold energy region. Otherwise, the reliability of the Born term model becomes questionable. Thus we set the threshold energy, E_{th}, of each reaction as the lowest bound to the incoming neutrino energy. As the energy increases beyond the threshold energy region, more and more resonances have to be included to obtain a reasonable result; this in turn gives rise to a number of complications. Moreover, since the muon is an on-shell particle, its energy can never be less than its mass, $m_\mu = 0.106\,\mathrm{GeV}$, as demanded by the relativistic energy-momentum relation. Note that the mass parameter M in the expression of the standard two-body weak transition of baryon, given in Eq. (5.5), is fixed at $M = 0.939$ GeV.

On the other hand, we suppose that in any of the reaction under consideration the final state lepton scattered at forward angles; hence we choose to fix its values at $\theta' = 0.5$ deg. Therefore, based on Eq. (3.5) one can finally reach at the following equation that allows us to numerically determine $E_{k'}$ provided that the values of Q^2, Ek and θ' are given.

$$\frac{Q^2 + m_l}{2E_k} = E_{k'} - \cos\theta'(E_{k'}^2 - m_l^2)^{\frac{1}{2}} \tag{7.1}$$

where m_l is the mass of the outgoing lepton. For the neutral current case this equation reduces to $Q^2 = 4E_kE_{k'}\sin^2(\theta'/2)$. One may use the Newton method of iteration to approximate the value of $E_{k'}$. Table. 7.2 and 7.3 summarize the kinematical inputs for the two fixed values of Q^2.

We recall that the general expression of the differential cross section for charged current reactions was derived in chapter 3 and written in Eq. (3.54). The dimension the expression becomes $\mathrm{GeV}^{-3}\,\mathrm{srad}^{-1}$. We convert the unit into $\mathrm{nbarn}\,\mathrm{GeV}^{-1}\,\mathrm{srad}^{-1}$ by using the following

Table. 7.2: The kinematical inputs E_k and $E_{k'}$ at fixed values $Q^2 = 0.035\,\mathrm{GeV}^2$ and $\theta' = 0.5$ deg.

E_k (GeV)	2.00	2.50	3.00	3.50	4.00	4.50	5.00
$E_{k'}$ (GeV)	0.50	0.61	0.74	0.86	1.00	1.11	1.23

Table. 7.3: The kinematical inputs E_k and $E_{k'}$ at fixed values $Q^2 = 0.25\,\mathrm{GeV}^2$ and $\theta' = 0.5$ deg.

E_k (GeV)	2.00	2.50	3.00	3.50	4.00	4.50	5.00
$E_{k'}$ (GeV)	0.12	0.13	0.15	0.17	0.19	0.21	0.23

relation

$$\mathrm{GeV}^2 = 0.389 \times 10^6 \mathrm{nb}. \tag{7.2}$$

Moreover, we adopt the following notations to label the generated curves: 's-chan', 't-chan', 'u-chan', and 'Full term' stand for the contribution of s-channel, t-channel, u-channel and the total contribution of all permissible tree diagrams to the particular reaction, respectively. In the plots that compare the contribution of the two helicity state of the final lepton the labels are 'h$' = -1$', 'h$' = +1$', and 'Total sum', which refer to the contributions of the negative helicity state, the positive helicity state, and the sum over the two possible helicity states, respectively. This goes in agreement with the idea that in this study we have chosen to investigate strange particle production reactions with unpolarized final state particles. Thus all the contributions and the total differential cross sections are obtained by summing over the helicity of the muon and the spin state of the hyperon. Note that the positive helicity survives partly due to the non-zero mass of the muon.

Fig. 7.1, 7.2, 7.3, and 7.4 are the angular distributions of the differential cross section with respect to the kaon angle θ'_1 for CC1, CC2, CC3, and CC4, respectively, at $Q^2 = 0.035\,\mathrm{GeV}^2$ and $\theta' = 0.5$ deg; and Fig. 7.6, 7.7, 7.8, and 7.9 are also the corresponding angular distributions at $Q^2 = 0.25\,\mathrm{GeV}^2$ and $\theta' = 0.5$ deg.

The seven plots of CC1 for both cases have shown that the differential cross section of the process is forward-peaked and starts to fall as the kaon angle increases. This pattern remains unchanged for the range of the incident neutrino energy, E_k, that runs from 2.0 Gev to 5.0 GeV. In addition, the cross section increases with E_k (more significantly at its peak).

Since the contribution of the u-channel comes from Λ and Σ^0 exchanges, it dominants the contribution that comes from the t-channel. The differential cross section contribution of the u-channel from Λ exchange dominants the one from Σ^0 exchange; the corresponding differential cross section contributions of the u-channel are proportional to the square of the strong coupling constants $g_{K^+\Lambda p}$ and $g_{K^+\Sigma^0 p}$. Hence it can be checked in chapter 5 that $g^2_{K^+\Lambda p}$ is greater than $g^2_{K^+\Sigma^0 p}$ (approximately by a factor of 10). At forward angles the full term curve is suppressed relative to that of the u-channel which indicates that the t-channel, which contributes only to the axial part, destructively interferes with the u-channel.

For the case of CC2 we deduce the following. In this reaction only the s- and u-channels contribute. In general, the u-channel dominates for the two choices of Q^2 (see Fig. 7.2 and 7.7). However, at the smaller value of Q^2 the s-channel shifts the peak to the right. The higher the incident energy gets, the farther the peak slides away from the forward angle. The same trend would have been observed at the higher value of Q^2, had it not been for the relatively negligible contribution from s-channel. The curves level off as θ'_1 gets higher and higher; and also the two channels together enhance the full term cross section. Moreover, the peak of the differential cross section of the full term increases with E_k.

The plots of CC3, on the other hand, display that s- and t-channels together cause a significant suppression of the full term cross section with respect to the u-channel at forward angle. In the case of $Q^2 = 0.035\,\mathrm{GeV}^2$ (see Fig. 7.3), the u-channel dominates the full term without interruption in the E_k range from 2.0 to 3.5 GeV. However, for the energy above this range that is not the case. In a similar manner to CC2, the peak of the cross section shifts toward $\theta'_1 = 20$ deg as E_k keeps increasing; and this possibly accounts for the presence of the s-channel in the Born diagram of the reaction. The same applies for the case of $Q^2 = 0.25\,\mathrm{GeV}^2$ except for the suppression of the full term occurs only at forward angles for all input E_k's (see Fig. 7.8). However, as the kaon angle increases the contribution of s- and t-channels, significantly the former, start to enhance the full term cross section above all the contributions until it reaches its peak and then smoothly falls down.

Now we turn our attention to the plots of CC4 given in Fig. 7.4 and 7.9. We first consider Fig. 7.4. The differential cross section is no longer forward-peaked due to the fact that u-channel does not show a strict dominance over the others even though it seems to be largest. However, as the kaon angle increases the peak is formed within a range of $20 - 40$ deg where the s-channel shows a significant dominance over the other channels. In fact, the contributions of all three channels appear to be quite relevant. Here, the s-channel and t-channel, particularly the former, creates the peak away from the forward angle and as the incident energy increases

they start to influence the shape of the full term differential cross section too. The shifting of the peak of the cross sections of CC4 reaction shows a significant influence of these channels. However, in most of the reactions the t-channel contribution is negligible. The same applies to CC3 too.

In the case of Fig. 7.9 the full term attains its peak at forward angle. Here s-channel does not play the same role in affecting the shape of the full term, noticeably as it did in the former case, even though it is still shows dominance over the others and also slows the rapid fall of the cross section as θ_1' increases, particularly for $E_k = 4.50$ and 5.00 GeV. Generally, the last plots in the two figures show that the differential cross section increases with the incident energy and the gap gets bigger and bigger at the peak.

One may also compare CC3 and CC4 because of the fact that both involve almost identical particles. For instance, their final state hyperons Σ^0 and Λ have the same quark structure. It also is also notable from Fig. 7.3 and 7.4 that at the low Q^2 their cross sections are approximately similar in shape even though this changes as Q^2 relatively gets bigger (compare Fig. 7.8 and 7.9). However, a closer look at the cross sections of the two reactions shows a significant difference between them. For instance, in CC3 case the u-channel strictly dominates all the others, whereas in CC4 s-channel dominates in a wide range of kaon angle. These differences may be explained in terms the SU(3) isospin symmetry. Clearly, Σ^0 belongs to isospin triplet state ($I = 1$) and Λ, on the other hand, forms isospin singlet state (I = 0); and hence the channels of CC3 and CC4 have different weak transition form factors and the strong coupling constants. Moreover, there is a difference between their masses.

Even though we have employed the SU(3) exact symmetry in order to determine the parametrization form factors for the weak transition of these channels, one may also employ the SU(2) isospin symmetry without the knowledge of SU(3) to derive the form factors for the s-channel; and hence this channel may not be considered as a nice candidate to test SU(3) flavour quark model. So we can safely state that the dynamics of SU(3) exact symmetry strongly comes through u-channel and t-channel.

In summary, one of the peculiar features of these plots is that almost all of the differential cross sections attain their peaks at forward angles. On the other hand, the curves display the rapid decrement as the kaon angle increases away from the forward angle. It is also clearly shown that the u-channel dominates all the other channels, particularly, in CC1 and CC2 the major contribution comes form this channel.

At this point, we look at Fig. 7.5 and 7.10 in order to compare the differential cross sections

that come from the negative helicity and the positive helicity states of the muon. Fig. 7.5 shows the clear dominance of the contribution of the negative helicity state over the positive one. Especially at the peaks of the cross sections the dominance of more significantly large; and hence almost the total contribution to the differential cross section comes from the negative helicity state of the muon. On the other hand, Fig. 7.10 shows that the positive helicity state becomes dominant at $Q^2 = 0.25\,\mathrm{GeV}^2$ and $\theta' = 0.5$ deg. Thus one can observe the asymmetry that does exist in the weak interaction in choosing between the left-handed and right-handed leptons. In the former case if we compare the muon mass to its energy we clearly see why the negative helicity is dominant. Thus, left-handedness of leptons is a high energy phenomenon. Note that whenever we make a comparison we specifically refer to the peaks of the cross sections.

In general, the cross section increases with E_k in all of the four reactions. For very small Q^2 the differential cross section is no longer forward-peaked if the s-channel is present in the reaction rather the peak shifts to higher angle ranging from 15 to 40 deg. Apart from that, all the curve have the cutoff point that arises from the non-zero mass of the muon. Moreover, in Fig. 7.11 our result shows that at forward angle, the angular distribution of the differential cross section for CC1 clearly dominates all the others, whereas CC3 gives the lowest cross section and the rest lies between the two extremes (Note that the two plot at the top of Fig. 7.11 are for $Q^2 = 0.035\,\mathrm{GeV}^2$ and $\theta' = 0.5$ deg, whereas the two plots at the bottom are for the other case).

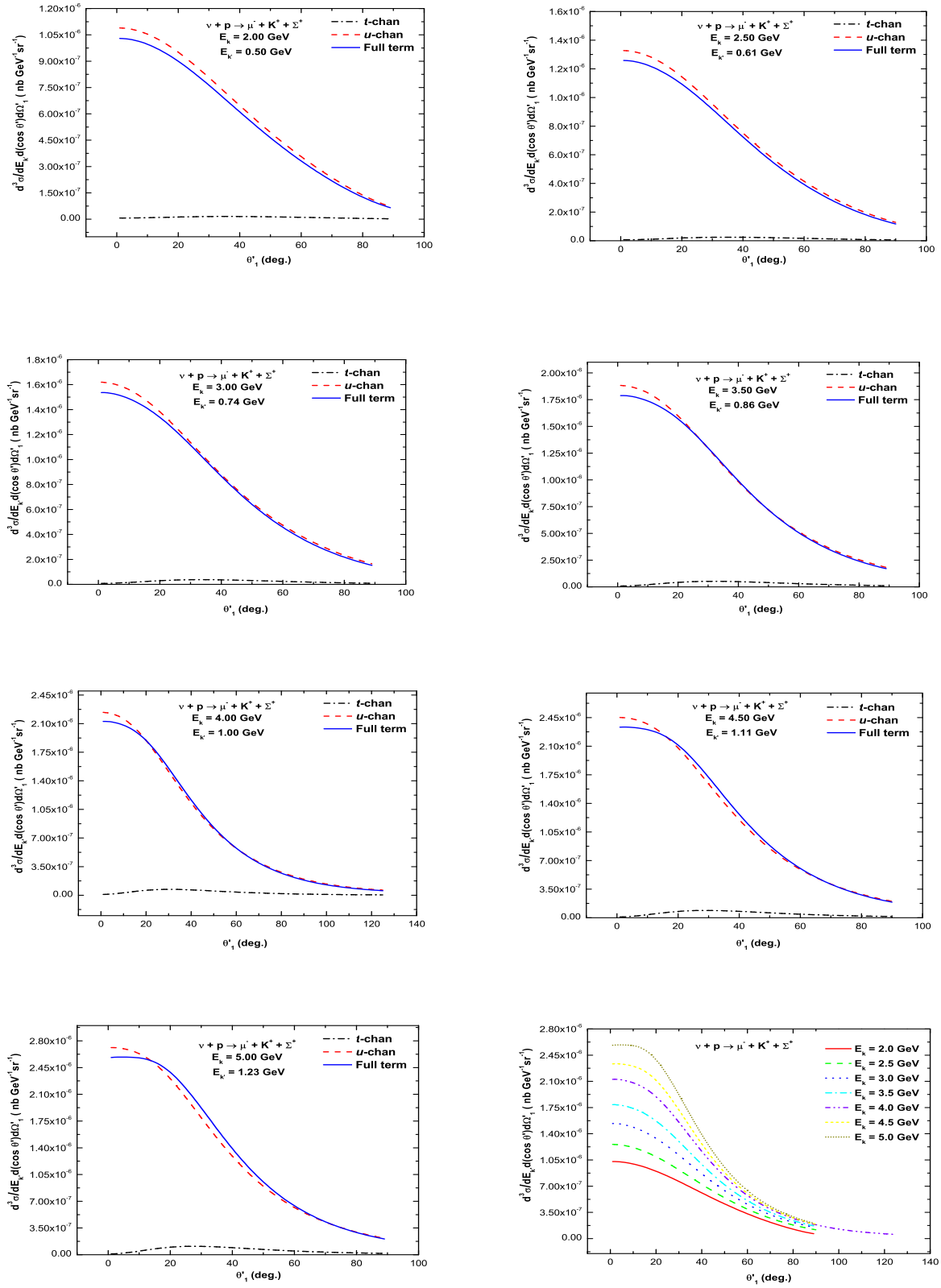

Fig. 7.1: The differential cross section against the kaon angle for CC1 at $Q^2 = 0.035\,\mathrm{GeV}^2$ and $\theta' = 0.5$ deg.

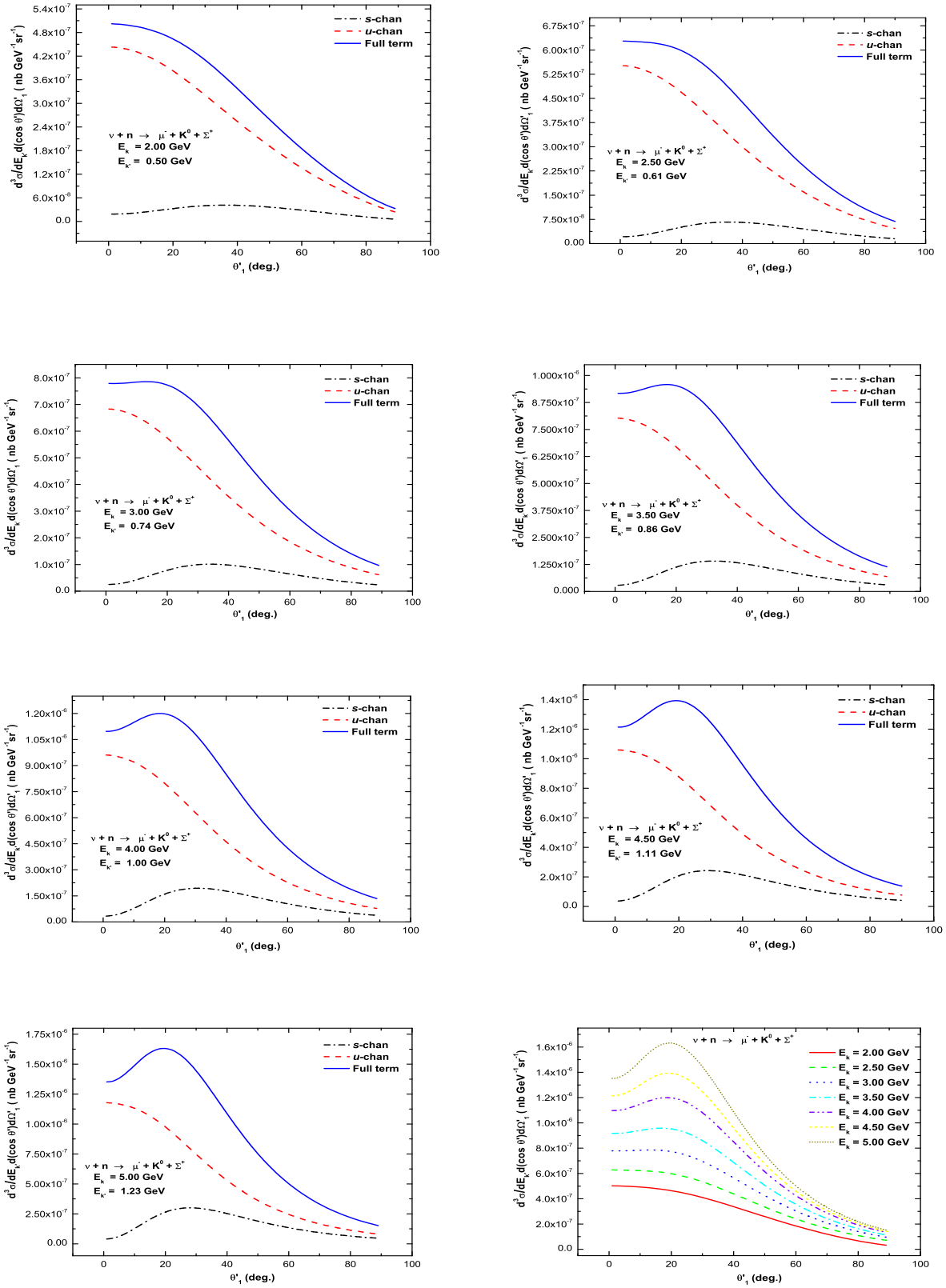

Fig. 7.2: The differential cross-section against the kaon angle for CC2 at $Q^2 = 0.035\,\mathrm{GeV}^2$ and $\theta' = 0.5$ deg.

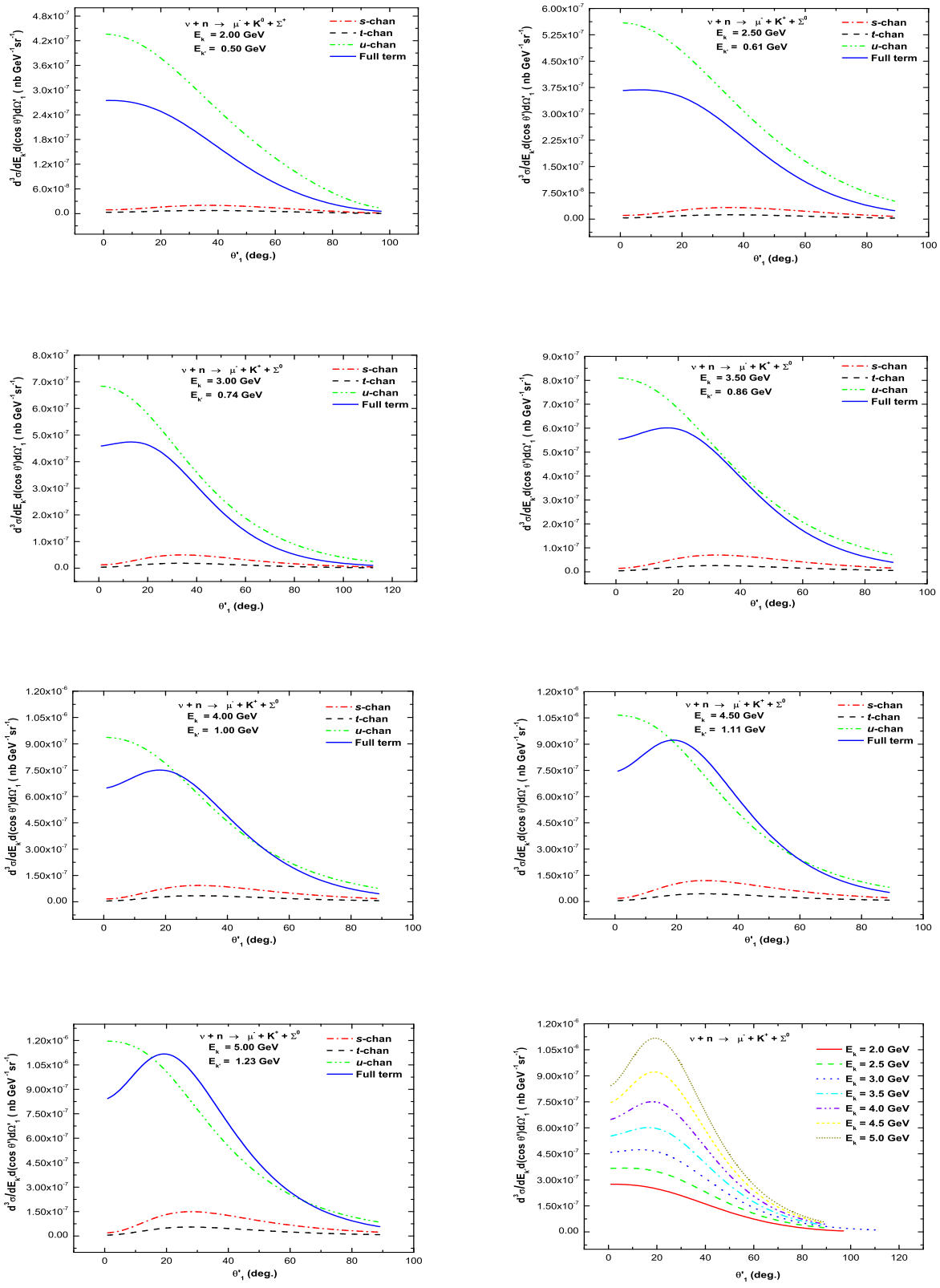

Fig. 7.3: The differential cross-section against the kaon angle for CC3 at $Q^2 = 0.035\,\mathrm{GeV}^2$ and $\theta' = 0.5$ deg.

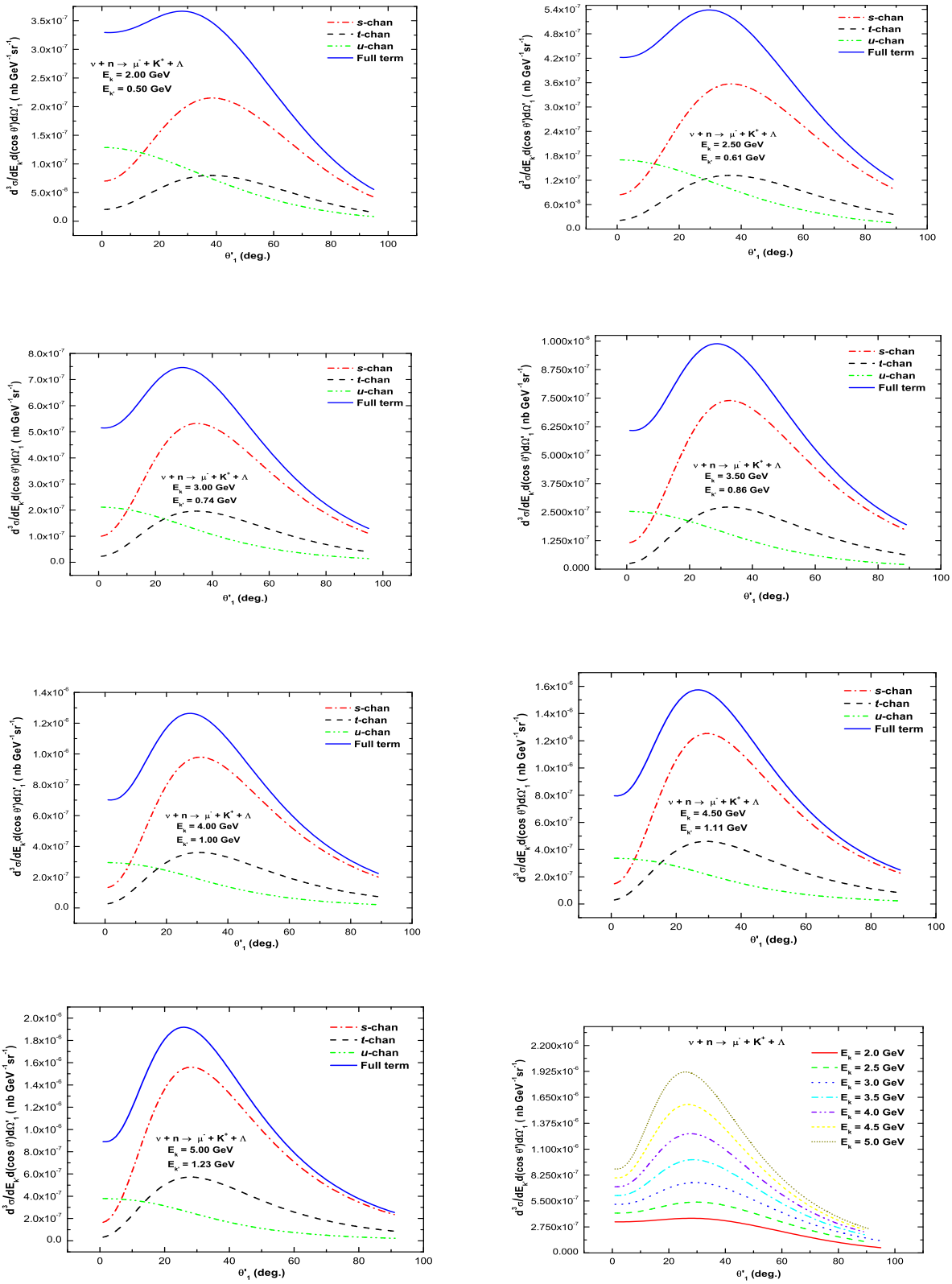

Fig. 7.4: The differential cross-section against the kaon angle for CC4 at $Q^2 = 0.035\,\mathrm{GeV}^2$ and $\theta' = 0.5$ deg.

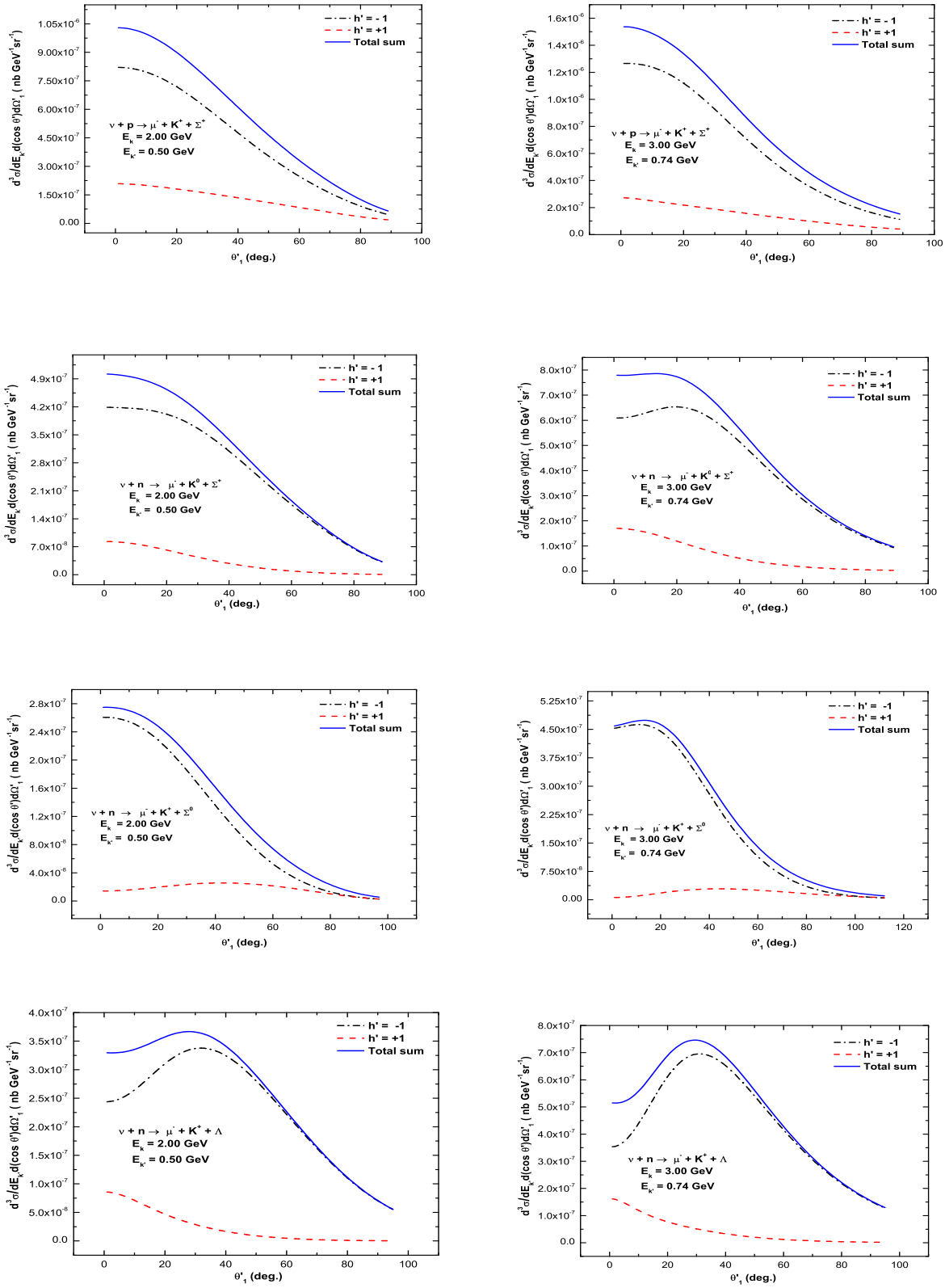

Fig. 7.5: The differential cross sections of CC1, CC2, CC3, and CC4 against the kaon angle for $h' = -1$ and $h' = +1$ helicity states as well as by summing over the two states at $Q^2 = 0.035\,\mathrm{GeV}^2$ and $\theta' = 0.5$ deg.

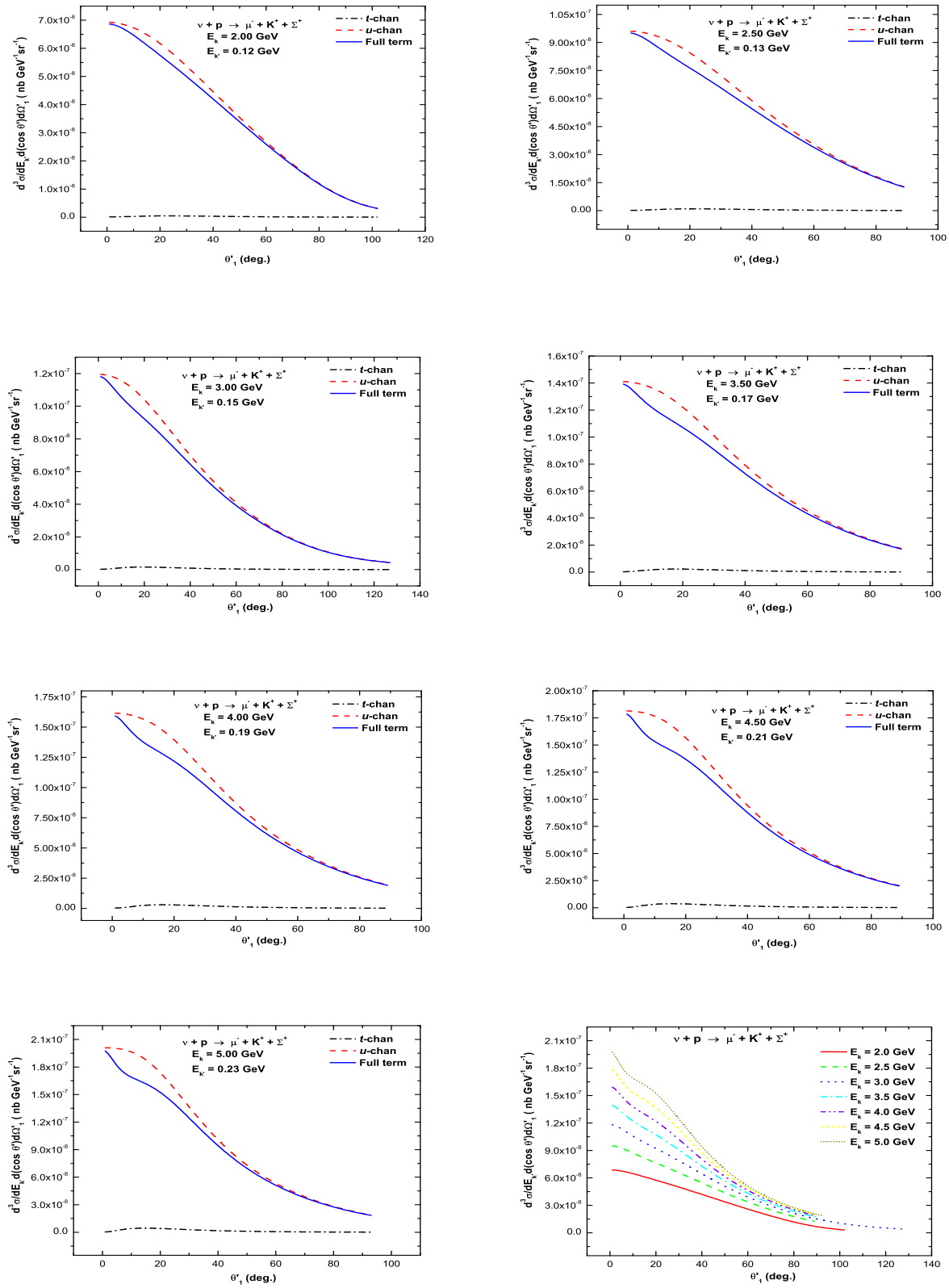

Fig. 7.6: The differential cross section against the kaon angle for CC1 at $Q^2 = 0.25\,\mathrm{GeV}^2$ and $\theta' = 0.5$ deg.

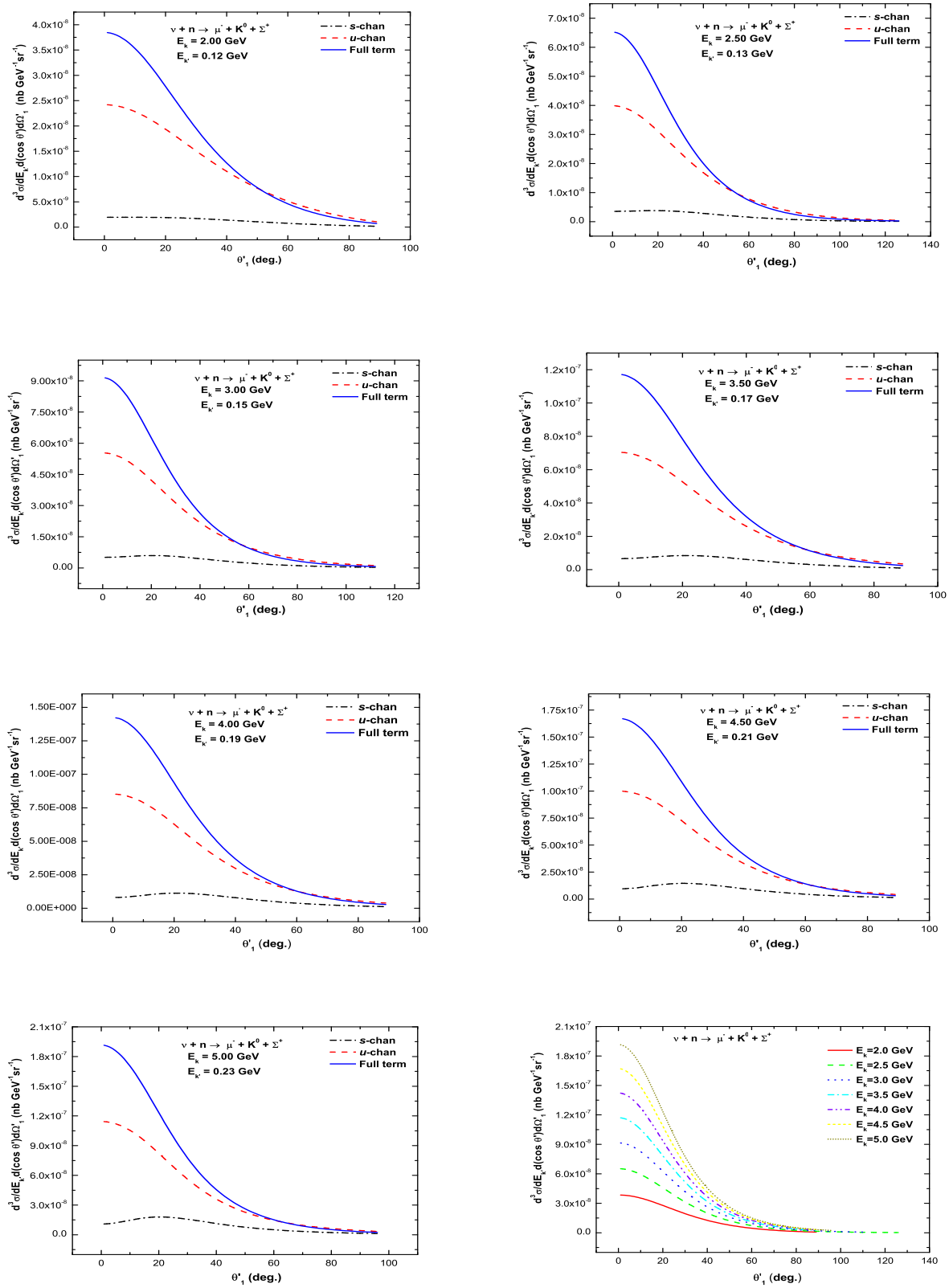

Fig. 7.7: The differential cross section against the kaon angle for CC2 at $Q^2 = 0.25\,\mathrm{GeV}^2$ and $\theta' = 0.5$ deg.

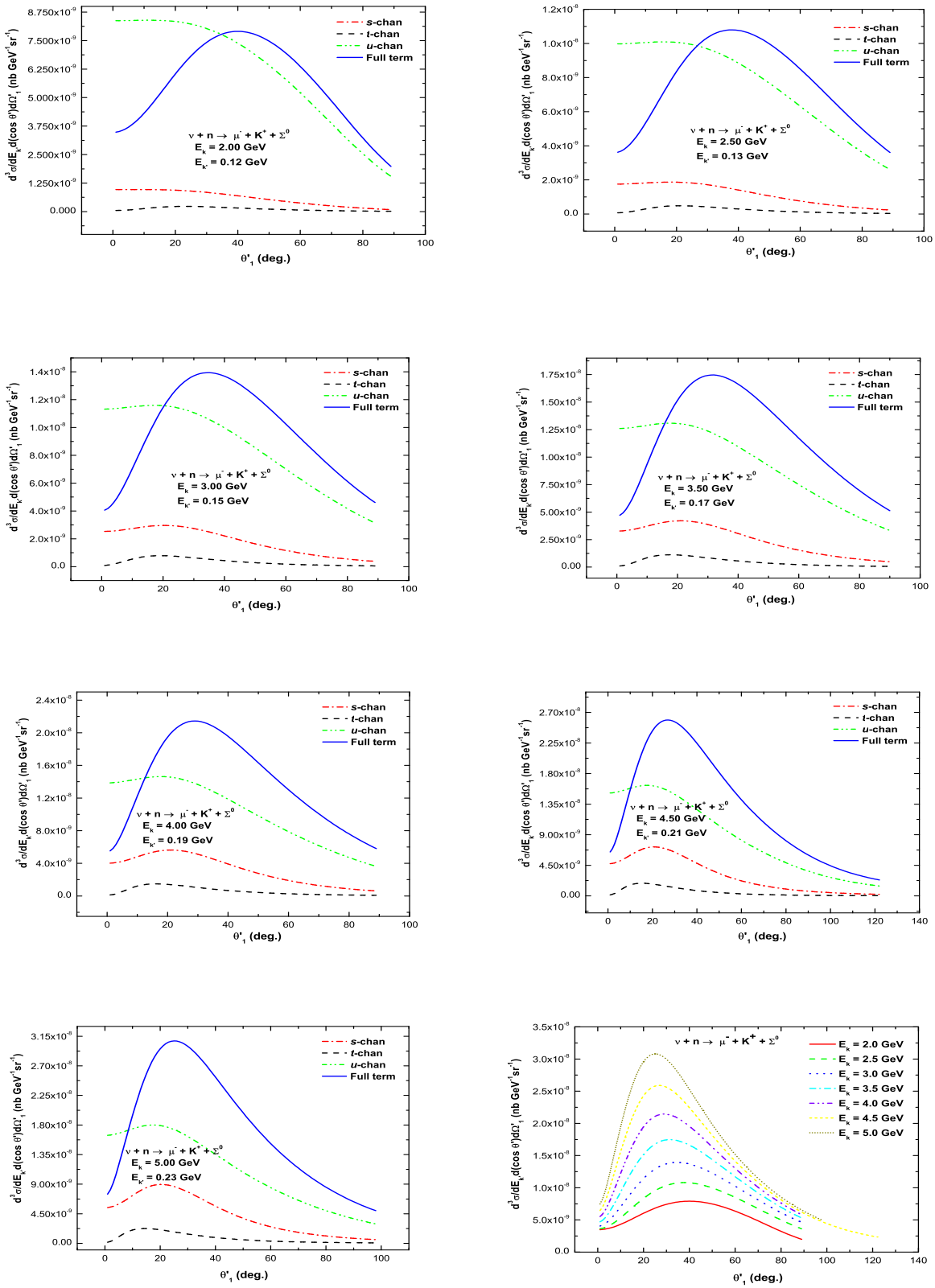

Fig. 7.8: The differential cross section against the kaon angle for CC3 at $Q^2 = 0.25\,\mathrm{GeV}^2$ and $\theta' = 0.5$ deg.

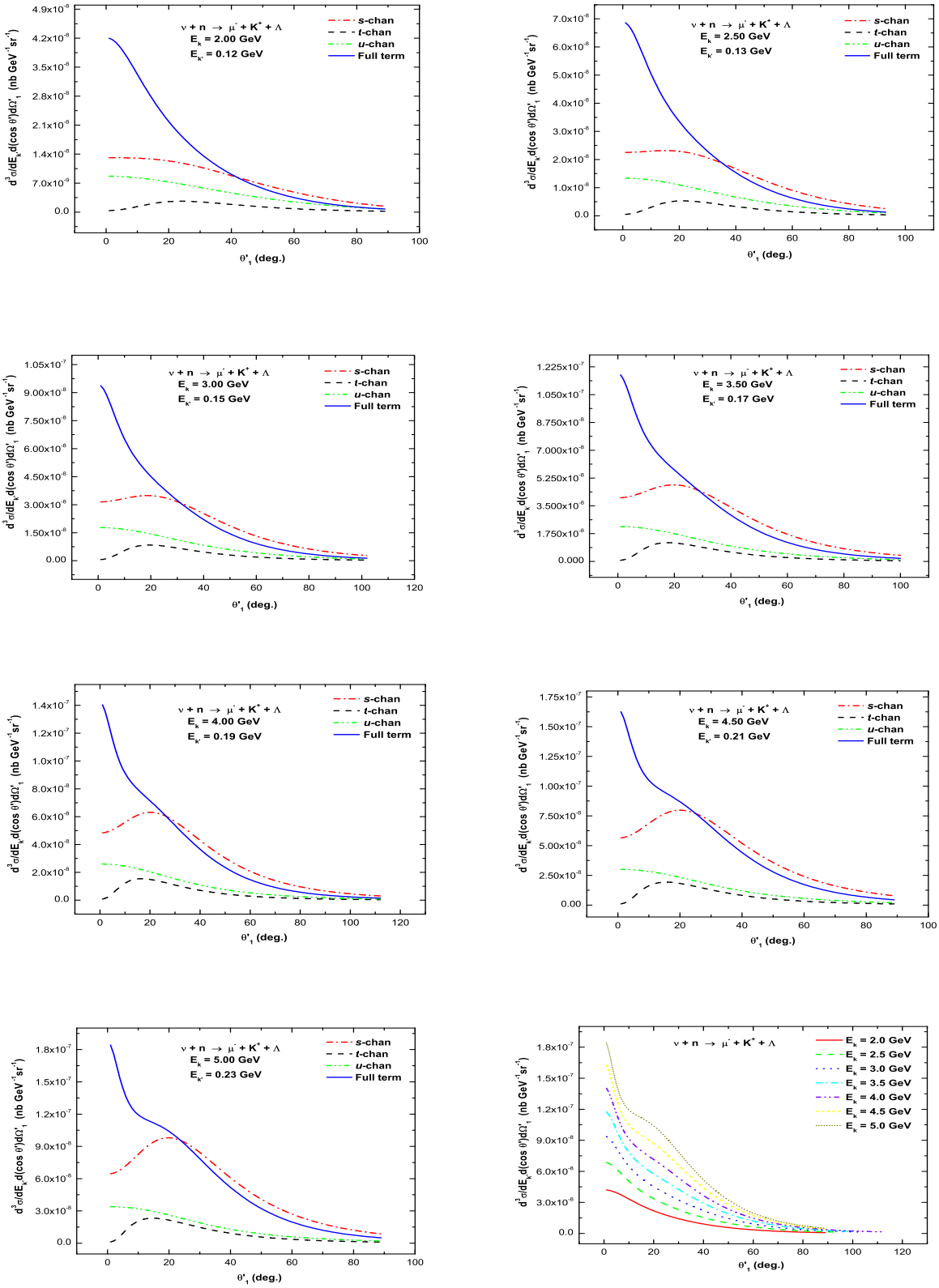

Fig. 7.9: The differential cross section against the kaon angle for CC4 at $Q^2 = 0.25\,\mathrm{GeV}^2$ and $\theta' = 0.5$ deg.

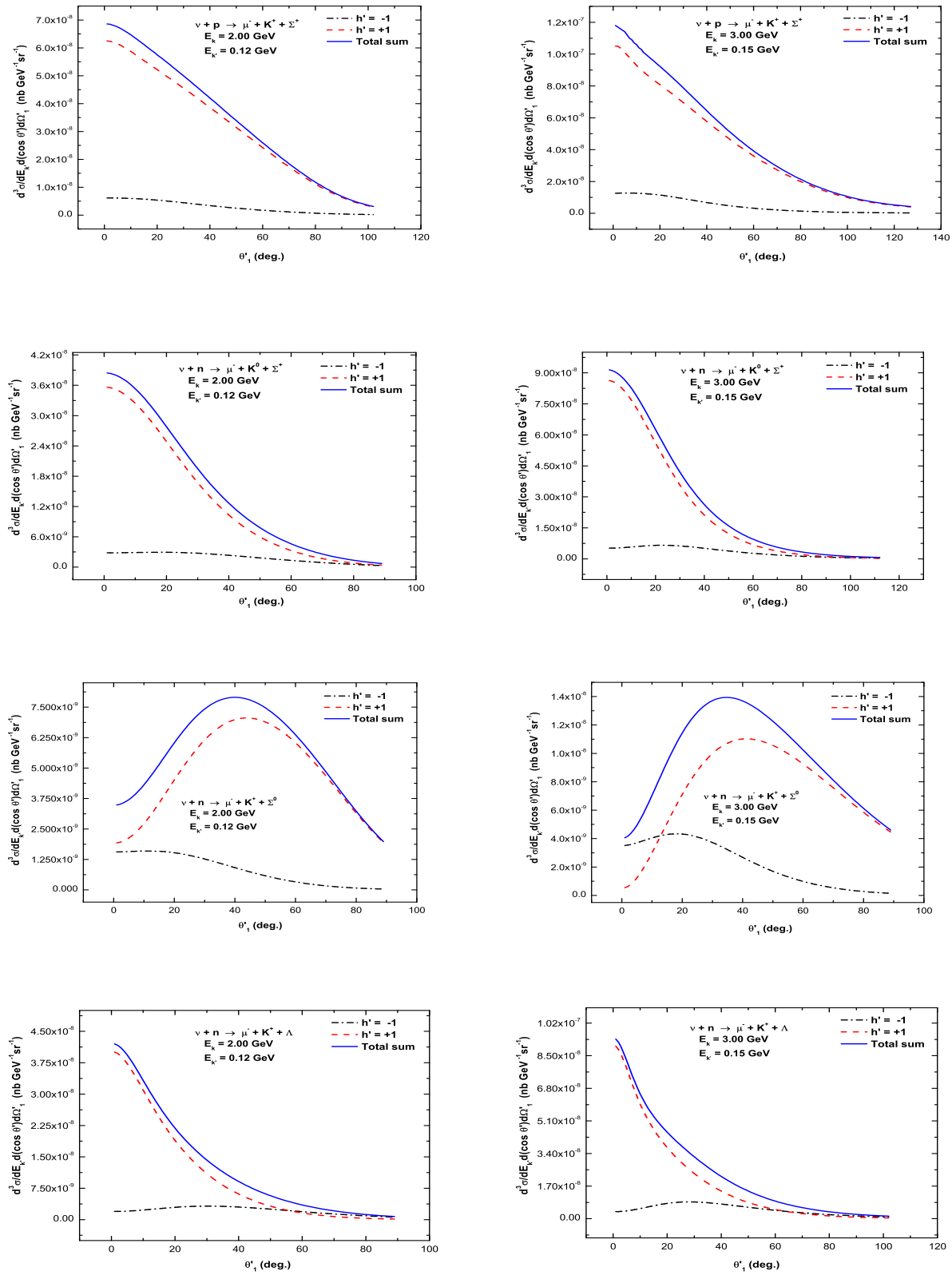

Fig. 7.10: The differential cross sections of CC1, CC2, CC3, and CC4 against the kaon angle for $\mathrm{h}' = -1$ and $\mathrm{h}' = +1$ helicity states as well as the total by summing over the two states at $Q^2 = 0.25\,\mathrm{GeV}^2$ and $\theta' = 0.5$ deg.

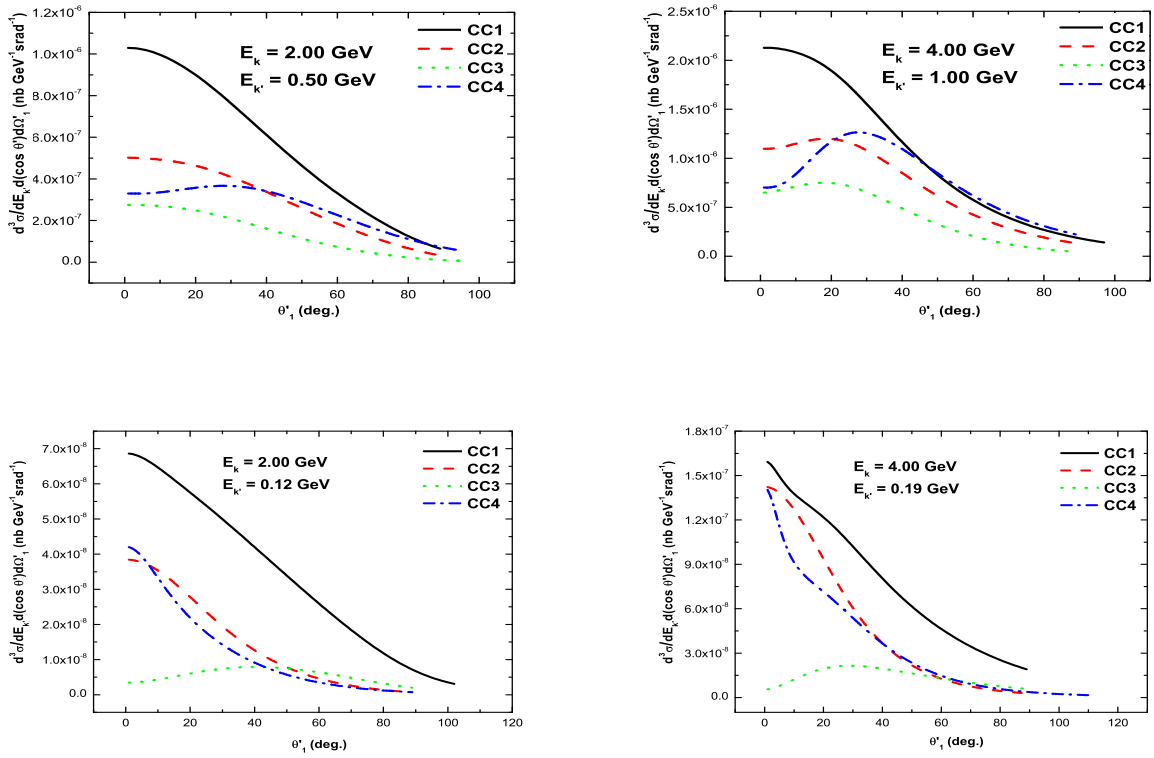

Fig. 7.11: The comparison of the angular distribution of the differential cross sections of CC1, CC2, CC3, and CC4 at $Q^2 = 0.035\,\mathrm{GeV}^2$ and $\theta' = 0.5$ deg (top) as well as $Q^2 = 0.25\,\mathrm{GeV}^2$ and $\theta' = 0.5$ deg (bottom).

Chapter 8

Summary and Conclusions

We have developed the most general relativistic formalism of the differential cross section for the neutrino-induced weak production of strange particles. The derivation is made for both CC and NC reactions in order to investigate the angular distribution of the differential cross section with respect to the outgoing kaon angle. In the case of CC reactions, we take into account the fact that the outgoing muon is a detectable particle such that the general form could also be used to study the differential cross section as a function of muon energy and the angular distribution with respect to the muon angle. However, this does not apply to the NC processes, because the outgoing neutrino can not be observed experimentally; thus we integrated over both muon energy and angle [32].

The norm squared invariant matrix element has been derived as the contraction between the leptonic tensor and the hadronic tensor. The leptonic tensor can be calculated in the framework of the electroweak theory. The helicity dependence comes through the anti-symmetric component of the leptonic tensor. We have realized that as the energy of the muon increases relative to its mass, the CC reactions appear to be in favour of the muon with the negative helicity state. We have employed the algebraic interpretation of the most appropriate Feynman diagram to derive the general form of the hadronic tensor.

Unlike the leptonic transition current, there are no well developed and tested gauge theories that allow us to calculate the hadronic weak transition current or the hadronic tensor. Therefore, we have developed the new model-independent approach to calculate the invariant matrix element by deriving the most general weak hadronic current in terms of eighteen parametrization form factors. In this derivation, we make use of the Dirac equation of the on-shell particle, the Dirac algebra of gamma matrices, and most importantly the nature of the weak interaction in violating certain conservation laws which makes it unrestricted by

the conditions imposed by their symmetries. We have applied this method to investigate the Born term approximation strictly in the threshold energy region in order to maintain the dominance of the contribution of the tree diagrams over the nearby resonances.

In our numerical study the computation has been done for CC and $\Delta S = 0$ associated production reactions labeled as: CC1 ($K^+\Sigma^+$), CC2 ($K^0\Sigma^+$), CC3 ($K^+\Sigma^0$), and CC4 ($K^+\Lambda$). In the calculation of the Born term model, the Cabibbo V-A theory and SU(3) exact symmetry have been used to determine the standard weak transition form factors via the CVC hypothesis. We have found that the contribution of the u-channel in the Born model approximation can be used to test SU(3) symmetry. The first three reactions have shown the definite dominance of the u-channel over the other channels; and this channel is always forward-peaked. Moreover, we have compared the relative contribution of two u-channels to the cross section for both CC1 and CC2; the one with Λ exchange dominates the others. This clearly indicates the sensitivity of the cross section to the strong coupling constant in agreement with the result of [12].

In conclusion, our results indicate that the validy of the Cabibbo V-A theory and SU(3) symmetry for the study of the neutrino-induced strange particle production reactions can be tested. The most general form of the hadronic weak current operator is applicable to any weak production of three-body processes. It also gives the general form for the differential cross section. Therefore, this new expression of the weak current operator avoids the recalculation of the differential cross section whenever we consider various reactions, introduce other models, or add more diagrams such as resonances to the tree diagrams. Instead our formalism of the differential cross section can be used in all other considerations by only updating the eighteen invariant amplitudes of the most general hadronic weak current.

This study will be extended to the CC and $\Delta S = 1$ as well as the NC strange particle production reactions. In addition, the calculation will include spin observables by focusing on polarized particles in the final states. Resonance contributions that are relevant in the threshold region will be added to the Born diagram. We can also investigate the sensitivity of the differential cross section to the variation of the coupling constants within their experimental bound and also other parameters. As far as our calculations go we can safely conclude that, the CC strange particle production reactions having the u-channel dominance can be used to test the validity of SU(3) symmetry. Especially, the CC1 reaction provides a wide range of kaon angles for such experimental study. Therefore, we hope that, our predictions motivate the undertaking of further experiments in the area of neutrino and hadron physics.

Appendix A

Dirac Algebra of Gamma Matrix

Pauli Matrices

These are the three Hermitian, unitary 2×2 matrices:

$$\sigma_1 = \begin{pmatrix} 0 & 1 \\ 1 & 0 \end{pmatrix}, \qquad \sigma_2 = \begin{pmatrix} 0 & -i \\ i & 0 \end{pmatrix}, \qquad \sigma_3 = \begin{pmatrix} 1 & 0 \\ 0 & -1 \end{pmatrix}. \tag{A.1}$$

Product rules

$$\begin{aligned} &\sigma_1^2 = \sigma_2^2 = \sigma_3^2 = I, \\ &\{\sigma_i, \sigma_j\} = 2\delta_{ij}. \end{aligned} \tag{A.2}$$

Dirac Matrices

These are four unitary traceless 4×4 matrices

$$\begin{aligned} &\gamma^0 = \begin{pmatrix} I & 0 \\ 0 & -I \end{pmatrix}; \qquad \gamma^k = \begin{pmatrix} 0 & \sigma^k \\ -\sigma^k & 0 \end{pmatrix}, \ k = 1, 2, 3 \\ &\gamma_5 = i\gamma^0\gamma^1\gamma^2\gamma^3 = \begin{pmatrix} 0 & I \\ I & 0 \end{pmatrix}, \end{aligned} \tag{A.3}$$

where I is 2×2 identity matrix and 0 is 2×2 matrix of zero. And the following unitary equivalence relation also holds for gamma matrices

$$\begin{aligned} \overline{\gamma^\mu} = &\quad \gamma^0(\gamma^\mu)^\dagger\gamma^0 = \gamma^\mu \\ \overline{i\gamma^5} = &\quad \gamma^0(i\gamma^5)^\dagger\gamma^0 = i\gamma^5 \\ \overline{\gamma^\mu\gamma^5} &= \gamma^0(\gamma^\mu\gamma^5)^\dagger\gamma^0 = \gamma^\mu\gamma^5 \end{aligned} \tag{A.4}$$

A.1 Dirac Algebra

Some of the most important properties associated with gamma matrices are listed below

Table. A.1: The summary of the Dirac gamma matrix properties.

$\{\gamma^\mu, \gamma^\nu\} = 2g^{\mu\nu}$	$\{\gamma_5, \gamma^\mu\} = 0$
$\gamma_5 = -\frac{i}{4!}\epsilon_{\mu\nu\alpha\beta}\gamma^\mu\gamma^\nu\gamma^\alpha\gamma^\beta$	$\sigma^{\mu\nu} = \frac{i}{2}\left[\gamma^\mu, \gamma^\nu\right]$
$\gamma^\mu\gamma^\nu = g^{\mu\nu} - i\sigma^{\mu\nu}$	$\gamma_5\sigma^{\mu\nu} = \frac{i}{2}\epsilon^{\mu\nu\alpha\beta}\sigma_{\alpha\beta}$
$\gamma_5\sigma^{\mu\nu} = 0$	$(\gamma^0)^2 = (\gamma^5)^2 = -(\gamma^k)^2 = I$

where $g^{\mu\nu}$ is the metric tensor which is given by

$$g^{\mu\nu} = \begin{pmatrix} 1 & 0 & 0 & 0 \\ 0 & -1 & 0 & 0 \\ 0 & 0 & -1 & 0 \\ 1 & 0 & 0 & -1 \end{pmatrix} \tag{A.5}$$

and $\epsilon^{\mu\nu\alpha\beta}$ is anti-symmetric Levi-Cevita tensor which is the four dimensional generalization of ϵ^{ijk}; it is conventionally defined as

$$\epsilon^{\mu\nu\alpha\beta} = \begin{cases} +1, & \text{if } \mu\nu\alpha\beta \text{ is an even permutation of 0123} \\ -1, & \text{if } \mu\nu\alpha\beta \text{ is an odd permutation of 0123} \\ 0, & \text{otherwise.} \end{cases} \tag{A.6}$$

We notice that $\epsilon_{\mu\nu\alpha\beta} = -\epsilon^{\mu\nu\alpha\beta}$. The following identities of the gamma matrices in combination with Levi-Cevita tensor and four-vectors is found to be important. Let a and b be

arbitrary four-vectors, Then

$$(a^\mu b^\nu \pm b^\mu a^\nu)\gamma_\nu = a^\mu \not{b} \pm b^\mu \not{a} \tag{A.7}$$

$$a^\mu b^\nu \sigma_{\mu\nu} = \begin{cases} i(\not{a}\not{b} - b\cdot a) & \text{or} \\ i(b\cdot a - \not{a}\not{b}) \end{cases} \tag{A.8}$$

$$(a^\mu b^\nu - a^\nu b^\mu)\sigma_{\mu\nu} = \begin{cases} 2i(\not{a}\not{b} - b\cdot a) & \text{or} \\ 2i(b\cdot a - \not{a}\not{b}) \end{cases} \tag{A.9}$$

$$\epsilon^{\mu\nu\alpha\beta}\gamma_\beta = i(g^{\mu\alpha}g^{\nu\beta} - g^{\mu\nu}g^{\alpha\beta})\gamma_5\gamma_\beta + \gamma_5\gamma^\mu\sigma^{\nu\alpha} \tag{A.10}$$

$$\epsilon^{\mu\nu\alpha\beta}\gamma_5\gamma_\beta = i(g^{\mu\nu}\gamma^\alpha - g^{\mu\alpha}\gamma^\nu + g^{\nu\alpha}\gamma^\mu) - i\gamma^\mu\gamma^\nu\gamma^\alpha \tag{A.11}$$

$$\epsilon^{\mu\nu\alpha\beta}a_\alpha b_\beta\gamma_\nu = i(a^\mu\not{b} + b^\mu\not{a})\gamma_5 + i\gamma_5\gamma^\mu(a\cdot b - \not{a}\not{b}) \tag{A.12}$$

In addition the following identities are found to be useful

$$\not{a}\not{b} = 2a\cdot b - \not{b}\not{a} \tag{A.13}$$

$$\not{a}\gamma^\mu = 2a^\mu - \gamma^\mu\not{a} \tag{A.14}$$

$$\not{a}\gamma^\mu\gamma_5 = 2a^\mu\gamma_5 + \gamma^\mu\gamma_5\not{a} \tag{A.15}$$

$$\not{a}\not{b}\gamma^\mu\gamma_5 = 2a\cdot b\gamma^\mu\gamma_5 - 2\not{b}a^\mu\gamma_5 - \not{b}\gamma^\mu\gamma_5\not{a} \tag{A.16}$$

$$\sigma^{\mu\nu}a_\nu = \begin{cases} i(a^\mu - \not{a}\gamma^\mu) & \text{or} \\ i(\gamma^\mu\not{a} - a^\mu) \end{cases} \tag{A.17}$$

$$\sigma^{\mu\nu}a_\nu\not{a} = i(a^2\gamma^\mu - \not{a}a^\mu) \tag{A.18}$$

$$\sigma^{\mu\nu}a_\nu\not{b} = i(a^\mu\not{b} - \not{a}b^\mu + 2a\cdot b\gamma^\mu - \not{b}\not{a}) \tag{A.19}$$

A.2 Trace Theorems

Note that the slash notation $\gamma\cdot a = \not{a}$.

Theorem 1

$$\mathrm{Tr}[\gamma^\mu\gamma^\nu] = 4g^{\mu\nu}, \tag{A.20}$$

and

$$\mathrm{Tr}[\gamma^\mu\gamma^\nu\gamma^\alpha\gamma^\beta] = 4(g^{\mu\nu}g^{\alpha\beta} - g^{\mu\alpha}g^{\nu\beta} + g^{\mu\beta}g^{\nu\alpha}), \tag{A.21}$$

Theorem 2

The trace of an odd number of γ matrices is zero. (A.22)

Theorem 3

For any arbitrary four-vectors a and b,

$$\mathrm{Tr}[\not{a}\not{b}] = 4a \cdot b \tag{A.23}$$

Theorem 4

For any arbitrary four-vectors a, b, c and d,

$$\mathrm{Tr}[\not{a}\not{b}\not{c}\not{d}] = 4[(a \cdot b)(c \cdot d) - (a \cdot c)(b \cdot d) + (a \cdot d)(b \cdot c)] \tag{A.24}$$

The following are additional trace theorems for the product of gamma matrices involving γ_5:

$$\begin{aligned}
&\mathrm{Tr}[\gamma^5 \times \text{odd number of gamma matrices}] = 0 \\
&\mathrm{Tr}[\gamma^5 \gamma^\mu \gamma^\nu] = 0 \\
&\mathrm{Tr}[\gamma^5 \gamma^\mu \gamma^\nu \gamma^\alpha \gamma^\beta] = i4\epsilon^{\mu\nu\alpha\beta} \\
&\mathrm{Tr}[\gamma^5 \not{a}\not{b}\not{c}\not{d}] = i4\epsilon^{\mu\nu\alpha\beta} a_\mu b_\nu c_\alpha d_\beta
\end{aligned} \tag{A.25}$$

Appendix B

Leptonic Tensor

A given leptonic weak current can be either charged current (CC) or neutral current (NC). The CC leptonic weak current always couples with the $W^{\pm}$ gauge bosons; whereas the NC leptonic weak current couples with Z^0. In order to evaluate the leptonic tensor we start with the construction of the invariant matrix element, in the framework of the electroweak theory, form the appropriate Feynman diagrams such as shown in Fig. B.1.

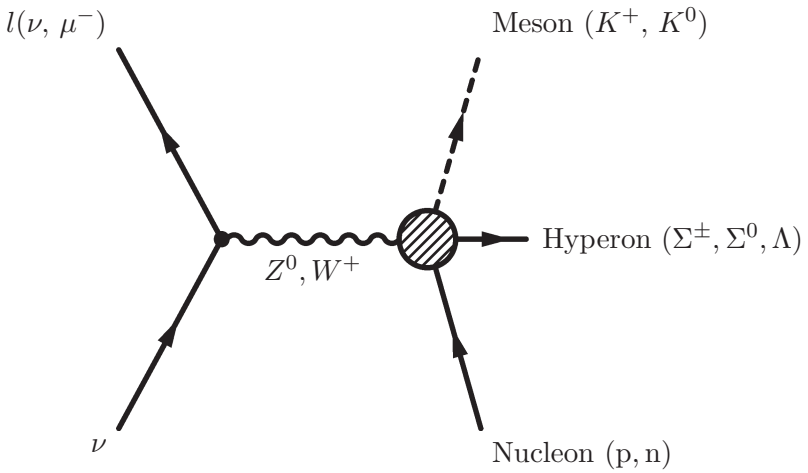

Fig. B.1: The Feynman diagram for neutrino-nucleon interactions.

B.1 Weak Neutral Current

The NC weak transition of the neutrino is shown in Fig. B.2. The invariant matrix element for the weak NC neutrino-induced weak production of strange particles from the nucleon can

be written as

$$-i\mathcal{M} = \left(\bar{\nu}_\mu(k',h')\left[\frac{-igM_Z}{4M_W}\gamma_\mu(1-\gamma_5)\right]\nu_\mu(k,h)\right) iD^{\mu\nu}\left(\bar{u}_Y(p',s')\frac{-igM_Z}{4M_W}\hat{J}_\nu u_N(p,s)\right), \tag{B.1}$$

where

$$D^{\mu\nu} = \frac{-g^{\mu\nu} + q^\mu q^\nu/M_Z^2}{q^2 - M_Z^2}, \tag{B.2}$$

and M_Z is the mass the the neutral gauge boson, $\nu_\mu(k,h)$ is the spinor field of muon-neutrino with four-momentum k and helicity eigenvalue h, $u_N(p,s)$ is the spinor field for the Nucleon with four-momentum p and spin state s, $\bar{u}_Y(p',s')$ is the spinor field for final state hyperon, $\hat{J}^\mu$ is a matrix or Lorentz vector that represents the blob at hadronic vertex, and q^μ is the

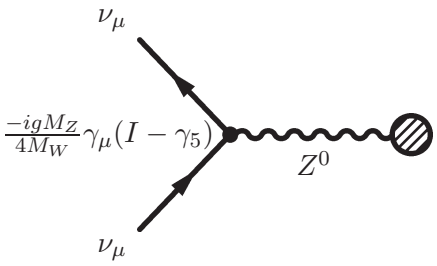

Fig. B.2: The Feynman diagram of the neutral current transition of the lepton.

four-momentum transfer. In order to avoid confusion from now on we write the Dirac spinor for the muon-neutrino without the subscript μ. In a situation where $q^2 \ll M_Z^2$, Eq. (B.1) becomes

$$\mathcal{M} = \frac{G_F}{2\sqrt{2}}[\bar{\nu}(k',h')\gamma_\mu(1-\gamma_5)\nu(k,h)][\bar{u}_H(p',s')\hat{J}^\mu u_N(p,s)] \tag{B.3}$$

The square of the norm of the invariant amplitude, therefore, becomes

$$\begin{aligned}|\mathcal{M}|^2 = \quad & \left(\frac{G_F}{2\sqrt{2}}\right)^2 [\bar{\nu}(k',h')\gamma_\mu(1-\gamma_5)\nu(k,h)]\,[\bar{u}_Y(p',s')\hat{J}^\mu u_N(p,s)] \\ & \times [\bar{\nu}(k',h')\gamma_\mu(1-\gamma_5)\nu(k,h)]^*\,[\bar{u}_Y(p',s')\hat{J}^\nu u_N(p,s)]^*.\end{aligned} \tag{B.4}$$

If we now consider the leptonic current since $[\bar{\nu}(k',h')\gamma_\mu(1-\gamma_5)\nu(k,h)]$ is an element of complex number, we can write

$$\begin{aligned}[\bar{\nu}(k',h')\gamma_\mu(1-\gamma_5)\nu(k,h)]^* &= [\bar{\nu}(k',h')\gamma_\mu(1-\gamma_5)\nu(k,h)]^\dagger \\ &= (\nu(k,h))^\dagger\,[\gamma_\mu(1-\gamma_5)]^\dagger\,(\bar{\nu}(k',h'))^\dagger.\end{aligned} \tag{B.5}$$

It is known that $\bar{u} = u^\dagger\gamma_0$. For any arbitrary matrices A and B of the same dimension, $(AB)^\dagger = B^\dagger A^\dagger$; noting also that $\gamma_5\gamma_\mu = -\gamma_\mu\gamma_5$, and $\gamma_0\gamma_0 = I$, we can write Eq. (B.5) as

$$\begin{aligned}(\nu(k,h))^\dagger\,[\gamma_\mu(1-\gamma_5)]^\dagger\,(\bar{\nu}(k',h'))^\dagger &= \bar{\nu}(k,h)\,[\,\bar{\gamma}_\nu - \overline{\gamma_\nu\gamma_5}]\,\nu(k',h') \\ &= \bar{\nu}(k,h)\,[\gamma_\mu(1-\gamma_5)]\,\nu(k',h'),\end{aligned} \tag{B.6}$$

where we have used $\bar{\gamma}_\mu = \gamma_0\gamma_\mu^\dagger\gamma_0 = \gamma_\mu$ and $\overline{\gamma_\mu\gamma_5} = \gamma_0(\gamma_\mu\gamma_5)^\dagger\gamma_0 = \gamma_\mu\gamma_5$. In a similar fashion we can also obtain for the hadronic current that

$$\begin{aligned}[\bar{u}_Y(p',s')\hat{J}^\nu u_N(p,s)]^* &= [\bar{u}_N(p,s)(\gamma^0(\hat{J}^\nu)^\dagger\gamma^0)u_Y(p',s')] \\ &= [\bar{u}_N(p,s)\hat{\bar{J}}^\nu u_Y(p',s')],\end{aligned} \tag{B.7}$$

where $\hat{\bar{J}}^\nu = \gamma^0(\hat{J}^\nu)^\dagger\gamma^0$. Thus Eq. (B.4) becomes

$$\begin{aligned}|\mathcal{M}|^2 &= \left(\frac{G_F}{2\sqrt{2}}\right)^2 [\bar{\nu}(k',h')\gamma_\mu(1-\gamma_5)\nu(k,h)][\bar{u}_Y(p',s')\hat{J}^\mu u_N(p,s)] \\ &\quad\times[\bar{\nu}(k,h)(\gamma_\nu(I-\gamma_5))\nu(k',h')][\bar{u}_N(p,s)\hat{\bar{J}}^\nu u_Y(p',s')] \\ &= \left(\frac{G_F}{2\sqrt{2}}\right)^2 [\bar{\nu}(k',h')\gamma_\mu(1-\gamma_5)\nu(k,h)][\bar{\nu}(k,h)\gamma_\nu(I-\gamma_5)\nu(k',h')] \\ &\quad\times[\bar{u}_Y(p',s')\hat{J}^\mu u_N(p,s)][\bar{u}_N(p,s)\hat{\bar{J}}^\nu u_Y(p',s')] \\ &= \left(\frac{G_F}{2\sqrt{2}}\right)^2 L_{\mu\nu}W^{\mu\nu},\end{aligned} \tag{B.8}$$

where

$$L_{\mu\nu} = [\bar{\nu}(k',h')\gamma_\mu(1-\gamma_5)\nu(k,h)][\bar{\nu}(k,h)\gamma_\nu(I-\gamma_5)\nu(k',h')] \tag{B.9}$$

is a leptonic tensor; and

$$W^{\mu\nu} = [\bar{u}_Y(p',s')\hat{J}^\mu u_N(p,s)][\bar{u}_N(p,s)\hat{\bar{J}}^\nu u_H(p',s')] \tag{B.10}$$

is the hadronic tensor.

B.1.1 Feynman's Trace Technique

Now we focus on the leptonic tensor. We want to find the expression of leptonic tensor that does not contain any Dirac spinor. So Feynman trace technique helps us to reach at the result without explicit use of Dirac spinor and gamma matrices. Note that Eq. (B.9) can be considered as the matrix multiplication of two 4×1 column, two 1×4 row and two 4×4 matrices. This allows us to re-express Eq. (B.9) in terms of indices representation. That is

$$\begin{aligned}L_{\mu\nu} &= \{\bar{\nu}(k',h')\}_k\{\gamma_\mu(I-\gamma_5)\}_{kl}\{\nu(k,h)\}_l\{\bar{\nu}(k,h)\}_m\{\gamma_\nu(I-\gamma_5)\}_{mn}\{\nu(k',h')\}_n \\ &= \{\gamma_\mu(I-\gamma_5)\}_{kl}\{\nu(k,h)\}_l\{\bar{\nu}(k,h)\}_m\{\gamma_\nu(I-\gamma_5)\}_{mn}\{\nu(k',h')\}_n\{\bar{\nu}(k',h')\}_k.\end{aligned} \tag{B.11}$$

From Eq. (2.35) we have

$$\{\nu(k,h=-1)\}_l\{\bar{\nu}(k,h=-1)\}_m = \left\{\frac{\not{k}}{2E}\ \frac{I+\gamma_5}{2}\right\}_{lm}. \tag{B.12}$$

Now we use the fact that

$$A_{ij}B_{jr}C_{ri} = Tr[ABC] = Tr[BCA] = Tr[CAB], \tag{B.13}$$

i.e., trace of ABC, where A, B and C are any arbitrary square matrices of the same dimension and the summation convention applies to repeated indices. Thus Eq. (B.11) becomes

$$\begin{aligned} L_{\mu\nu} &= \mathrm{Tr}\left[\gamma_\mu(I-\gamma_5)\nu(k,h)\bar{\nu}(k,h)\gamma_\nu(I-\gamma_5)\nu(k',h')\bar{\nu}(k',h')\right] \\ &= \mathrm{Tr}\left[\gamma_\mu(I-\gamma_5)\left(\frac{\not{k}}{2E_k}\,\frac{I+\gamma_5}{2}\right)\gamma_\nu(I-\gamma_5)\left(\frac{\not{k}'}{2E_{k'}}\,\frac{I+\gamma_5}{2}\right)\right] \\ &= \frac{k^\alpha k'^\beta}{16E_kE_{k'}}\mathrm{Tr}\left[\gamma_\mu(I-\gamma_5)\gamma_\alpha(I+\gamma_5)\gamma_\nu(I-\gamma_5)\gamma_\beta(I+\gamma_5)\right] \end{aligned} \tag{B.14}$$

So by using the following properties

$$(I\pm\gamma_5)(I\pm\gamma_5) = 2(I\pm\gamma_5) \tag{B.15}$$

and

$$(I\pm\gamma_5)\gamma_\mu = \gamma_\mu(I\mp\gamma_5), \tag{B.16}$$

we can get

$$L_{\mu\nu} = \frac{8k^\alpha k'^\beta}{16E_kE_{k'}}\mathrm{Tr}\left[\gamma_\mu\gamma_\alpha\gamma_\nu\gamma_\beta(I+\gamma_5)\right]. \tag{B.17}$$

For any matrices A and B, $Tr[A+B] = Tr[A] + Tr[B]$. So by using this identity we can separate the symmetric and anti-symmetric parts of $L_{\mu\nu}$. That is

$$L_{\mu\nu} = (L_{\mu\nu})_s + (L_{\mu\nu})_a, \tag{B.18}$$

where the symmetric component is

$$(L_{\mu\nu})_s = \frac{k^\alpha k'^\beta}{2E_kE_{k'}}\mathrm{Tr}\left[\gamma_\mu\gamma_\alpha\gamma_\nu\gamma_\beta\right] \tag{B.19}$$

and the anti-symmetric component is

$$\begin{aligned} (L_{\mu\nu})_a &= \frac{k^\alpha k'^\beta}{2E_kE_{k'}}\mathrm{Tr}\left[\gamma_\mu\gamma_\alpha\gamma_\nu\gamma_\beta\gamma_5\right] \\ &= \frac{k^\alpha k'^\beta}{2E_kE_{k'}}\mathrm{Tr}\left[\gamma_5\gamma_\mu\gamma_\alpha\gamma_\nu\gamma_\beta\right] \end{aligned} \tag{B.20}$$

So based on the trace theorems given in Appendix A, one can show that

$$\begin{aligned} (L_{\mu\nu})_s &= \frac{2k^\alpha k'^\beta}{E_kE_{k'}}(g_{\mu\alpha}g_{\nu\beta} - g_{\mu\nu}g_{\alpha\beta} + g_{\mu\beta}g_{\alpha\nu}) \\ &= \frac{2}{E_kE_{k'}}(k_\mu k'_\nu + k_\nu k'_\mu - k\cdot k' g_{\mu\nu}) \end{aligned} \tag{B.21}$$

and

$$\begin{aligned}(L_{\mu\nu})_a &= \frac{-i2}{E_k E_{k'}}\epsilon_{\mu\alpha\nu\beta}k^\alpha k'^\beta \\ &= \frac{i2}{E_k E_{k'}}\epsilon_{\mu\nu\alpha\beta}k^\alpha k'^\beta\end{aligned} \tag{B.22}$$

Therefore, the total leptonic tensor for charge conserving weak current becomes

$$L_{\mu\nu} = \frac{2}{E_k E_{k'}}(k_\mu k'_\nu + k_\nu k'_\mu - k\cdot k' g_{\mu\nu} + i\epsilon_{\mu\nu\alpha\beta}k^\alpha k'^\beta). \tag{B.23}$$

B.2 Weak Charged Current

In this case the leptonic transition of the weak interaction is from neutrino to muon ($\nu \to \mu$) as shown in Fig. B.3.

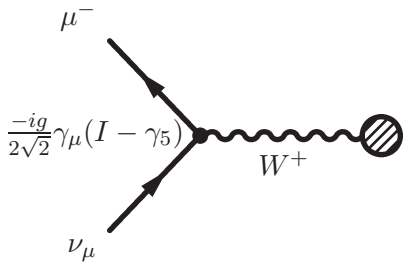

Fig. B.3: The Feynman diagram of the charged current weak leptonic transition.

By following similar procedure as in section B.1, the leptonic tensor for charged weak current interaction may be written as

$$L_{\mu\nu} = \mathrm{Tr}[\gamma_\mu(I-\gamma_5)\nu(k,h)\bar{\nu}(h,k)\gamma_\nu(I-\gamma_5)\mu(k',h')\bar{\mu}(k',h')] \ . \tag{B.24}$$

Recalling that

$$\{\nu(k,h=-1)\}_\alpha\{\bar{\nu}(k,h=-1)\}_\beta = \left(\frac{\not{k}}{2E_k}\ \frac{I+\gamma_5}{2}\right)_{\alpha\beta} \tag{B.25}$$

and

$$\{\mu(k',h')\}_\alpha\{\bar{\mu}(k',h')\}_\beta = \left(\frac{\not{k}'+m}{2E_{k'}}\right)\left(\frac{I+h'\gamma_5\not{s}'}{2}\right)_{\alpha\beta}, \tag{B.26}$$

one can find that

$$L_{\mu\nu} = \frac{k^\alpha}{16E_kE_{k'}}\mathrm{Tr}[\gamma_\mu(I-\gamma_5)\gamma_\alpha(I+\gamma_\alpha)\gamma_\nu(I-\gamma_5)(\not{k}'+m)(I+h'\gamma_5\not{s}')] \tag{B.27}$$

where

$$s'^\mu = \left(\frac{|\mathbf{k}'|}{m},\ \frac{E_{k'}}{m}\hat{\mathbf{k}}'\right). \tag{B.28}$$

By using Eq. (B.15) and (B.16), the leptonic tensor reduces to

$$\begin{aligned} L_{\mu\nu} &= \frac{k^\alpha}{4E_k E_{k'}} \mathrm{Tr}[\gamma_\mu \gamma_\alpha \gamma_\nu (I - \gamma_5)(\not{k}' + m + h'\gamma_5 m \not{s}')] \\ &= (L_{\mu\nu})_1 + (L_{\mu\nu})_2 + (L_{\mu\nu})_3 \end{aligned} \tag{B.29}$$

where

$$\begin{aligned} (L_{\mu\nu})_1 &= \frac{k^\alpha k'^\beta}{4E_k E_{k'}} \mathrm{Tr}[\gamma_\mu \gamma_\alpha \gamma_\nu \gamma_\beta (I + \gamma_5)] \\ (L_{\mu\nu})_2 &= \frac{m k^\alpha}{4E_k E_{k'}} \mathrm{Tr}[\gamma_\mu \gamma_\alpha \gamma_\nu (I - \gamma_5)] \quad . \\ (L_{\mu\nu})_3 &= \frac{-h' m k^\alpha s'^\beta}{4E_k E_{k'}} \mathrm{Tr}[\gamma_\mu \gamma_\alpha \gamma_\nu \gamma_\beta (I + \gamma_5)] \end{aligned} \tag{B.30}$$

The trace theorems would simply yield

$$(L_{\mu\nu})_2 = 0. \tag{B.31}$$

Thus Eq. (B.29) becomes

$$L_{\mu\nu} = \frac{k^\alpha K^\beta}{4E_k E_{k'}} \mathrm{Tr}[\gamma_\mu \gamma_\alpha \gamma_\nu \gamma_\beta (I + \gamma_5)] \tag{B.32}$$

where

$$K^\beta = \frac{1}{2}(k'^\beta - h' m s'^\beta). \tag{B.33}$$

Therefore, the total leptonic tensor for charge changing weak interaction may be written as

$$L_{\mu\nu} = \frac{2}{E_k E_{k'}} (k_\mu K_\nu + k_\nu K_\mu - g_{\mu\nu}\, k \cdot K + i\epsilon_{\mu\nu\alpha\beta} k^\alpha K^\beta). \ . \tag{B.34}$$

Appendix C

Gordon-like Identities

In the derivation of the most general form of invariant amplitude for the electromagnetic and weak interaction of spin - $\frac{1}{2}$ particles, the Gordon-like identities ($\mathcal{GLI}$'s) play important role. In what follows we make an attempt to list down the major identities that are widely employed in reducing the number of terms appearing in the expansion of the interaction matrix element that represent the vertex of the interaction. The Dirac free particle equation and the Dirac algebra of gamma matrices are vastly used in the derivation of $\mathcal{GLI}$'s. The above argument is true as far as the electromagnetic or weak current operator is sandwiched between the Dirac spinors.

Let consider the coupling of the photon with electromagnetic current of the Dirac particle. One can assume that the incoming and the outgoing particles are the same. The expectation value of such current is given by

$$\langle p_2|j^\mu(0)|p_1\rangle. \tag{C.1}$$

The translational invariance relates the current at 0 space-time point at any other arbitrary point x as

$$j_\mu^{(\hat{P})}(x) = e^{i\hat{P}\cdot x} j_\mu^{(\hat{P})}(0) e^{-i\hat{P}\cdot x} \tag{C.2}$$

where $\hat{P}$ is the total four-momentum operator. Eq. (C.1) becomes

$$\langle p_2|j^\mu(x)|p_1\rangle = e^{-i(p_1-p_2)\cdot x}\langle p_2|j^\mu(0)|p_1\rangle. \tag{C.3}$$

The matrix element at the right-hand side of Eq. (C.3), for apparent reason, must be of the form

$$\langle p_2|j^\mu(0)|p_1\rangle = \bar{u}_2\mathcal{O}^\mu u_1 \tag{C.4}$$

Identifying the general properties of the operator will allow us to obtain its explicit expression. Note that whenever the operator $\mathcal{O}^\mu$ is sandwiched between the Dirac spinors it becomes a

Lorentz vector. If we refer the right-hand side of Eq. (C.4), we notice that $\mathcal{O}^\mu$ the 4×4 matrix operator that acts on the Dirac spinors. Besides it carries only a single Lorentz index, in other word, it is a first rank tensor. Therefore, it is well known that any 4×4 matrix placed between the Dirac spinors can be expanded in terms of the complete set of five basis elements

$$\Gamma = \{I, \gamma^0, \gamma^\mu, \gamma^0\gamma^\mu, \sigma^{\mu\nu}\}, \tag{C.5}$$

where I is 4×4 identity matrix. Moreover, we have a set of two independent four-momenta either $\{p_1, p_2\}$, $\{p_1, q\}$, or $\{p_2, q\}$ at our disposal, where $q^\mu = p_2^\mu - p_1^\mu$. Here one notices the importance of $\mathcal{GLI}$'s for minimising the number of terms in the decomposition of the current operator. For convenience, we start with treating both particles having identical mass m. Therefore, by using $(\not{p} - m)u(\mathbf{p}, s) = 0$ and Table. A.1 in Appendix A, we can derive the $\mathcal{GLI}$'s given in Table. C.1 [35].

Table. C.1: Summary of Gordon-like identities for identical mass case

$\bar{u}_2\gamma^\mu u_1 = \frac{1}{2m}\bar{u}_2\left[l^\mu + i\sigma^{\mu\nu}q_\nu\right]u_1$	$\bar{u}_2\gamma^\mu\gamma_5 u_1 = \frac{1}{2m}\bar{u}_2\gamma_5\left[q^\mu + i\sigma^{\mu\nu}l_\nu\right]u_1$
$\bar{u}_2 i\sigma^{\mu\nu}l_\nu u_1 = -\bar{u}_2 q^\mu u_1$	$\bar{u}_2 i\sigma^{\mu\nu}q_\nu u_1 = \bar{u}_2\left[2m\gamma^\mu - l^\mu\right]u_1$
$\bar{u}_2 i\sigma^{\mu\nu}\gamma_5 q_\nu u_1 = -\bar{u}_2 l^\mu\gamma_5 u_1$	

where $l^\mu = p_1^\mu + p_2^\mu$. If we now assume that the initial particle and the final one have different masses m_1 and m_2, respectively, then the modified $\mathcal{GLI}$'s are given in Table.C.2

Table. C.2: Summary of Gordon-like identities for different mass case

$\bar{u}_2\gamma^\mu u_1 = \frac{1}{2}\bar{u}_2\left[L^\mu + i\sigma^{\mu\nu}Q_\nu\right]u_1$	$\bar{u}_2\gamma^\mu\gamma_5 u_1 = \frac{1}{2}\bar{u}_2\left[\gamma_5 Q^\mu + i\gamma_5\sigma^{\mu\nu}L_\nu\right]u_1$
$\bar{u}_2 i\sigma^{\mu\nu}L_\nu u_1 = -\bar{u}_2 Q^\mu u_1$	$\bar{u}_2 i\sigma^{\mu\nu}Q_\nu u_1 = \bar{u}_2\left[2\gamma^\mu - L^\mu\right]u_1$
$\bar{u}_2 i\sigma^{\mu\nu}\gamma_5 Q_\nu u_1 = -\bar{u}_2 L^\mu\gamma_5 u_1$	

where we have defined L^μ and Q^μ such that the $\mathcal{GLI}$ equations for different mass case would also have similar structures as those of identical mass ones.

$$L^\mu = \frac{p_1^\mu}{m_1} + \frac{p_2^\mu}{m_2}; \quad Q^\mu = \frac{p_2^\mu}{m_2} - \frac{p_1^\mu}{m_1}, \tag{C.6}$$

or

$$L^\mu + Q^\mu = \frac{l^\mu + q^\mu}{m_2}; \quad L^\mu - Q^\mu = \frac{l^\mu - q^\mu}{m_1}. \tag{C.7}$$

To show how one can easily apply Eq. (2.5) and Table. A.1 in Appendix A to derive these identities of Table.C.2; the proof of the first identity in Table. C.1 may be illustrated as follows.

$$\bar{u}_2 \gamma^\mu \not{p}_1 u_1 = m \bar{u}_2 \gamma^\mu u_1, \tag{C.8}$$

where we have used $\not{p}_1 u_1 = m u_1$. We rewrite $\not{p}_1$ as $\gamma^\nu p_{1\nu}$; then we use the property $\gamma^\mu \gamma^\nu = g^{\mu\nu} - i\sigma^{\mu\nu}$ and then by making some re-arrangement we finally obtain

$$\bar{u}_2 \gamma^\mu u_1 = \frac{1}{m} \bar{u}_2 \left[p_1^\mu + i\sigma^{\mu\nu} p_{1\nu} \right] u_1. \tag{C.9}$$

Similarly, we follow the same argument for $\bar{u}_2 \not{p}_2 = m \bar{u}_2$ to reach at

$$\bar{u}_2 \gamma^\mu u_1 = \frac{1}{m} \bar{u}_2 \left[p_2^\mu - i\sigma^{\mu\nu} p_{2\nu} \right] u_1. \tag{C.10}$$

Adding these last equations together and then multiplying a factor of $\frac{1}{2}$ both sides would eventually yields

$$\bar{u}_2 \gamma^\mu u_1 = \frac{1}{2m} \bar{u}_2 \left[l^\mu + i\sigma^{\mu\nu} q_\nu \right] u_1. \tag{C.11}$$

Besides, by subtracting Eq. (C.9) from (C.10) one can easily show that

$$\bar{u}_2 i\sigma^{\mu\nu} l_\nu u_1 = -\bar{u}_2 q^\mu u_1. \tag{C.12}$$

The same procedure can also be followed to derive all other $\mathcal{GLI}$'s listed in Table. C.1 as well as the ones in Table. C.2

Appendix D

Born Approximation of the Weak Hadronic Current Amplitudes

In Table. 2.6 we specified four CC and $\Delta S = 0$ neutrino-induced weak processes. In chapter 6 we performed the model-dependent derivation for the $\nu \mathrm{n} \to \mu^- K^+ \Lambda$. Here we tabulate eighteen structure functions obtained from the Born term approximation for the rest of the CC and $\Delta S = 0$ associated production reactions.

Here we first consider $\nu \mathrm{p} \to \mu^- K^+ \Sigma^+$ reaction channel. The s-channel needs the exchange particle to have the electric charge quantum number $Q = 2$ which indicates that there can not be an s-channel contribution. t-channel is mediated by K^0; whereas the u-channel accompanied by two exchange particles, Λ and Σ^0 and hence it contributes twice. By following similar steps like it has been for $\nu \mathrm{n} \to \mu^- K^+ \Lambda$ in section 6.2, the t-channel contribution would take a form

$$J^{\mu}_{t,CC} = G_t \left\{ (F_{K^+,\,0}) q^{\mu} \gamma_5 + (2F_{K^+,\,0}) p_1^{\mu} - (2F_{K^+,\,0}) p'^{\mu}_2 \gamma_5 \right\}, \tag{D.1}$$

where

$$G_t = g_{K^0 \Sigma^+ p} \frac{1}{t - M^2_{K^0}}, \quad M_{K^0} = 0.498\mathrm{GeV} \tag{D.2}$$

Since the u-channel has contributions from tree diagrams with Λ and Σ^0 propagators. Thus the current is given by

$$J^{\mu}_{u,CC} = J^{\mu}_{u,CC_{(\Lambda)}} + J^{\mu}_{u,CC_{(\Sigma^0)}}, \tag{D.3}$$

where

$$
\begin{aligned}
J^{\mu}_{u,CC\,(\Lambda)} = \; & G_u^{(\Lambda)} \Big\{ 2G_A^{Y_1} q^{\mu} - 2G_A^{Y_1} p'^{\mu}_2 + \left[2F_1^{Y_1} + (M_{\Sigma^+} - M_{\Lambda}) \frac{F_2^{Y_1}}{2M} \right] q^{\mu}\gamma_5 - 2F_1^{Y_1} p'^{\mu}_2 \gamma_5 \\
& + (M_{\Sigma^+} - M_{\Lambda}) G_A^{Y_1} \gamma^{\mu} + \left[\left(\frac{q^2}{2} - q \cdot p'_2 \right) \frac{F_2^{Y_1}}{M} - (M_{\Sigma^+} + M_{\Lambda}) F_1^{Y_1} \right] \gamma_5 \gamma^{\mu} \\
& - \left[F_1^{Y_1} + (M_{\Sigma^+} - M_{\Lambda}) \frac{F_2^{Y_1}}{2M} \right] \gamma_5 \not{q} \gamma^{\mu} - \frac{F_2^{Y_1}}{2M} q^{\mu} \gamma_5 \not{q} + \frac{F_2^{Y_1}}{M} p'^{\mu}_2 \gamma_5 \not{q} - G_A^{Y_1} \not{q} \gamma^{\mu} \Big\},
\end{aligned}
\tag{D.4}
$$

where

$$
G_u^{(\Lambda)} = g_{K^+\Lambda p} \frac{1}{u - M_{\Lambda}^2}, \quad M_{\Lambda} = 1.116\text{Gev}. \tag{D.5}
$$

Note that the Σ^0 exchange diagram gives similar form for $J^{\mu}_{u,CC\,(\Sigma^0)}$ as Λ exchange in Eq. (D.4). That is, by simply substituting the label Λ by Σ^0 we may find.

$$
\begin{aligned}
J^{\mu}_{u,CC\,(\Sigma^0)} = \; & G_u^{(\Sigma^0)} \Big\{ 2G_A^{Y_2} q^{\mu} - 2G_A^{Y_2} p'^{\mu}_2 + \left[2F_1^{Y_2} + (M_{\Sigma^+} - M_{\Sigma^0}) \frac{F_2^{Y_2}}{2M} \right] q^{\mu}\gamma_5 - 2F_1^{Y_2} p'^{\mu}_2 \gamma_5 \\
& + (M_{\Sigma^+} - M_{\Sigma^0}) G_A^{Y_2} \gamma^{\mu} + \left[\left(\frac{q^2}{2} - q \cdot p'_2 \right) \frac{F_2^{Y_2}}{M} - (M_{\Sigma^+} + M_{\Sigma^0}) F_1^{Y_2} \right] \gamma_5 \gamma^{\mu} \\
& - \left[F_1^{Y_2} + (M_{\Sigma^+} - M_{\Sigma^0}) \frac{F_2^{Y_2}}{2M} \right] \gamma_5 \not{q} \gamma^{\mu} - \frac{F_2^{Y_2}}{2M} q^{\mu} \gamma_5 \not{q} + \frac{F_2^{Y_2}}{M} p'^{\mu}_2 \gamma_5 \not{q} - G_A^{Y_2} \not{q} \gamma^{\mu} \Big\},
\end{aligned}
\tag{D.6}
$$

where

$$
G_u^{(\Sigma^0)} = g_{K^+\Sigma^0 p} \frac{1}{u - M_{\Sigma^0}^2}, \quad M_{\Sigma^0} = 1.192\text{Gev}. \tag{D.7}
$$

Note that the SU(3) current algebra gives that

$$
F_i^{Y_1}(Q^2) = -\sqrt{\frac{3}{2}} f_i^n(Q^2), \qquad G_A^{Y_1}(Q^2) = \sqrt{\frac{2}{3}} \frac{D}{F+D} g_A(Q^2) \tag{D.8}
$$

$$
F_i^{Y_2}(Q^2) = -\frac{1}{\sqrt{2}} (2f_i^p(Q^2) + f_i^n(Q^2)), \quad G_A^{Y_2}(Q^2) = -\sqrt{2} \frac{F}{F+D} g_A(Q^2) \tag{D.9}
$$

Table. D.1 summarizes the Born diagram contributions to the reaction.

Now we turn our attention to $\nu n \to \mu^- K^0 \Sigma^+$. Demanding conservation of charge quantum number at the weak vertex of t-channel suggests the absence of the channel's contribution. However, s-channel contribute once due to proton propagator; whereas this u-channel contributes twice for having two physically allowed exchange particles (Λ and Σ^0) just like the previous reaction channel. Table. D.2 generalizes the Born model evaluation of the unknown amplitudes of the most general hadronic current for this reaction.

For this reaction, the common factors G'_s, $G'^{(\Lambda)}_u$, and $G'^{(\Sigma^0)}_u$ are

$$
G'_s = g_{K^0\Sigma^+ p} \frac{1}{s - M_N^2}, \quad G'^{(\Lambda)}_u = g_{K^0\Lambda n} \frac{1}{u - M_{\Lambda}^2}; \quad G'^{(\Sigma^0)}_u = g_{K^0\Sigma^0 n} \frac{1}{u - M_{\Sigma^0}^2} \tag{D.10}
$$

Table. D.1: Extraction of the unknown amplitudes for the $\nu p \to \mu^- K^+ \Sigma^+$ reaction process.

Structure function	u-channel. with Λ	u-channel with Σ^0	t-channel with K^0
$\tilde{A}_1$	$2G_u^{(\Lambda)} G_A^{Y_1}$	$2G_u^{(\Sigma^0)} G_A^{Y_2}$	–
$\tilde{A}_2$	–	–	–
$\tilde{A}_3$	$-2G_u^{(\Lambda)} G_A^{Y_1}$	$-2G_u^{(\Sigma^0)} G_A^{Y_2}$	–
$\tilde{A}_4$	–	–	–
$\tilde{B}_1$	$G_u^{(\Lambda)} \left[2F_1^{Y_1} + M_{(1-)} \frac{F_2^{Y_1}}{2M} \right]$	$G_u^{(\Sigma^0)} \left[2F_1^{Y_2} + M_{(2-)} \frac{F_2^{Y_2}}{2M} \right]$	$G_t F_{K^+,0}$
$\tilde{B}_2$	–	–	$2G_t F_{K^+,0}$
$\tilde{B}_3$	$-2G_u^{(\Lambda)} F_1^{Y_1}$	$-2G_u^{(\Sigma^0)} F_1^{Y_2}$	$-2G_t F_{K^+,0}$
$\tilde{B}_4$	–	–	–
$\tilde{C}_1$	$G_u^{(\Lambda)} M_{(1-)} G_A^{Y_1}$	$G_u^{(\Sigma^0)} M_{(2-)} G_A^{Y_2}$	–
$\tilde{C}_2$	–	–	–
$\tilde{C}_3$	–	–	–
$\tilde{C}_4$	–	–	–
$\tilde{D}_1$	$G_u^{(\Lambda)} \left[\left(\frac{q^2}{2} - q \cdot p'_2 \right) \frac{F_2^{Y_1}}{M} - M_{(1+)} F_1^{Y_1} \right]$	$G_u^{(\Sigma^0)} \left[\left(\frac{q^2}{2} - q \cdot p'_2 \right) \frac{F_2^{Y_2}}{M} - M_{(2+)} F_1^{Y_2} \right]$	–
$\tilde{D}_2$	$-G_u^{(\Lambda)} \frac{F_2^{Y_1}}{2M}$	$-G_u^{(\Sigma^0)} \frac{F_2^{Y_2}}{2M}$	–
$\tilde{D}_3$	–	–	–
$\tilde{D}_4$	$G_u^{(\Lambda)} \frac{F_2^{Y_1}}{M}$	$G_u^{(\Sigma^0)} \frac{F_2^{Y_2}}{M}$	–
$\tilde{D}_5$	$-G_u^{(\Lambda)} G_A^{Y_1}$	$-G_u^{(\Sigma^0)} G_A^{Y_2}$	–
$\tilde{D}_6$	$-G_u^{(\Lambda)} \left[F_1^{Y_1} + M_{(1-)} \frac{F_2^{Y_1}}{2M} \right]$	$-G_u^{(\Sigma^0)} \left[F_1^{Y_2} + M_{(2-)} \frac{F_2^{Y_2}}{2M} \right]$	–

Note that in Table. D.1 and D.2 we have denoted $M_{(2-)} = M_{\Sigma^+} - M_{\Sigma^0}$, $M_{(2+)} = M_{\Sigma^+} + M_{\Sigma^0}$, $M_{(1-)} = M_{\Sigma^+} - M_\Lambda$, and $M_{(1+)} = M_{\Sigma^+} + M_\Lambda$. Moreover, the standard Dirac, Pauli, and axial-vector form factors of transitions between two SU(3) octet baryons in the Born diagram of $\nu n \to \mu^- K^0 \Sigma^+$ are given as

$$F_i^{N'}(Q^2) = f_1^p(Q^2) - f_1^n(Q^2), \qquad G_A^{N'}(Q^2) = g_A(Q^2); \tag{D.11}$$

$$F_i^{Y'_1}(Q^2) = -\sqrt{\frac{3}{2}} f_i^n(Q^2), \qquad G_A^{Y'_1}(Q^2) = \sqrt{\frac{2}{3}} \frac{D}{F+D} g_A(Q^2); \tag{D.12}$$

$$F_i^{Y'_2}(Q^2) = -\frac{1}{\sqrt{2}}(2f_i^p(Q^2)) + f_i^n(Q^2), \quad G_A^{Y'_2}(Q^2) = -\sqrt{2} \frac{F}{F+D} g_A(Q^2). \tag{D.13}$$

Finally, the CC and $\Delta S = 0$ associated production reaction we want to look at is $\nu n \to \mu^- K^+ \Sigma^0$. All the three tree diagrams shown in Fig. D.1 contribute to the differential cross section of this reaction process. The s-, u-, and t-channels, respectively, are accompanied by the propagators of p, Σ^-, and K^0; and they contain $g_{K^+\Sigma^0 p}$, $g_{K^+\Sigma^- n}$, and $g_{K^0\Sigma^0 n}$ strong coupling constants. Then the common factors $\tilde{G}_s$, $\tilde{G}_u$, and $\tilde{G}_t$ are

Table. D.2: Extraction of the unknown amplitudes for the $\nu n \to \mu^- K^0 \Sigma^+$ reaction process.

Structure function	s-channel. with p	u-channel with Λ	u-channel with Σ^0
$\tilde{A}_1$	–	$2G_u^{(\Lambda)} G_A^{Y_1}$	$2G_u'^{(\Sigma^0)} G_A^{Y_2'}$
$\tilde{A}_2$	$-2G_s' G_A^{N'}$	–	–
$\tilde{A}_3$	–	$-2G_u'^{(\Lambda)} G_A^{Y_1'}$	$-2G_u'^{(\Sigma^0)} G_A^{Y_2'}$
$\tilde{A}_4$	–	–	–
$\tilde{B}_1$	$-G_s' \frac{M_N}{M} F_2^{N'}$	$G_u'^{(\Lambda)} \left[2F_1^{Y_1'} + M_{(1-)} \frac{F_2^{Y_1'}}{2M} \right]$	$G_u'^{(\Sigma^0)} \left[2F_1^{Y_2'} + M_{(2-)} \frac{F_2^{Y_2'}}{2M} \right]$
$\tilde{B}_2$	$2G_s' F_1^{N'}$	–	–
$\tilde{B}_3$	–	$-2G_u'^{(\Lambda)} F_1^{Y_1'}$	$-2G_u'^{(\Sigma^0)} F_1^{Y_2'}$
$\tilde{B}_4$	–	–	–
$\tilde{C}_1$	$2M_N G_s' G_A^{N'}$	$G_u'^{(\Lambda)} M_{(1-)} G_A^{Y_1'}$	$G_u'^{(\Sigma^0)} M_{(2-)} G_A^{Y_2'}$
$\tilde{C}_2$	–	–	–
$\tilde{C}_3$	–	–	–
$\tilde{C}_4$	–	–	–
$\tilde{D}_1$	$G_s' \left(\frac{q^2}{2} + p_1 \cdot q \right) \frac{F_2^{N'}}{M}$	$G_u'^{(\Lambda)} \left[\left(\frac{q^2}{2} - q \cdot p_2' \right) \frac{F_2^{Y_1'}}{M} - M_{(1+)} F_1^{Y_1'} \right]$	$G_u'^{(\Sigma^0)} \left[\left(\frac{q^2}{2} - q \cdot p'_2 \right) \frac{F_2^{Y_2'}}{M} - M_{(2+)} F_1^{Y_2'} \right]$
$\tilde{D}_2$	$-G_s' \frac{F_2^{N'}}{2M}$	$-G_u'^{(\Lambda)} \frac{F_2^{Y_1'}}{2M}$	$-G_u'^{(\Sigma^0)} \frac{F_2^{Y_2'}}{2M}$
$\tilde{D}_3$	$-G_s' \frac{F_2^{N'}}{M}$	–	–
$\tilde{D}_4$	–	$G_u'^{(\Lambda)} \frac{F_2^{Y_1'}}{M}$	$G_u'^{(\Sigma^0)} \frac{F_2^{Y_2'}}{M}$
$\tilde{D}_5$	$-G_s' G_A^{N'}$	$-G_u'^{(\Lambda)} G_A^{Y_1'}$	$-G_u'^{(\Sigma^0)} G_A^{Y_2'}$
$\tilde{D}_6$	$G_s' (F_1^{N'} + \frac{M_N}{M} F_2^{N'})$	$-G_u'^{(\Lambda)} \left[F_1^{Y_1'} + M_{(1-)} \frac{F_2^{Y_1'}}{2M} \right]$	$-G_u'^{(\Sigma^0)} \left[F_1^{Y_2'} + \left(M_{(2-)} \right) \frac{F_2^{Y_2'}}{2M} \right]$

$$\tilde{G}_s = g_{K^+\Sigma^0 p} \frac{1}{s - M_N^2}; \quad \tilde{G}_u = g_{K^+\Sigma^- n} \frac{1}{u - M_{\Sigma^-}^2}; \quad \tilde{G}_t = g_{K^0\Sigma^0 n} \frac{1}{t - M_{K^0}^2}. \tag{D.14}$$

The SU(3) algebra allows us to write the standard hadronic weak form factor of this reaction as follows

$$\tilde{F}_i^N(Q^2) = f_i^p(Q^2) - f_i^n(Q^2), \qquad \tilde{G}_A^N(Q^2) = g_A(Q^2); \tag{D.15}$$

$$\tilde{F}_i^Y(Q^2) = \frac{1}{\sqrt{2}}(2f_i^p(Q^2) + f_i^n(Q^2)), \quad \tilde{G}_A^Y(Q^2) = \sqrt{2}\frac{F}{F+D} g_A(Q^2). \tag{D.16}$$

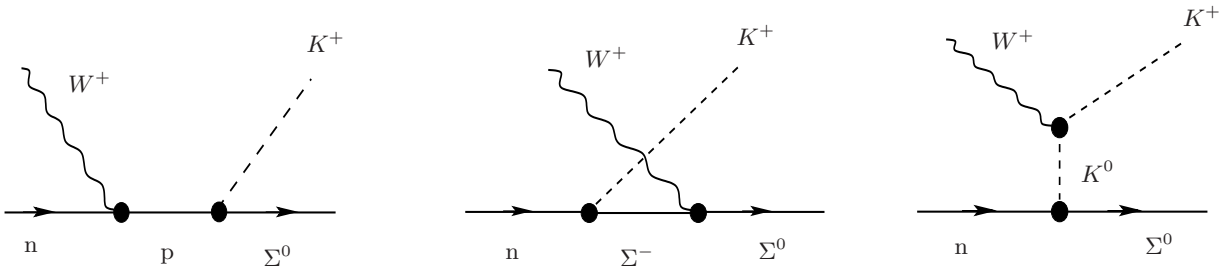

Fig. D.1: The Born diagram of $\nu n \to \mu^- K^+ \Sigma^0$ reaction channel.

Table. D.3: Extraction of the unknown amplitudes for the $\nu n \to \mu^- K^+ \Sigma^0$ reaction process.

Structure function	s-channel. with p	u-channel with Σ^-	t-channel with K^0
$\tilde{A}_1$	–	$2\tilde{G}_u G_A^Y$	–
$\tilde{A}_2$	$-2\tilde{G}_s \tilde{G}_A^N$	–	–
$\tilde{A}_3$	–	$-2\tilde{G}_u \tilde{G}_A^Y$	–
$\tilde{A}_4$	–	–	–
$\tilde{B}_1$	$-\tilde{G}_s \frac{M_N}{M} \tilde{F}_2^N$	$\tilde{G}_u \left[2\tilde{F}_1^Y + (M_{\Sigma 0} - M_{\Sigma^-}) \frac{\tilde{F}_2^Y}{2M} \right]$	$\tilde{G}_t F_{K^+,0}$
$\tilde{B}_2$	$2\tilde{G}_s \tilde{F}_1^N$	–	$2\tilde{G}_t F_{K^+,0}$
$\tilde{B}_3$	–	$-2\tilde{G}_u \tilde{F}_1^Y$	$-2\tilde{G}_t F_{K^+,0}$
$\tilde{B}_4$	–	–	–
$\tilde{C}_1$	$2M_N \tilde{G}_s \tilde{G}_A^N$	$\tilde{G}_u (M_{\Sigma 0} - M_{\Sigma^-}) \tilde{G}_A^Y$	–
$\tilde{C}_2$	–	–	–
$\tilde{C}_3$	–	–	–
$\tilde{C}_4$	–	–	–
$\tilde{D}_1$	$\tilde{G}_s \left(\frac{q^2}{2} + p_1 \cdot q \right) \frac{\tilde{F}_2^N}{M}$	$-\tilde{G}_u \left[(M_{\Sigma 0} + M_{\Sigma^-}) \tilde{F}_1^Y + \left(q \cdot p'_2 - \frac{q^2}{2} \right) \frac{\tilde{F}_2^Y}{M} \right]$	–
$\tilde{D}_2$	$-\tilde{G}_s \frac{\tilde{F}_2^N}{2M}$	$-\tilde{G}_u \frac{\tilde{F}_2^Y}{2M}$	–
$\tilde{D}_3$	$-\tilde{G}_s \frac{\tilde{F}_2^N}{M}$	–	–
$\tilde{D}_4$	–	$\tilde{G}_u \frac{\tilde{F}_2^Y}{M}$	–
$\tilde{D}_5$	$-\tilde{G}_s \tilde{G}_A^N$	$-\tilde{G}_u \tilde{G}_A^Y$	–
$\tilde{D}_6$	$\tilde{G}_s (\tilde{F}_1^N + \frac{M_N}{M} \tilde{F}_2^N)$	$-\tilde{G}_u \left[\tilde{F}_1^Y + (M_{\Sigma 0} - M_{\Sigma^-}) \frac{\tilde{F}_2^Y}{2M} \right]$	–

Bibliography

[1] S. k. Singh and M. J. Vicente Vacas. *arXiv:hep-ph/060235v1*, 2006.

[2] L. Alvarez-Rosu T. Leitner and U. Mosel. *arXiv:nucl-th/0601103v2*, 2006.

[3] M. K. Cheoun and K. S. Kim. *arXiv:nucl-th/0712.4097v1*, 2007.

[4] C. Giusti A. Meucci and F. D. Pacati. *arXiv:nucl-th/0601052v2*, 2006.

[5] P. Hutauruk A. Sulaksono, C. K. Williams and T. Mart. *Phys. Rev. C*, 73(025803), 2006.

[6] N. Jachowicz J. Rychebusch M. C. Martínez, P. Lava and K. Vantournhout. *arXive:nucl-th/0505008v2*, 2006.

[7] L. Bugel *et. al.* Finesse: a proposal for a near detector experiment on the booster neutrino beamline. 2003.

[8] L. Alvarez-Rosu T. Leitner and U. Mosel. *arXiv:nucl-th/0605405v2*, 2006.

[9] N. Solomey. *Nucl. Phys. B*, 142:74–78, 2005.

[10] N. Jachowicz C. Praet, O. Lalakulich and J. Rychebusch. *arXiv:0804.2750v1*, 2008.

[11] R. E. Shrock. *Phys. Rev. D*, 12, 1975.

[12] W. Mechlenburg. *Acta Phys. Aust.*, 48, 1976.

[13] H. K. Dewan. *Phys. Rev. D*, 24, 1980.

[14] S. D. Drell and F. Zachariasen. Electromagnetic structure of nucleons. Oxford University Press, 1961.

[15] M. Gell-Mann. *Phys. Lett.*, 8:214, 1964.

[16] G. Zweig. *CERN-8182-TH-401*, 1964.

[17] M. Gell-Mann. *Phys. Rev.*, 125:1067, 1962.

[18] T.-P. Cheng and L.-F. Li. *Gauge Theory of Elementary Particle Physics*. Oxford University Press, 1984.

[19] J. Bernstein. *Elementary Particles and Their Currents*. W. H. Freeman, 1968.

[20] T. D. Lee and C. N. Yang. *Phys. Rev.*, 104:254, 1956.

[21] C. S. Wu *et al. Phys. Rev.*, 105:1413, 1957.

[22] N. Cabibbo. *Phys. Rev. Let.*, 10(12), 1963.

[23] D. Griffiths. *Introduction to Elementary Particles*. Wiley, 1987.

[24] W. E. Burcham and M. Jobes. *Nuclear and Particle Physics*. Longman, 1995.

[25] F. Halzen and A. D. Martin. *QUARKS AND LEPTONS: an introductory course to modern particle physics*. wiley, 1984.

[26] P. Renton. *Electroweak Interactions: An Introduction The Physics of Quarks and Leptons*. Cambridge University Press, 1990.

[27] W. Anthony Mann. *NuMI-NOTE-GEN-927*, 2003.

[28] L. G. Hyman P. Schreiner R. Singer R. P. Smith S. J. Barish, M. Derrick and H. Yuta. *Phys. Rev. Lett.*, 33(24), 1974.

[29] J. D. Bjorken and S. D. Drell. *Relativistic Quantum Mechanics*. McGraw-Hill, 1964.

[30] I. J. R. Aitchison and A. J. G. Hey. *Gauge Theories in Particle Physics*. Adam Hilger, 1982.

[31] W. Greiner and J. Reinhardt. *Quantum Electrodynamics*. Springer Verlag, 1992.

[32] D. P. Murdock C. J. Horowitz, H. Kim and S. Pollock. *Phys. Rev. C*, 48(6), 1993.

[33] B. I. S. van der Ventel and J. Piekarewizc. *Phys. Rev. C*, 69, 2004.

[34] D. H. Perkins. *Introduction to High Energy Physics*. Cambridge University Press, 2000.

[35] E. A. Paschos M. Nowakowski and J. M. Rodríguez. *arXiv:physics/0402058*, 2, 2005.

[36] R. P. Feynman and M. Gell-Mann. *Phys. Rev. Let.*, 109:193, 1958.

[37] S. Weinberg. *Phys. Rev.*, 112:1375, 1958.

[38] S. M. Bilenky W. M. Alberico1 and C. Maieron. *arXiv:hep-ph/0311053v1*, 2003.

[39] B. I. S. van der Ventel and J. Piekarewicz. *Phys. Rev. C*, 73, 2006.

[40] K. S. Kim B. S. Han, M. K. Cheoun and I.-T. Cheon. *arXiv: nucl-th/9912011v1*, 1999.

[41] P. A. Carruthers. *Introduction to Unitary Symmetry.* John Wiley & Sons, 1966.

[42] R. A. Adelseck and B. Saghai. *Physc. Rev. C*, 42, 1990.

[43] C. Bennhold H. Haberzettl F. X. Lee, T. Mart and L. E. Wright. *Nucl. Phys. A*, 695:237, 2001.

[44] S. L. Adler and F. T. Gilman. *Phys. Rev.*, 152(4), 1966.

[45] H. W. Naus R. L. Workman and S. J. Pollock. *Phys. Rev. C*, 5(5), 1992.

[46] D. Drechsel and L. Tialor. *J. Phys. G: Nuvl. Part. Phys*, 18:449–497, 1992.

[47] Z.-P. Li Q. Zhao, J. S. Al-Khalili and R. L. Workman. *arXiv: nucl-th/0202067v1*, 2002.

[48] T. Mart. Multipole approach for kaon photoproduction, comparing the new saphir and clas data. Presentation given at Bosen, 2006.

[49] P. Ambrozewicz *et al. arXiv: hep-ex/0611036v1*, 2006.